Supplementary material for *Greater climate control of above- versus belowground communities* by Mod et al.

Appendix 1: A detailed description of the used data

Amphibians, reptiles

Data on amphibian and reptile distributions were provided by the *info fauna karch* (Pittet, 2017; Schmidt & Zumbach, 2019). The data are based on point observations collected by professional and amateur herpetologists and naturalists, where recording of coordinates have maximum precision of 100 m. The oldest records date back to 1965, yet for the large majority of points, the most recent observations were collected after 2000. Separately for amphibian and reptile datasets, absence of a species is assumed in the sites of presence observations of another species. To increase the reliability of absence observations, the reptile dataset was complemented with field observations in summer 2014 targeting to examine the zones which were defined as missing observations or as possible distribution boundary by the expert assessment of *info fauna karch.*

Grasshoppers, butterflies, bumblebees

During the vegetation growing seasons of 2009-2010, using net-capture and in-situ identification, grasshoppers (species belonging to order *Orthoptera*; i.e. including also crickets) and bumblebees (species belonging to genus *Bombus*) were investigated in 202 sites (Pellissier et al., 2013b; Pradervand et al., 2013), and butterflies (species belonging to order *Lepidoptera*, i.e. including also moths) in 208 sites (Pellissier et al., 2012). Presences (and absences) of species were first recorded in four sub-squares of 10 × 10 m located at the four cardinal points of the large square (50 × 50 m) and subsequently in the complete 50 m square.

Vascular plants

During the peak growing seasons of 2002-2009, 909 sites of 4 m^2 were surveyed (Dubuis et al., 2011). All vascular plant species (referred as plants in the main text) were exhaustively inventoried in each site, resulting in 795 species identified. As we were only interested in non-forested ecosystems, 15 species clearly belonging to forest ecosystems (e.g. seedlings of trees) were removed from the analyses.

Fungi (at genus level)

During the summer 2012, soil was sampled from 103 sites (Pinto-Figueroa et al., 2019). Samples were taken from top soil layer (0-5 cm) from the corners and centre of the sites after removing plant litter surface and then pooled together and homogenized. Fungal observational taxonomic units (OTUs) of each site were determined by metabarcoding internal transcribed spacer 1 (ITS1) at the Genomic Technology Facility of the University of Lausanne. PCR amplification and Hiseq Illumina sequencing resulted in 49 million demultiplex paired-end DNA sequences, that were closed-reference clustered against the ITS1_Hiseq dataset at 97% sequence identity in QIIME 1.8. After regular and recommended quality control and filtering see Pinto-Figueraoa (2016), the identified 2095 OTUs (occurring at least in three sites) were aggregated to genus level using the tax.abund function in the *ram* -R package (Chen, Simpson, & Levesque, 2016). Only OTUs assigned at the genus level retained for analyses. Subsequently, sequence counts were transformed

to presences, whereas zero counts represent absences. For the detailed description of the dataset and its preparation, see Pinto-Figueraoa (2016) and Pinto-Figueroa et al. (2019).

Fungi (at order level)

During the summer 2009, soil was sampled from 198 sites (Pagni et al., 2013). The composition of fungal communities is based on DNA extraction from five air-dried samples per site and pyro-sequencing the pooled ITS1 DNA amplicons. OTUs were clustered using the DBC454 hierarchical clustering algorithm. Out of the resulting 1199 OTUs were assigned with order level using NCBI taxonomy database. OTUs without order level assignment (607) were removed. Subsequently, sequence counts were transformed to presences, whereas zero counts represent absences. For the detailed description of the dataset and its preparation, see Pagni et al. (2013), and Pellissier et al. (2013a), (2014).

Bacteria

In addition to data collected in 2012 (see Yashiro et al., 2016 and sampling description for fungi genera dataset), soil was additionally sampled in summer 2013 resulting in total of 258 sites. Following Yashiro et al. (2016), assemblage of bacterial OTUs per site was determined by metabarcoding of the V5 hypervariable region of the 16S rRNA gene by HiSeq Illumina sequencing at the Genomic Technology Facility of the University of Lausanne. The sequences were clustered into OTUs and taxonomically assigned in QIIME v.1.7.0 at the 97 % similarity threshold using the gg_13_8 database from Greengenes as a reference and the pick_closed_reference_otus.p (DeSantis et al., 2006). After regular and recommended quality control based filtering (see Yashiro et al., 2016), from the pooled samples of 2012 and 2013, ~15 500 OTUs were identified. For the datasets at genus and order levels, the OTUs without respective assignment were removed (11411 and 2056 OTUs, respectively). Finally, sequence counts were transformed to presences, whereas no counts represent absences. For the detailed description of the dataset and its preparation, see Yashiro et al. (2016)ˈ(2018).

Protista

Out of DNA extractions from soil samples collected in 2013 (see bacteria datasets), 220 sites were analysed for their Protista content (Seppey et al., 2019). The metabarcoding of the V4 region of the ribosomal RNA small sub-unit gene was done at the Molecular Systematics & Environmental Genomics Laboratory at University of Geneva. Following amplification of DNA extractions, three replicate pools of PCR for each sample were pair-end sequenced by MiSeq Illumina. After quality control and subsequent sequence removal (see Seppey et al., 2019), the replicates were pooled and OTUs were built with the program swarm v. 2.1.8 (Mahe, Rognes, Quince, de Vargas, & Dunthorn, 2015). The 41 050 identified OTUs were then taxonomically assigned at genus and order levels based on the dominant sequence by aligning it to the trimmed PR^2 database using the global pairwise alignment program ggsearch v. 36.3.6 (Pearson, 2000; Guillou et al., 2013). For the detailed description of the dataset and its preparation, see Seppey et al. (2019).

~23 000 OTUs belonging to other taxa than protists, being clear misclassifications, or with lower percentage of identity than 65 % were removed following Seppey et al. (2019). At genus level, ~10 000 OTUs, with missing or unclear taxonomy were removed. Finally, sequence counts were transformed to presences, whereas zero counts represent absences.

Environmental data

The environmental variables used to calibrate the models represent climatic and topographic conditions of the study area: mean annual temperature (mean T), annual temperature range (T range), sum of annual precipitation (P sum), topographic position index (TPI), slope and potential annual solar radiation. Annual values were used instead of seasonal because each taxonomical group might have a different growing season. All predictors were produced for the study area at a 25 m resolution (see Figures S1-10 in Appendix 1). The climatic predictors were derived from daily MeteoSwiss gridded data covering period 1981-2010 at 1 km resolution (meteoswiss.ch), and subsequently downscaled to 25 m using local linear regressions with elevation in a moving window of 5 km radius (CHclim25 dataset; https://www.unil.ch/ecospat/en/home/menuguid/ecospat-resources/data.html). TPI and slope were derived from a 25 m resolution DEM (Federal Office of Topography; swisstopo.ch) following Zimmermann and Kienast (1999). Potential solar radiation was calculated for each month with module ta_lighting in SAGA GIS at 2 m resolution and subsequently resampled to 25 m by averaging, and the monthly values were summed as annual.

For future climate projections of temperature and precipitation, we used the grids at 0.02° (~2.2 km) developed by Zubler et al. (2014), themselves based on scenarios by the Swiss Climate Change Scenario CH2011 project from the Center for Climate Systems Modeling (http://www.c2sm.ethz.ch/). Projections are averaged based on ARPEGEALADIN, ECHAM5-REMO and HadCM3Q0-CLM, coupling regional and global climatic models. Anomalies for the scenarios A1B and A2, and for the time slices 2020-2049, 2045-2074, and 2070-2099 (hereafter called 35, 60 and 85, respectively) were downscaled with bilinear interpolation at 25m and added to current climatic variables across the study area. Although the whole quantile range of estimates is available for each scenario and time slice, only median estimates were used here. The climate change scenarios, from current to future, indicate increase in annual mean temperature and temperature range, and decrease in annual precipitation sum (Figures S21 in Appendix 1). Despite the correlation between mean T and P sum; Figures S11-20 in Appendix 1), all predictors were used for the models of all taxa, as future changes in temperature and precipitation are of opposite direction.

Figures S1-S10 (the following 11 pages): Maps of spatial distribution of sampling sites per taxonomic group (black dots) and current and future environmental predictors. Yellow (red for solar radiation) indicates non-analogous environmental space relative to coverage of species sampling. Green indicate location of forest (shown only for taxonomic groups sampled from non-forested sites). T = temperature, P = precipitation, TPI = topographic position index

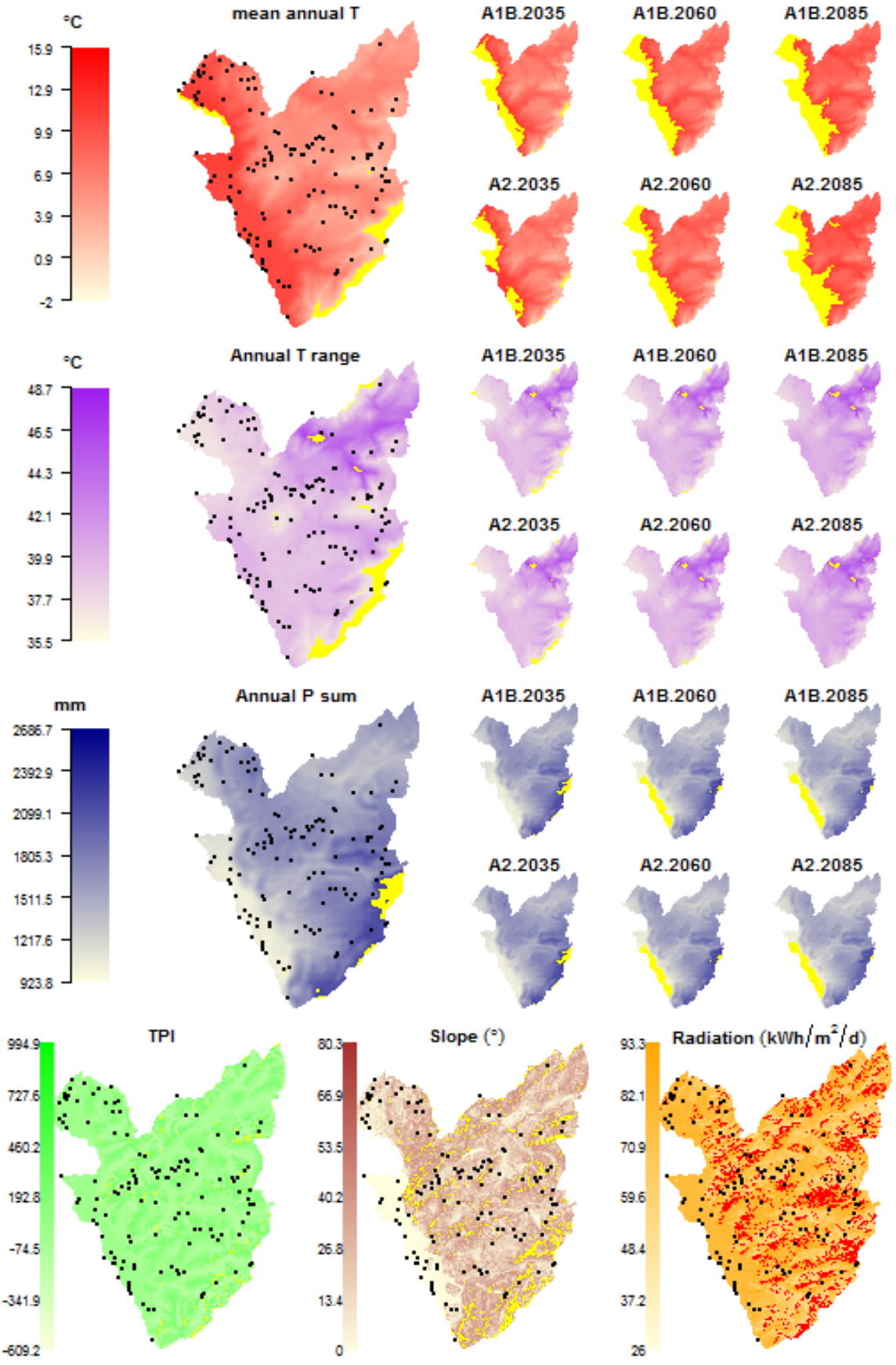

Figure S1. Amphibians

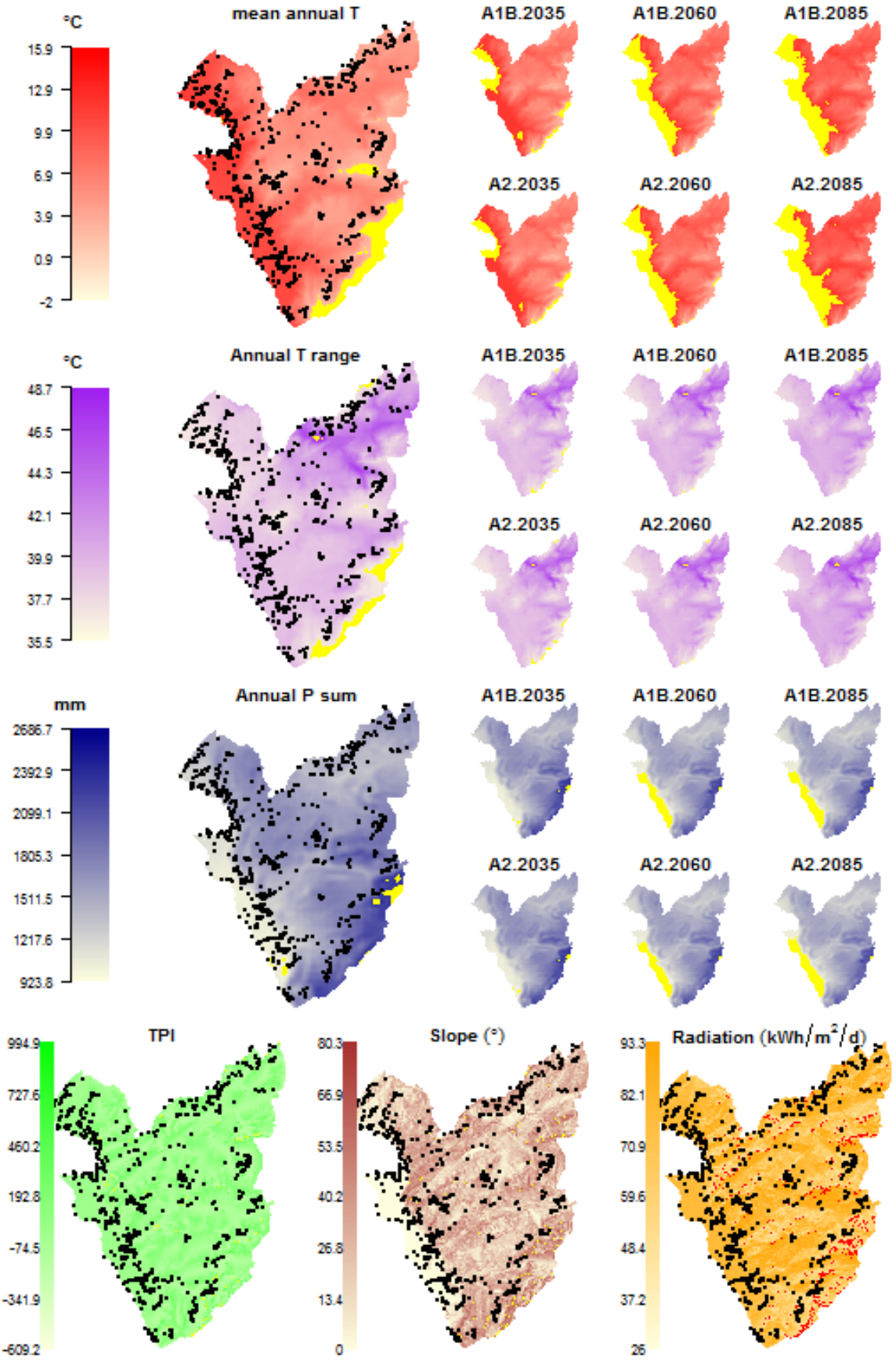

Figure S2. Reptiles

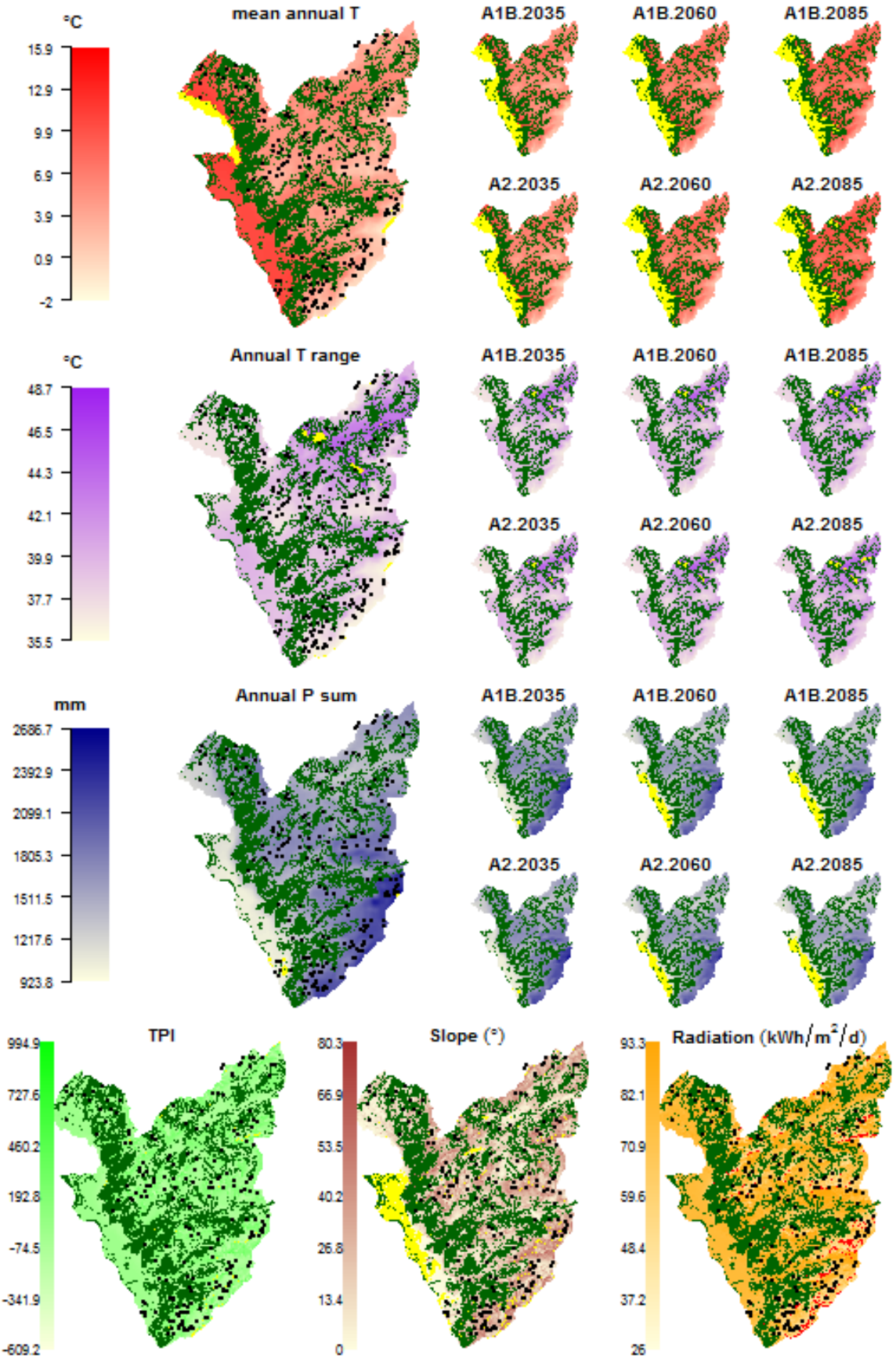

Figure S3. Grasshoppers

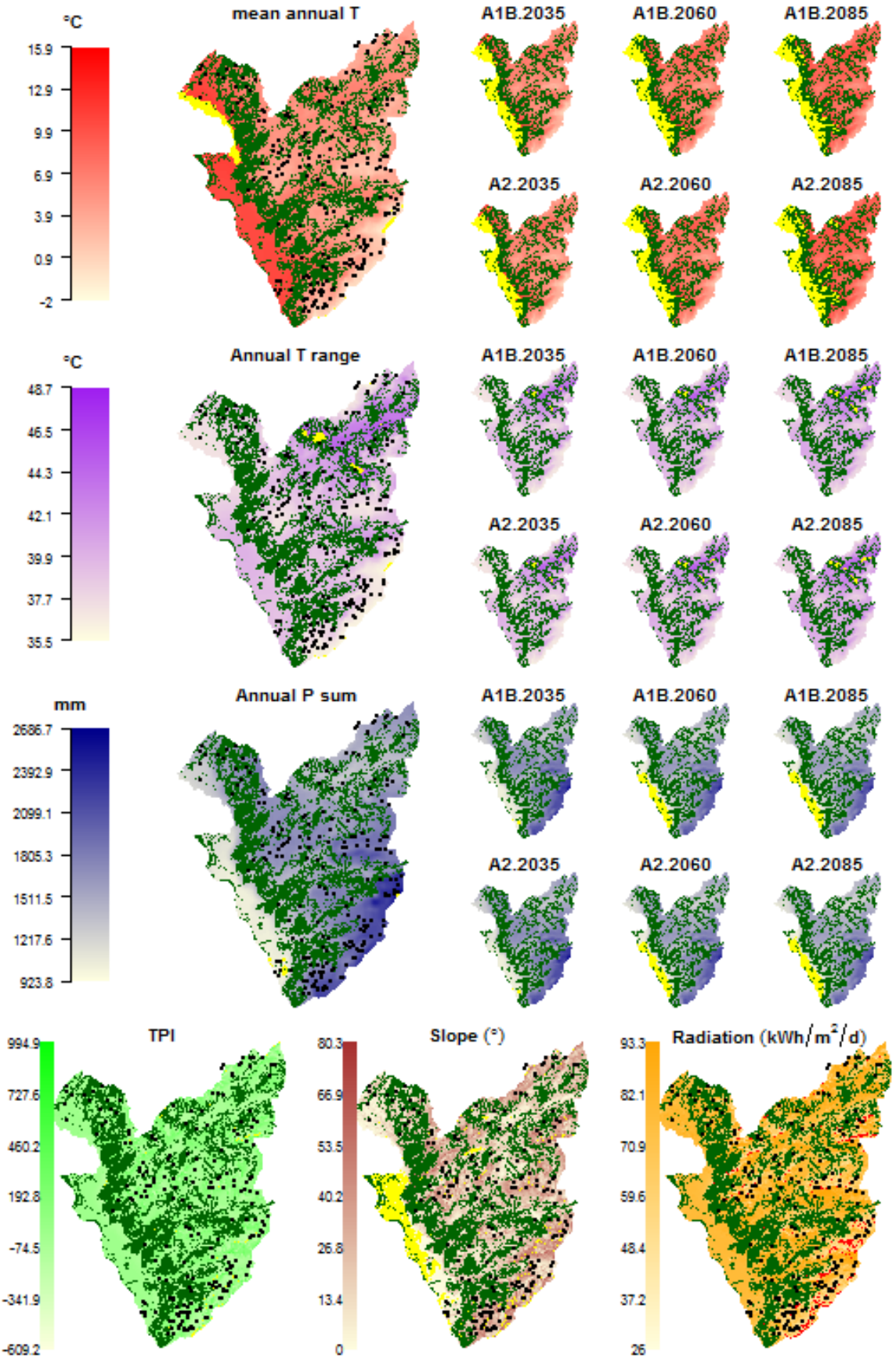

Figure S4. Butterflies

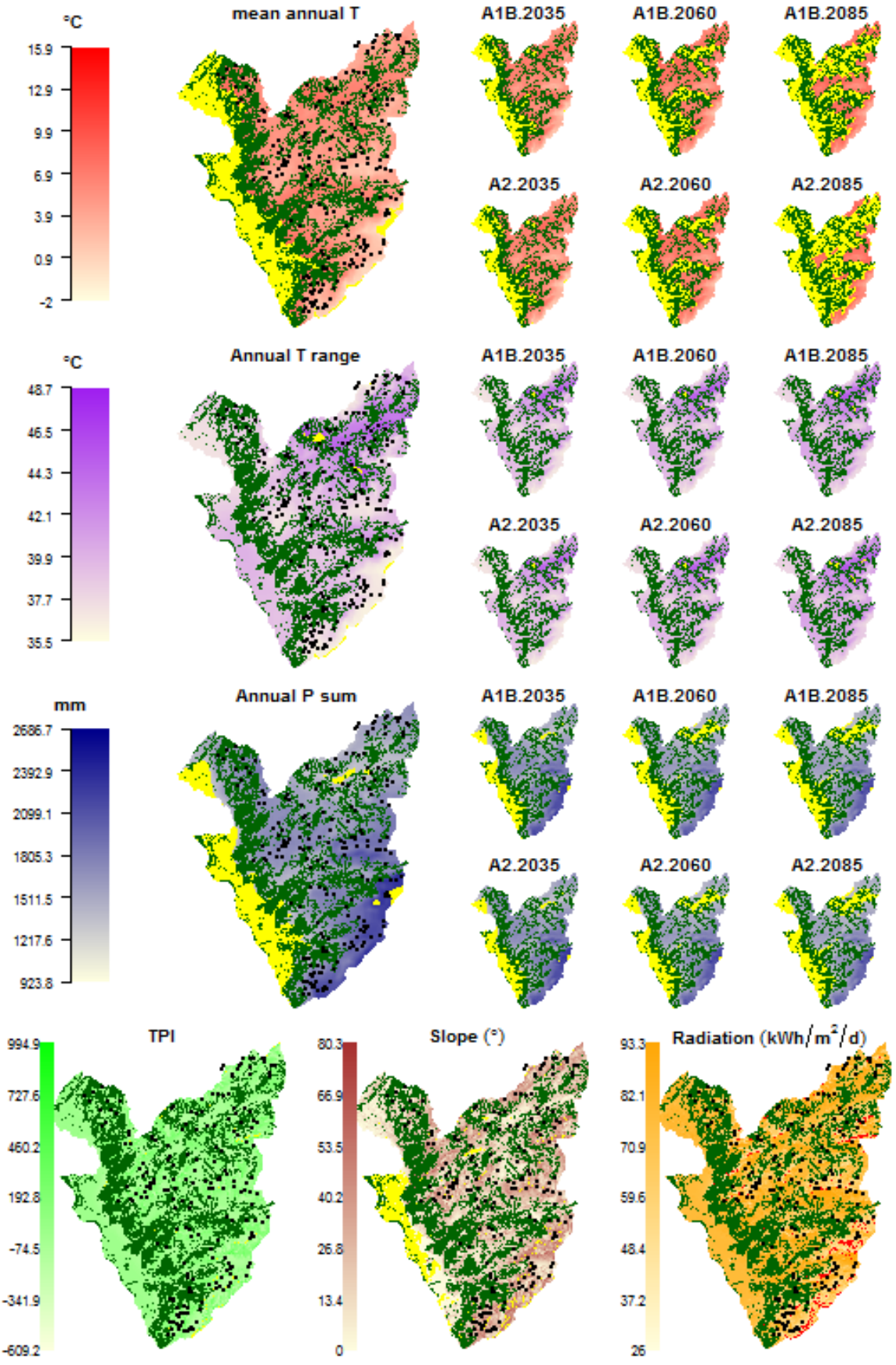

Figure S5. Bumblebees

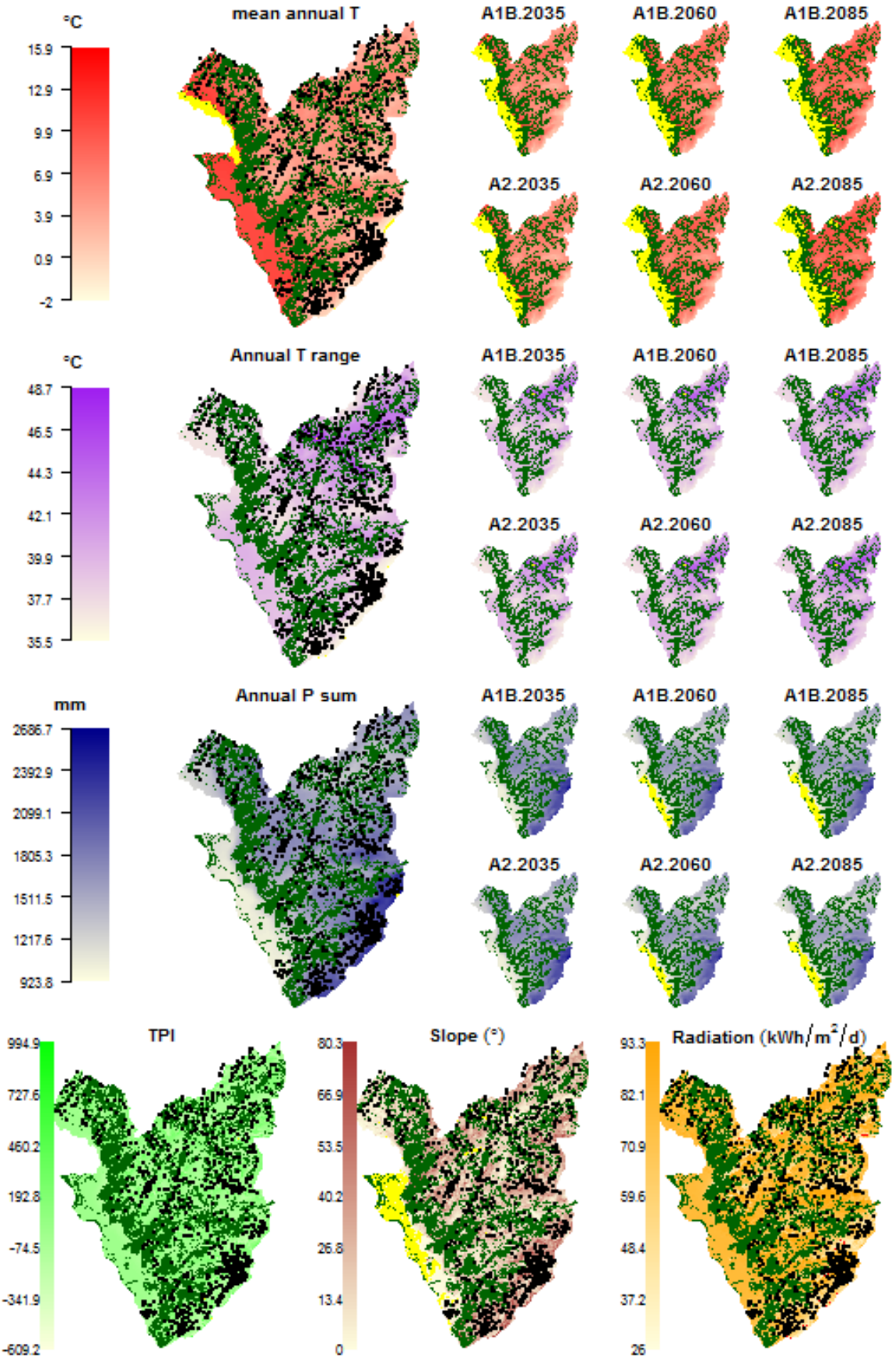

Figure S6. Plants.

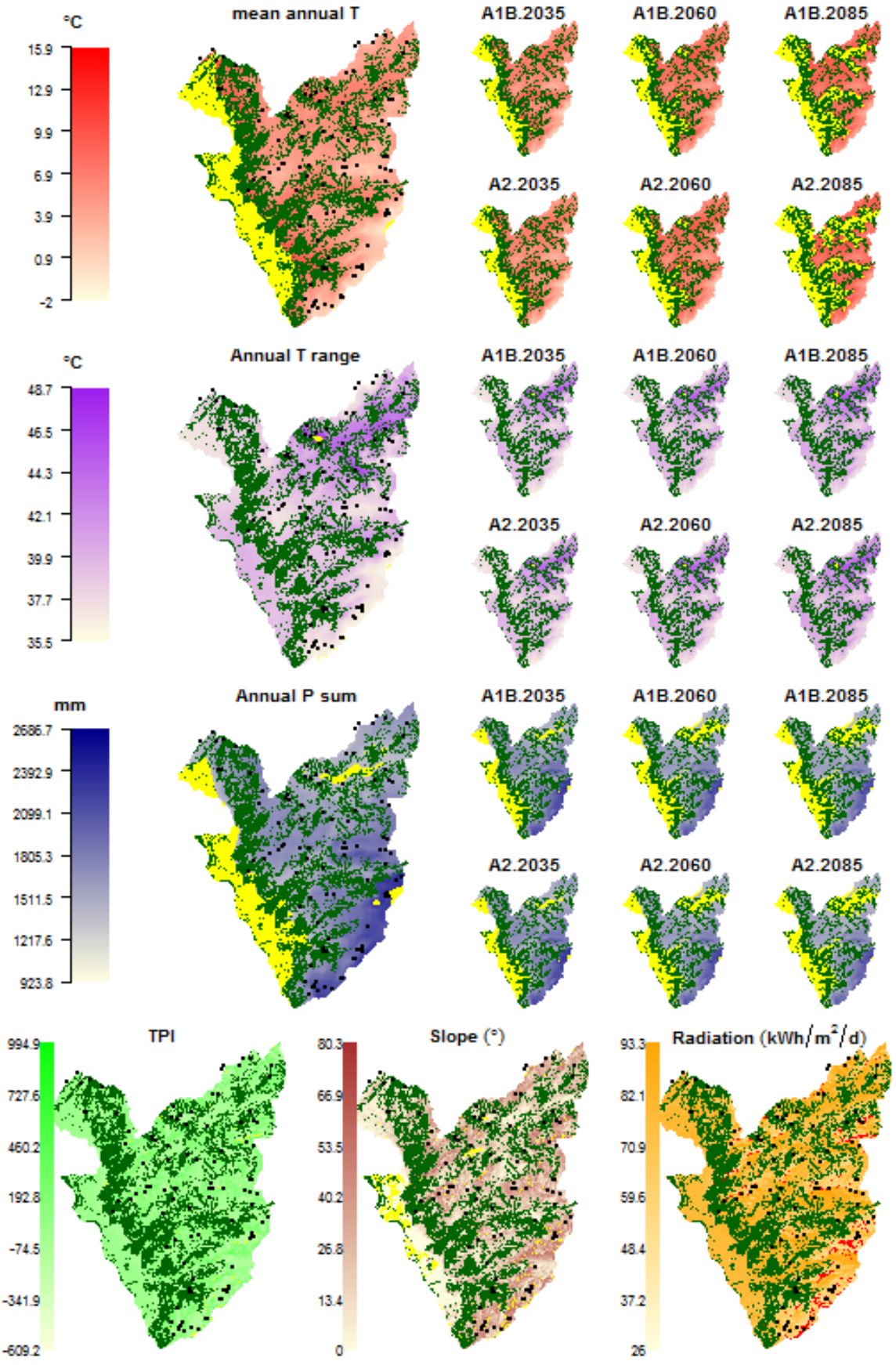

Figure S7. Fungus genera

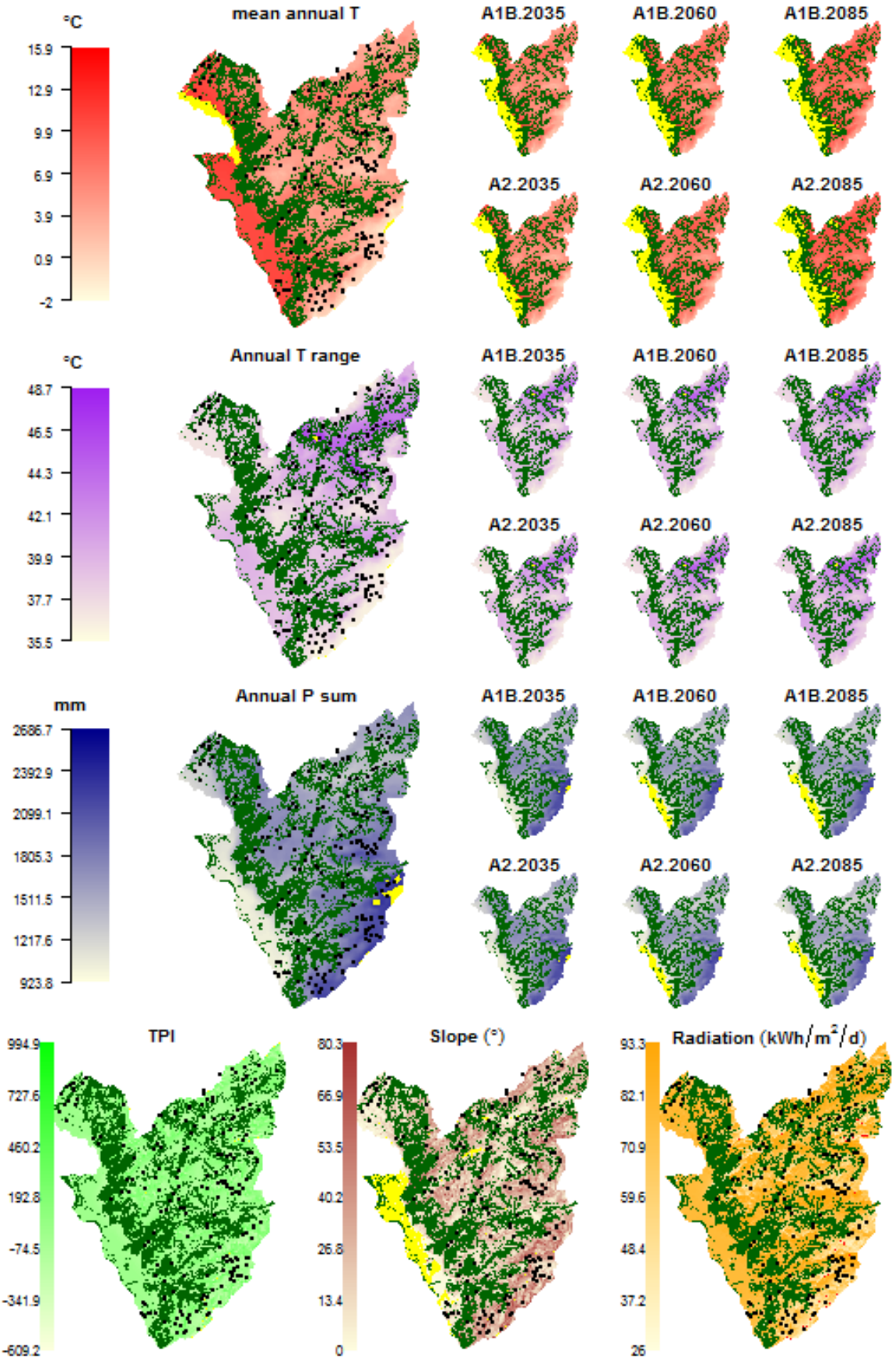

Figure S8. Fungus orders

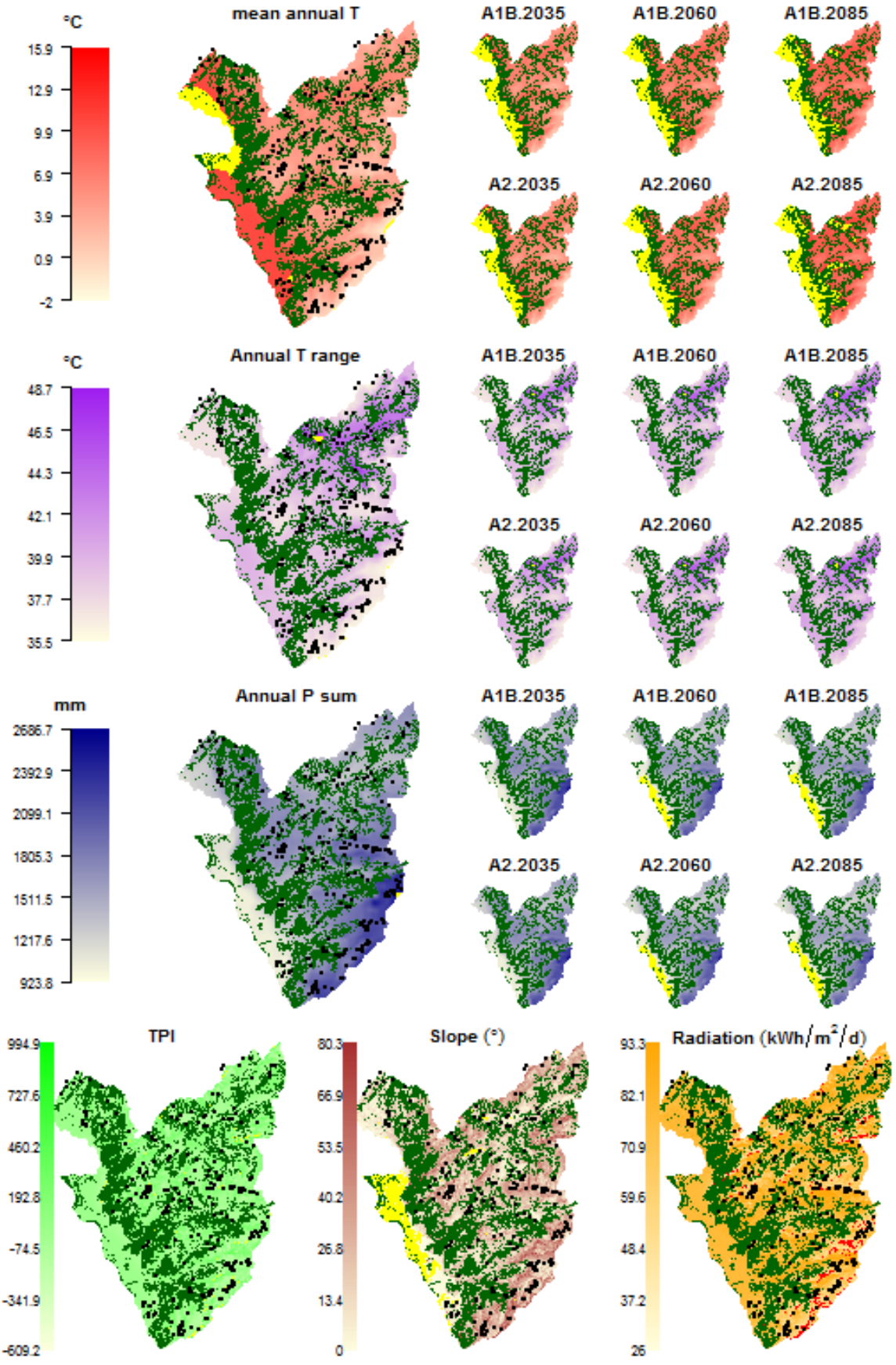

Figure S9. Bacteria

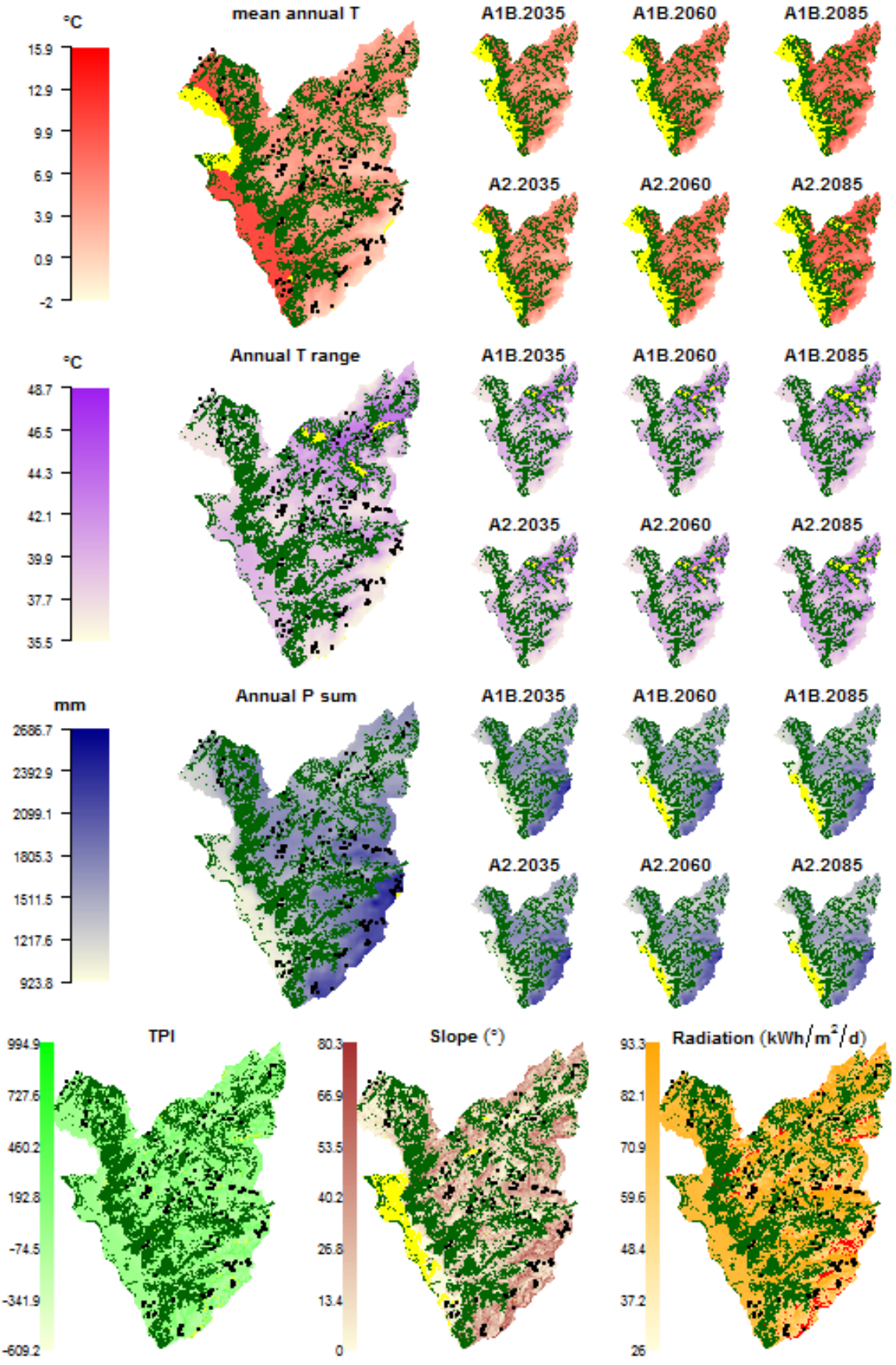

Figure S10. Protists

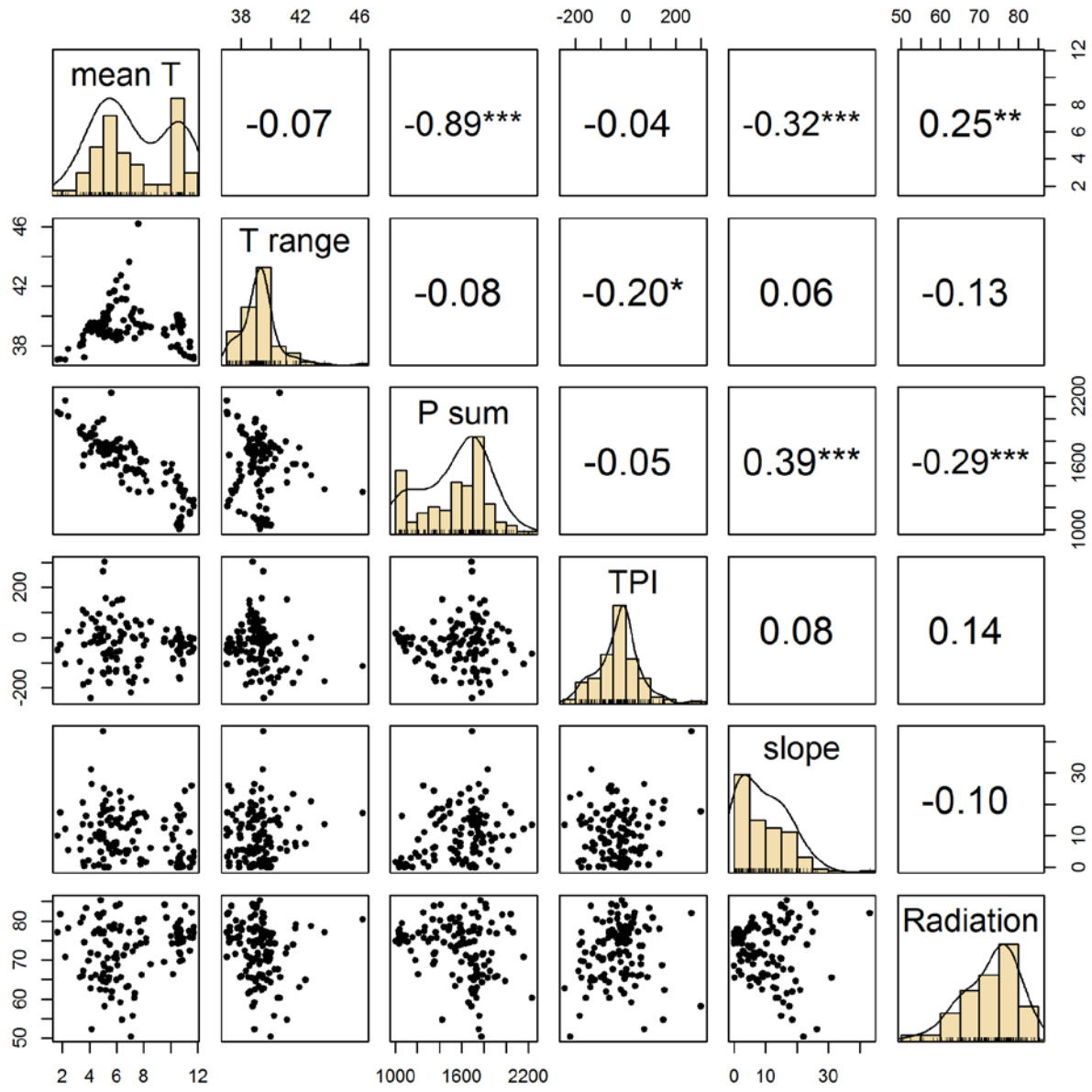

*Figure S11. Distributions and relationships of environmental predictors extracted for sampling sites of **amphibians**. Upper right panels are Pearson correlations with significance levels (* p < 0.05, ** p < 0.01, *** p < 0.001). T = temperature (°C), P = precipitation (mm), TPI = topographic position index, slope (°) and Radiation = potential annual solar radiation (in kWh/m^2/day).*

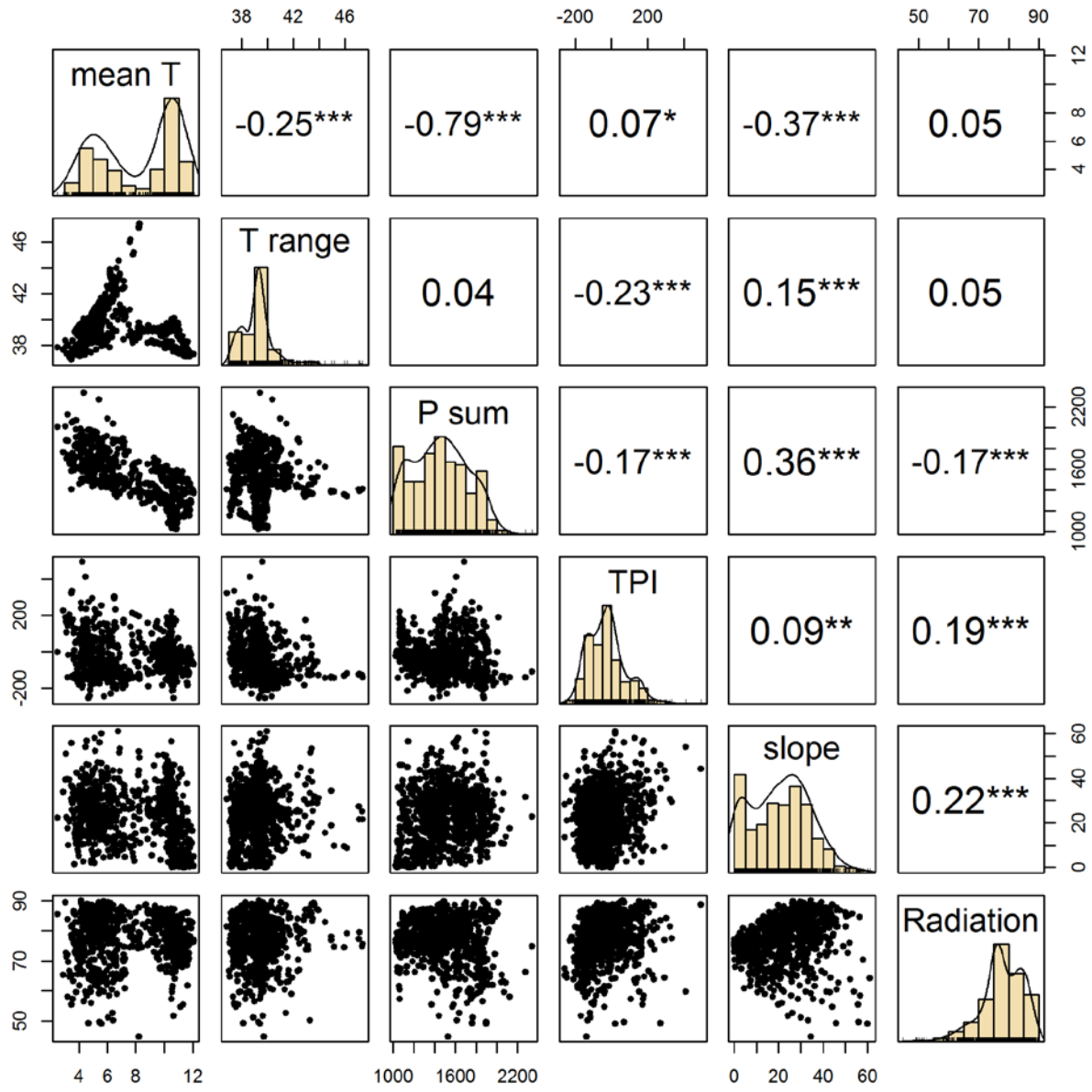

*Figure S12. Distributions and relationships of environmental predictors extracted for sampling sites of **reptiles**. Upper right panels are Pearson correlations with significance levels (* p < 0.05, ** p < 0.01, *** p < 0.001). T = temperature (°C), P = precipitation (mm), TPI = topographic position index, slope (°) and Radiation = potential annual solar radiation (in kWh/m^2/day).*

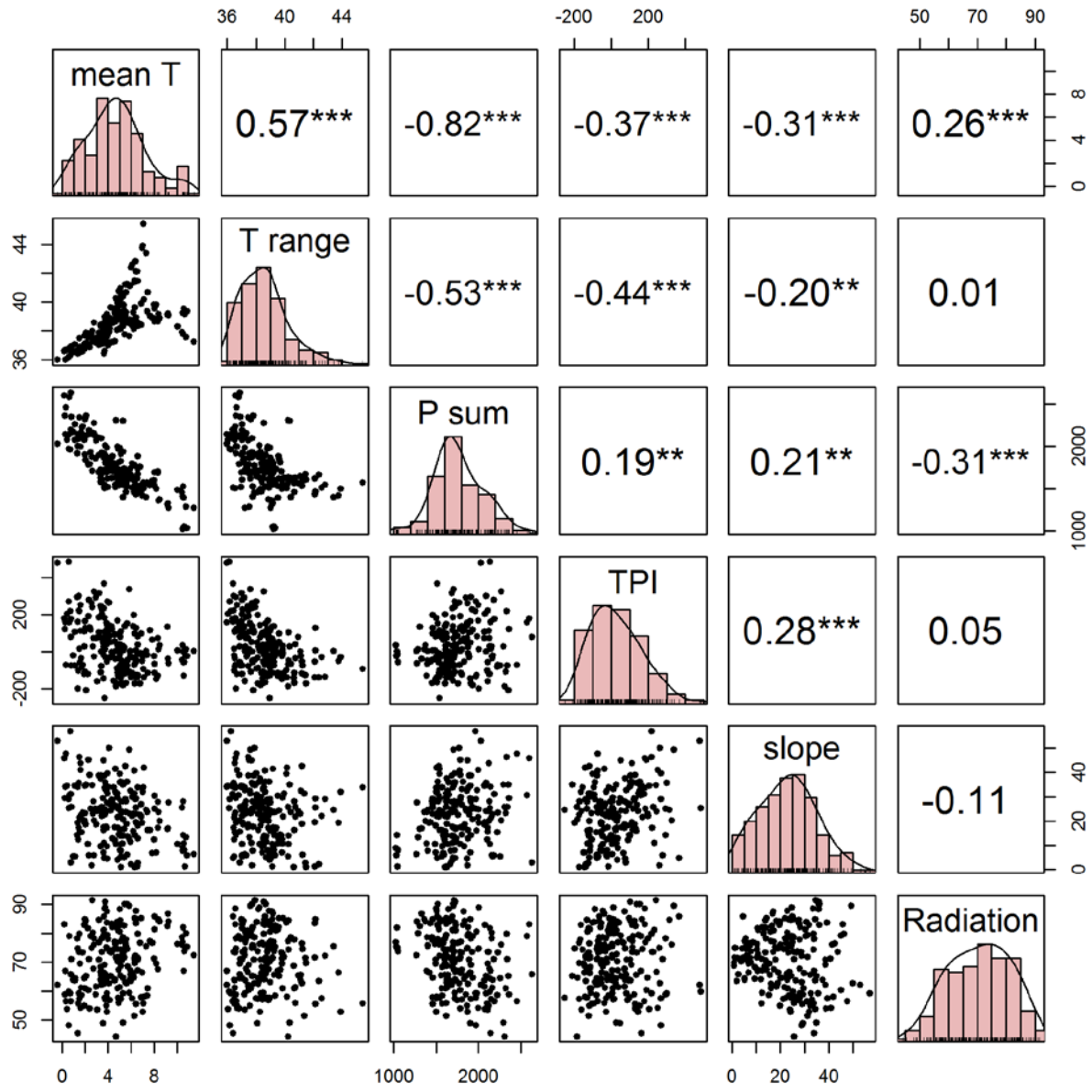

*Figure S13. Distributions and relationships of environmental predictors extracted for sampling sites of **grasshoppers**. Upper right panels are Pearson correlations with significance levels (* p < 0.05, ** p < 0.01, *** p < 0.001). T = temperature (°C), P = precipitation (mm), TPI = topographic position index, slope (°) and Radiation = potential annual solar radiation (in kWh/m^2/day).*

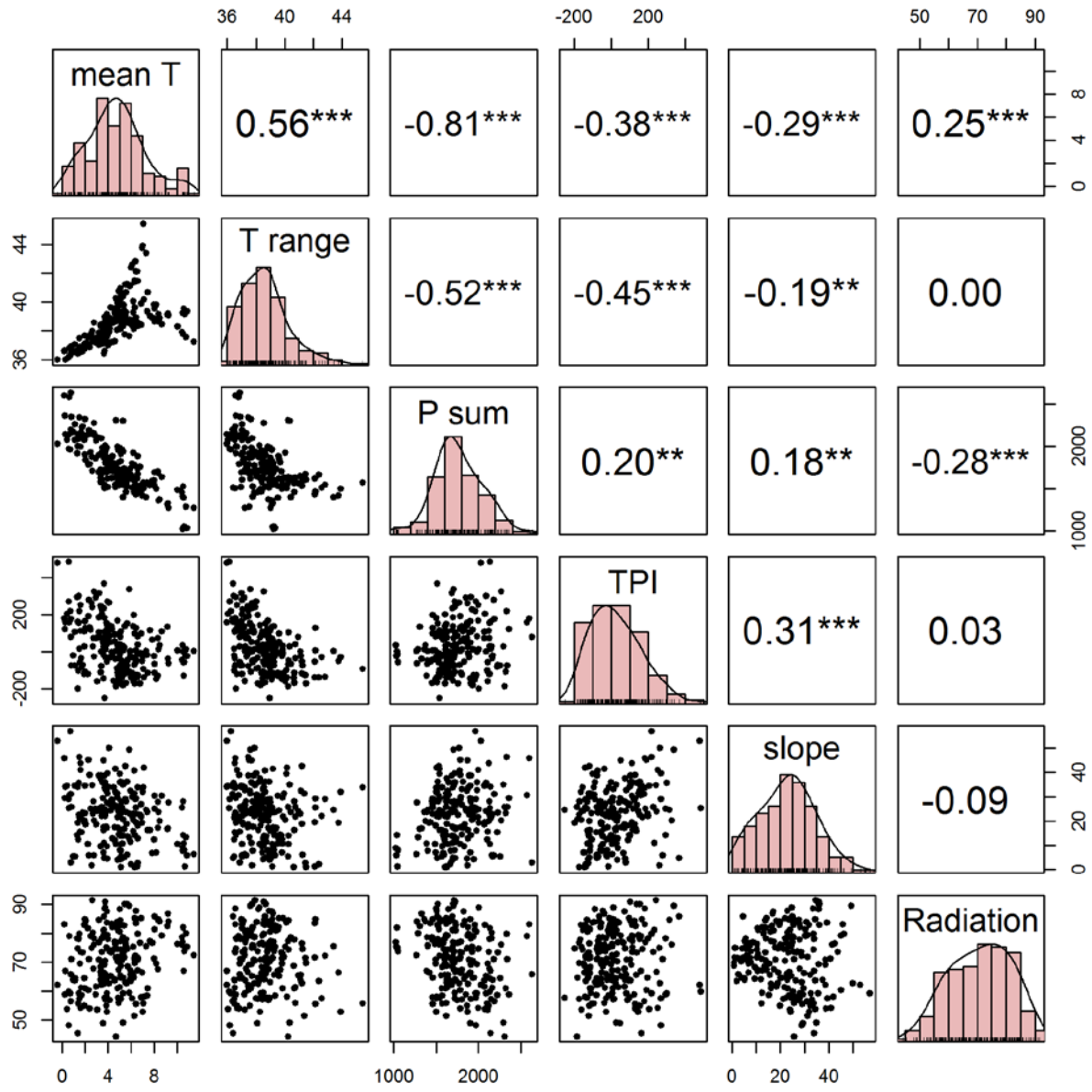

*Figure S14. Distributions and relationships of environmental predictors extracted for sampling sites of **butterflies**. Upper right panels are Pearson correlations with significance levels (* p < 0.05, ** p < 0.01, *** p < 0.001). T = temperature (°C), P = precipitation (mm), TPI = topographic position index, slope (°) and Radiation = potential annual solar radiation (in kWh/m^2/day).*

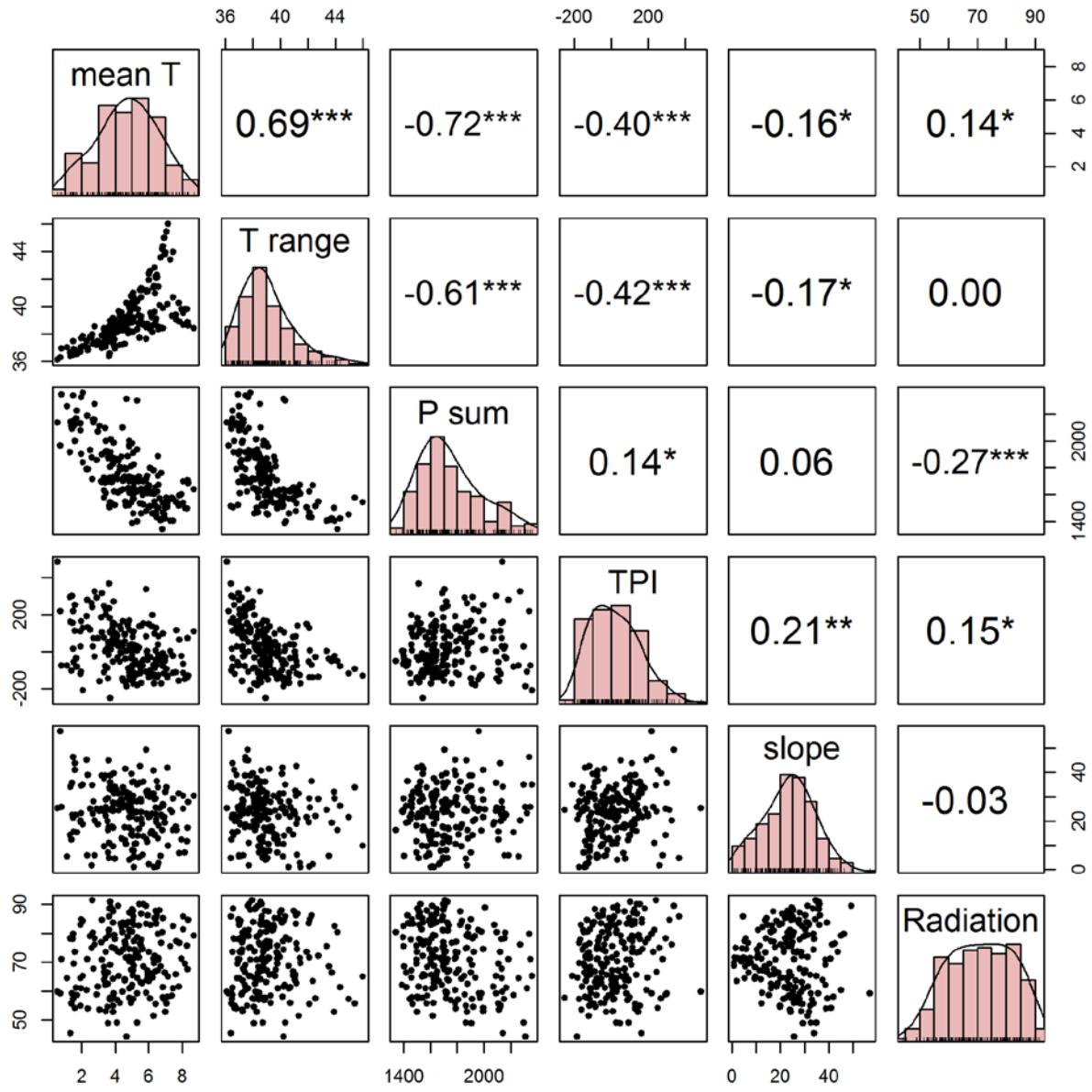

*Figure S15. Distributions and relationships of environmental predictors extracted for sampling sites of **bumblebees**. Upper right panels are Pearson correlations with significance levels (* p < 0.05, ** p < 0.01, *** p < 0.001). T = temperature (°C), P = precipitation (mm), TPI = topographic position index, slope (°) and Radiation = potential annual solar radiation (in kWh/m^2/day).*

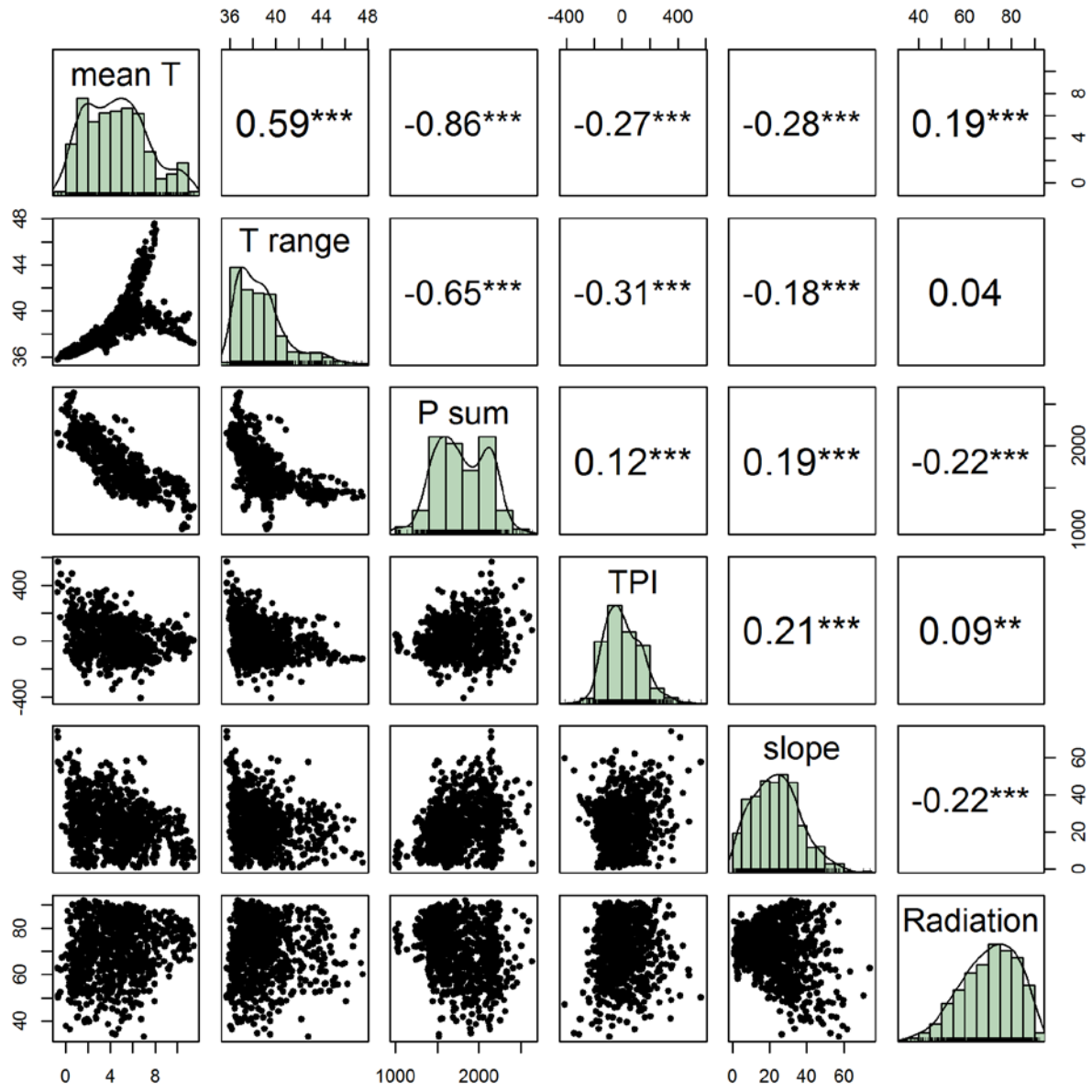

*Figure S16. Distributions and relationships of environmental predictors extracted for sampling sites of **plants**. Upper right panels are Pearson correlations with significance levels (* p < 0.05, ** p < 0.01, *** p < 0.001). T = temperature (°C), P = precipitation (mm), TPI = topographic position index, slope (°) and Radiation = potential annual solar radiation (in kWh/m^2/day).*

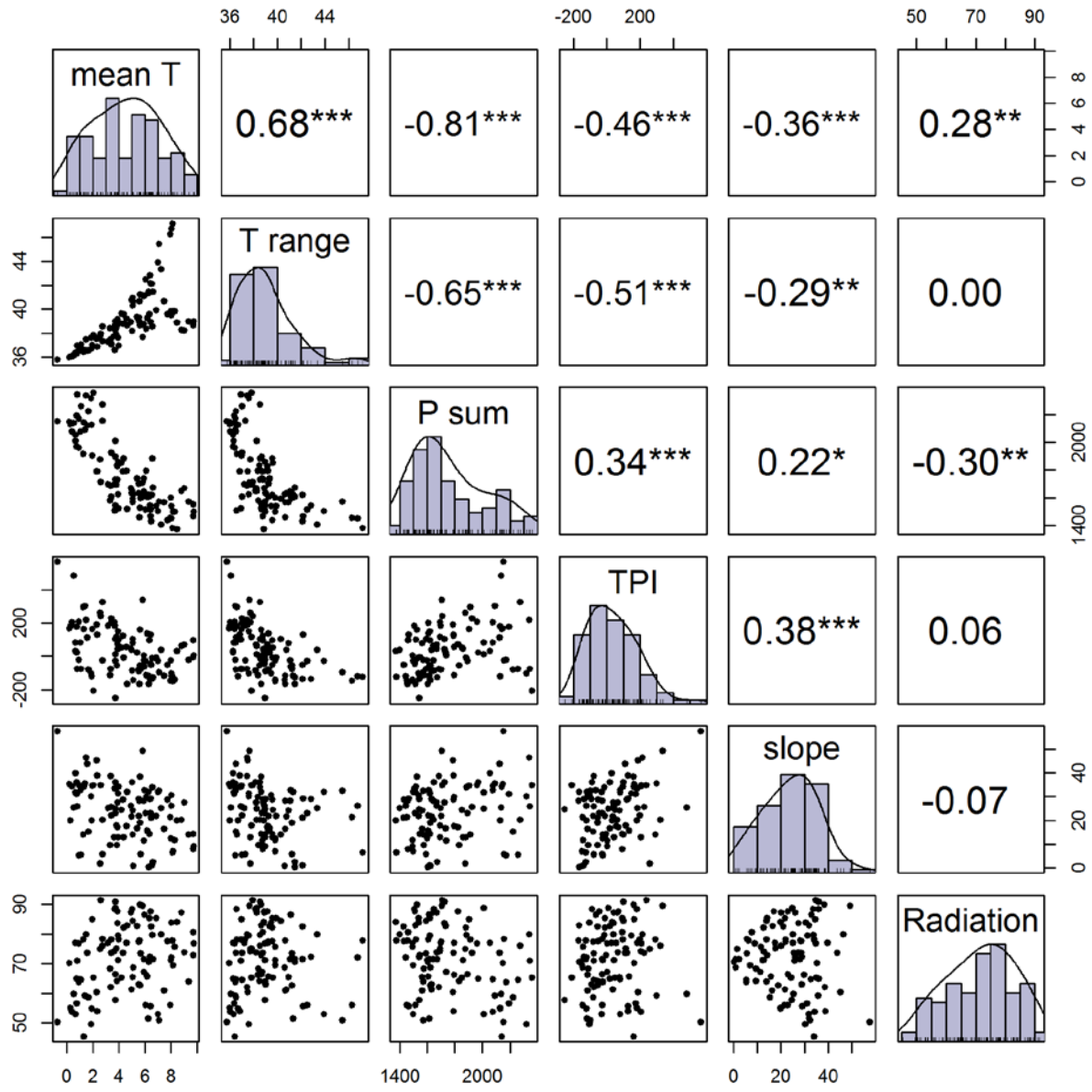

*Figure S17. Distributions and relationships of environmental predictors extracted for sampling sites of **fungi genus**. Upper right panels are Pearson correlations with significance levels (* p < 0.05, ** p < 0.01, *** p < 0.001). T = temperature (°C), P = precipitation (mm), TPI = topographic position index, slope (°) and Radiation = potential annual solar radiation (in kWh/m^2/day).*

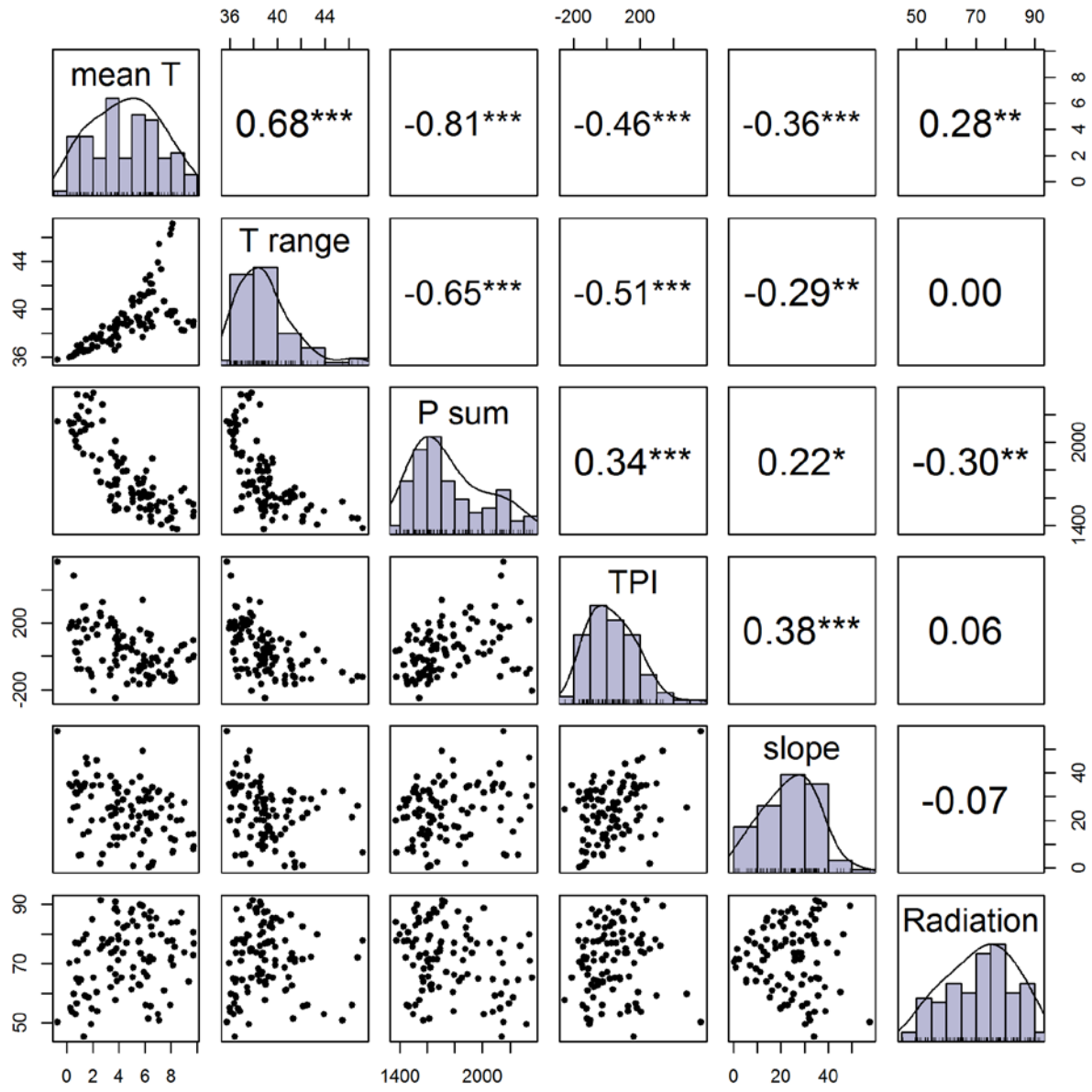

*Figure S18. Distributions and relationships of environmental predictors extracted for sampling sites of **fungi orders**. Upper right panels are Pearson correlations with significance levels (* p < 0.05, ** p < 0.01, *** p < 0.001). T = temperature (°C), P = precipitation (mm), TPI = topographic position index, slope (°) and Radiation = potential annual solar radiation (in kWh/m^2/day).*

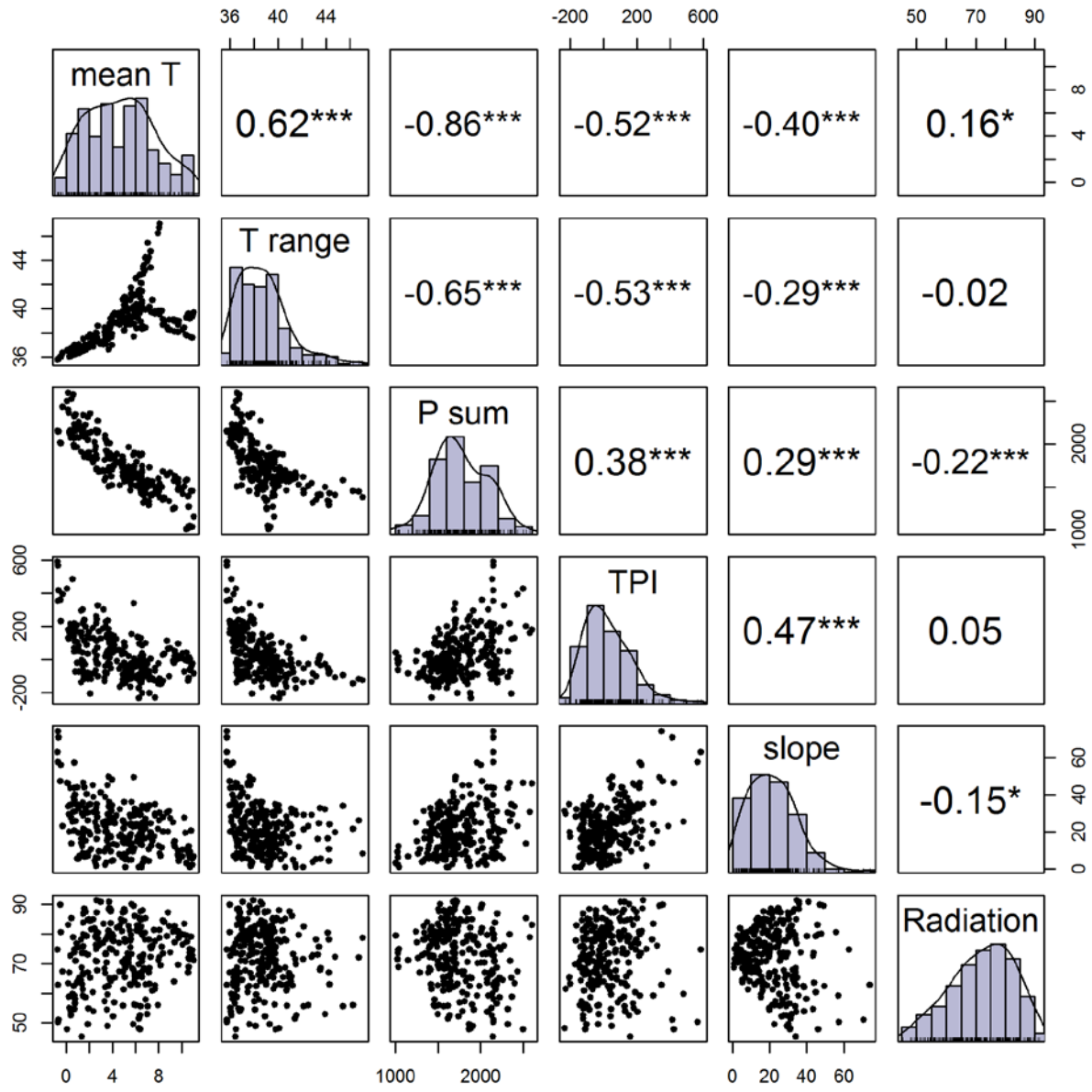

*Figure S19. Distributions and relationships of environmental predictors extracted for sampling sites of **bacteria**. Upper right panels are Pearson correlations with significance levels (* p < 0.05, ** p < 0.01, *** p < 0.001). T = temperature (°C), P = precipitation (mm), TPI = topographic position index, slope (°) and Radiation = potential annual solar radiation (in kWh/m^2/day).*

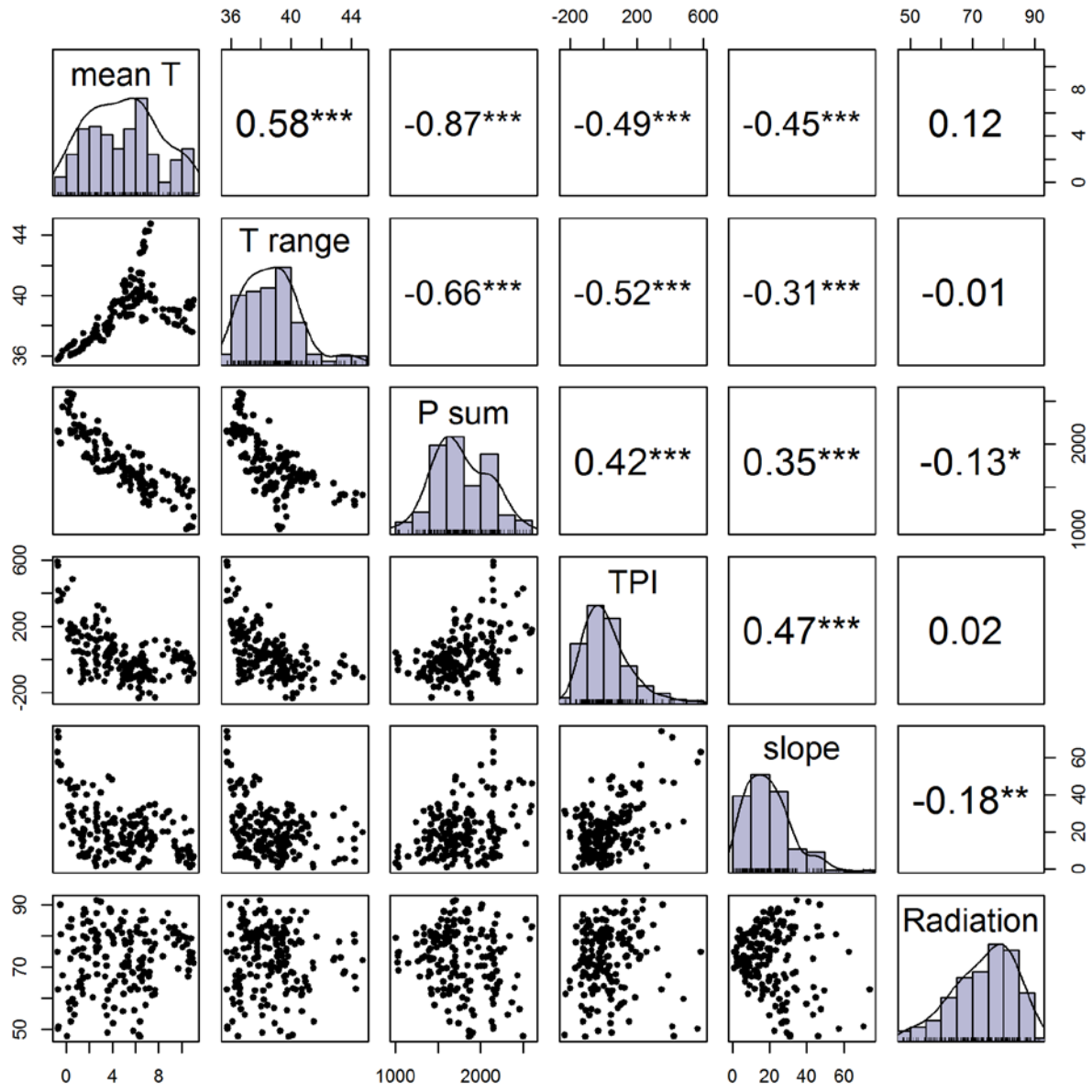

*Figure S20. Distributions and relationships of environmental predictors extracted for sampling sites of **protists**. Upper right panels are Pearson correlations with significance levels (* p < 0.05, ** p < 0.01, *** p < 0.001). T = temperature (°C), P = precipitation (mm), TPI = topographic position index, slope (°) and Radiation = potential annual solar radiation (in kWh/m^2/day).*

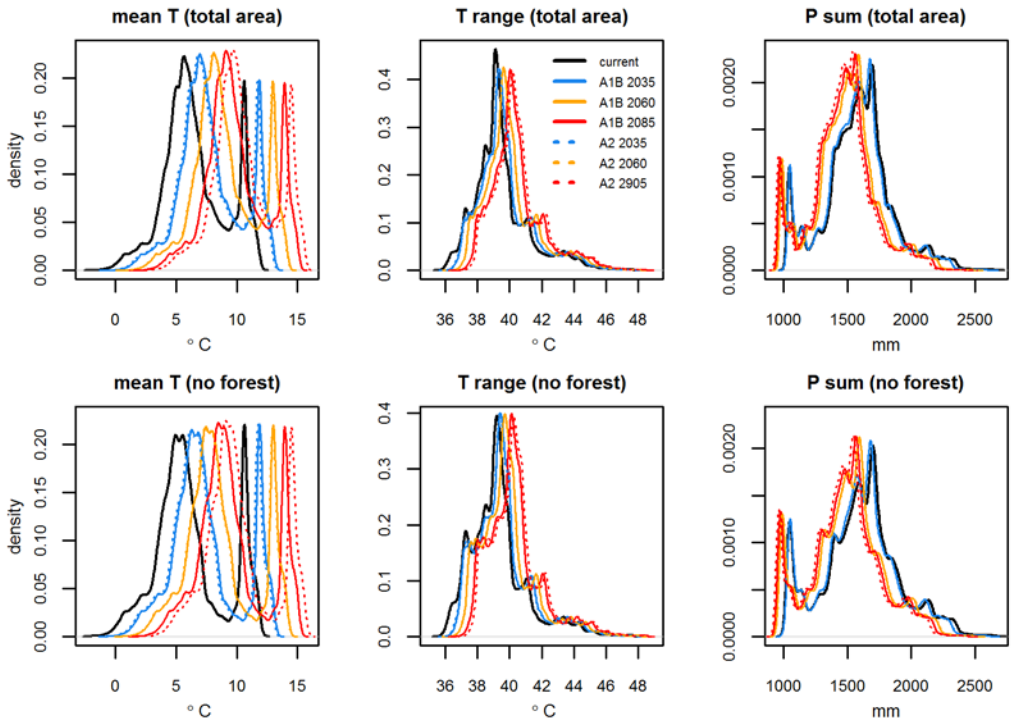

Figure S21. Distribution of climatic conditions in the study area under current climate and future scenarios with and without forested areas. T = temperature, P = precipitation

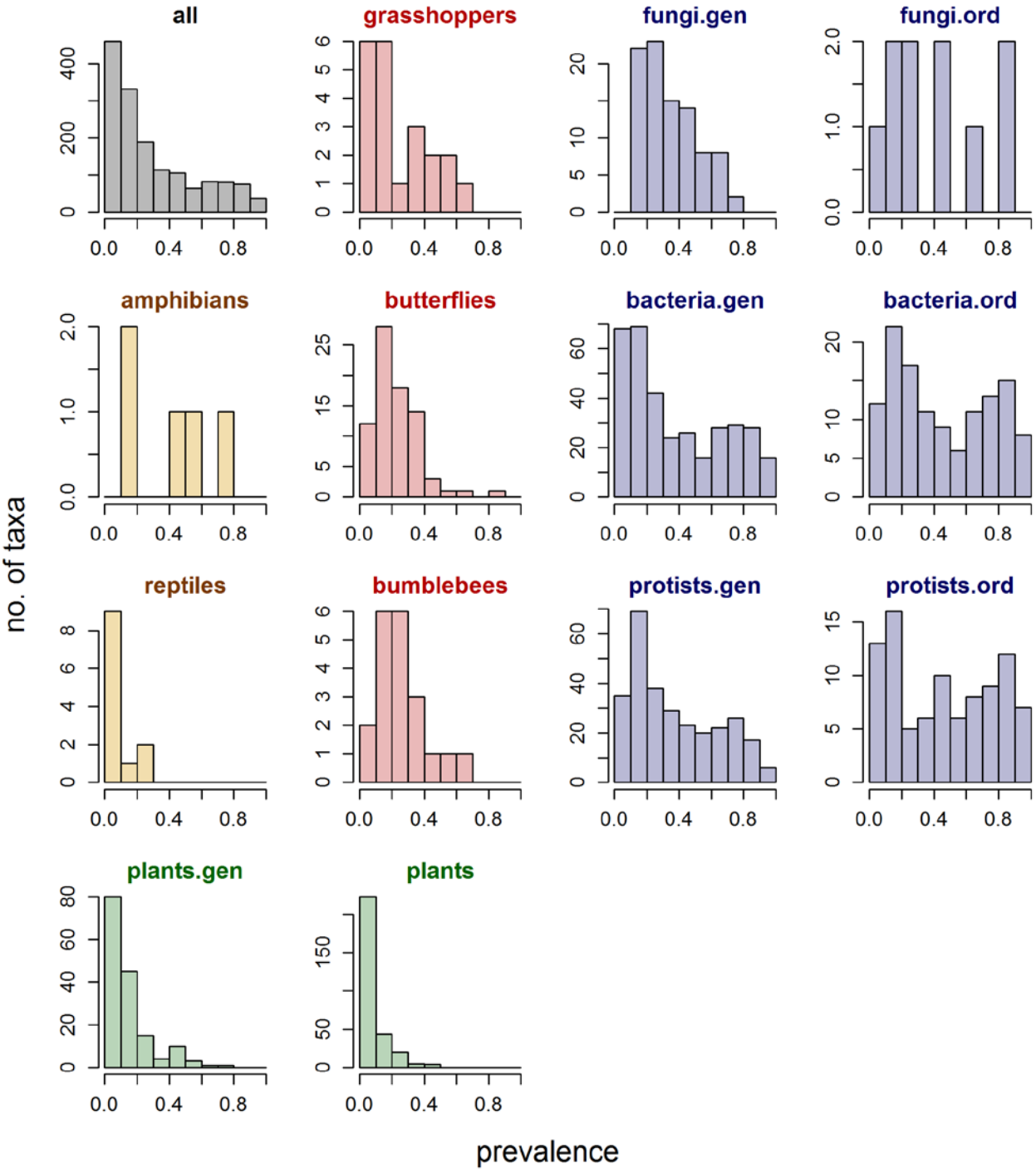

Figure S22. Histograms of prevalence of taxa for all taxa and per taxonomic group.

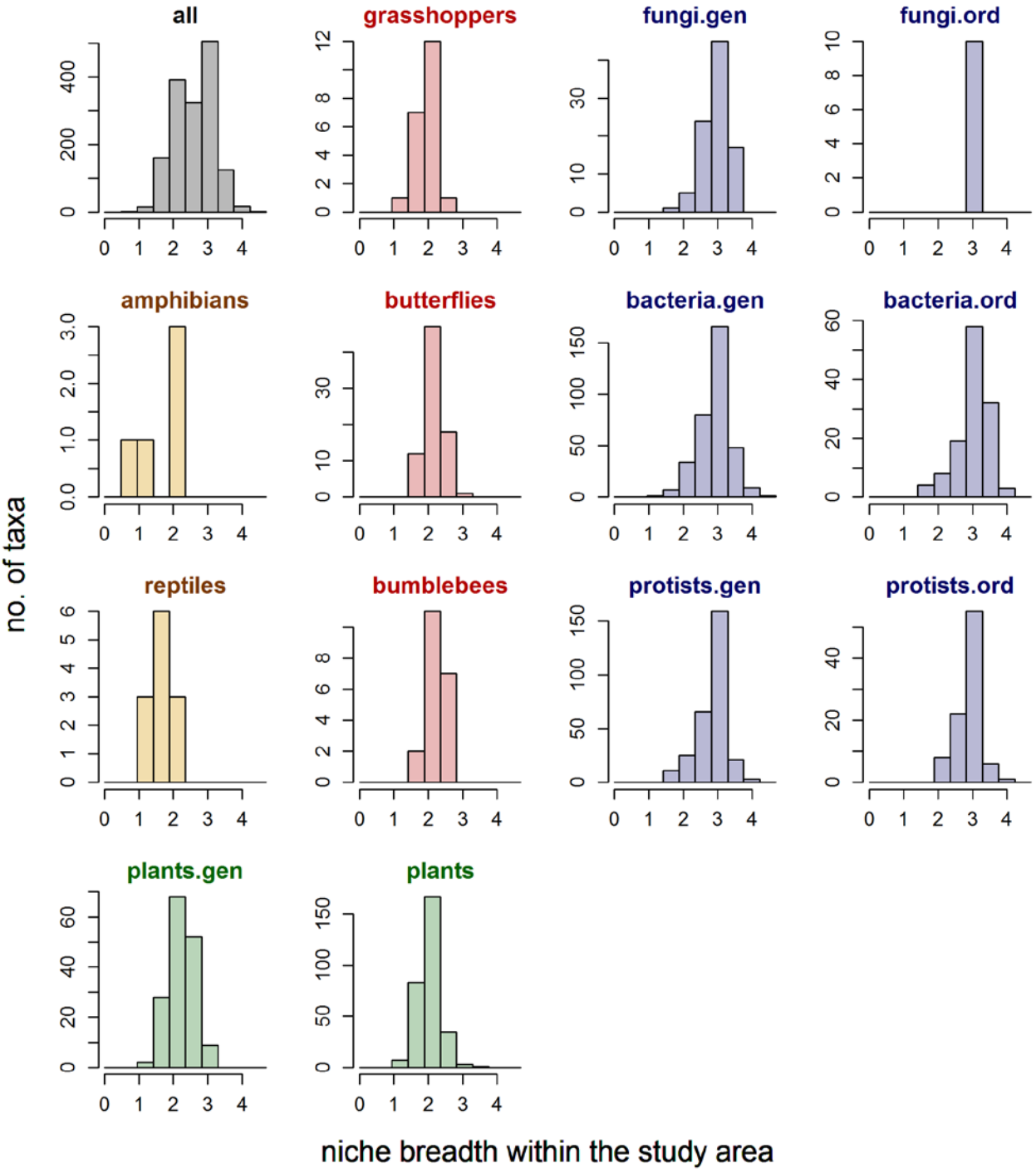

Figure S23. Histograms of niche breadths of taxa within the study area for all taxa and per taxonomic group.

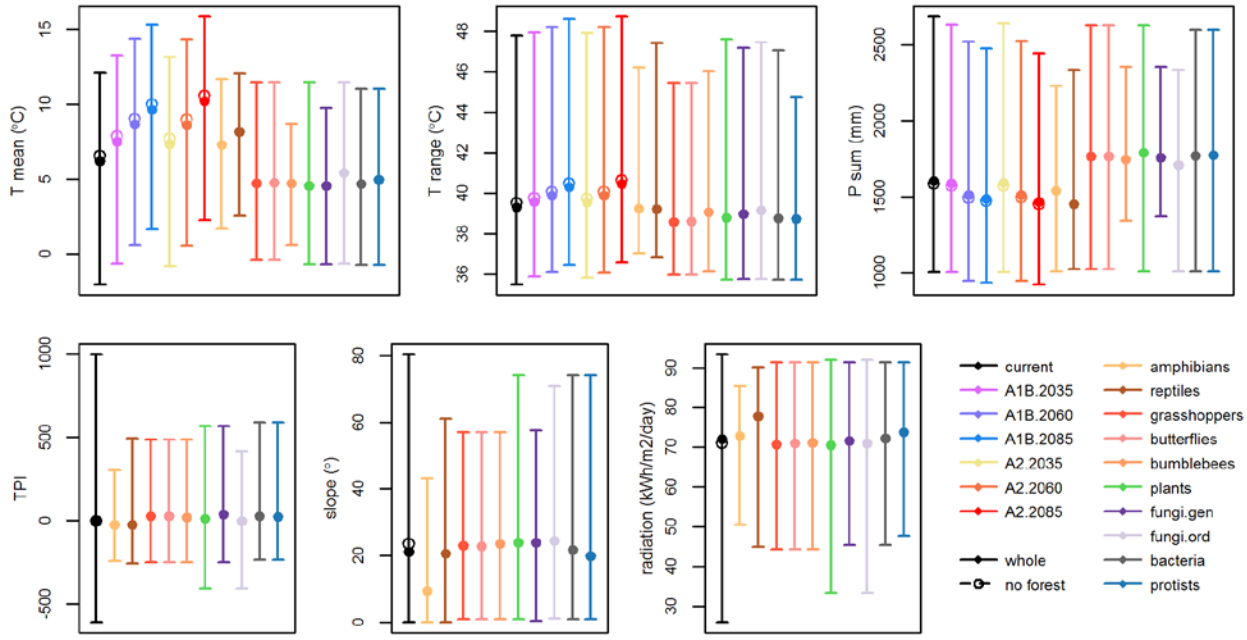

Figure S24. Minimum, mean and maximum values of the environmental predictors in the study area under current conditions (and future scenarios for climatic factors; with and without masking forest) and within the taxon datasets. T = temperature, P = precipitation, TPI = topographic position index

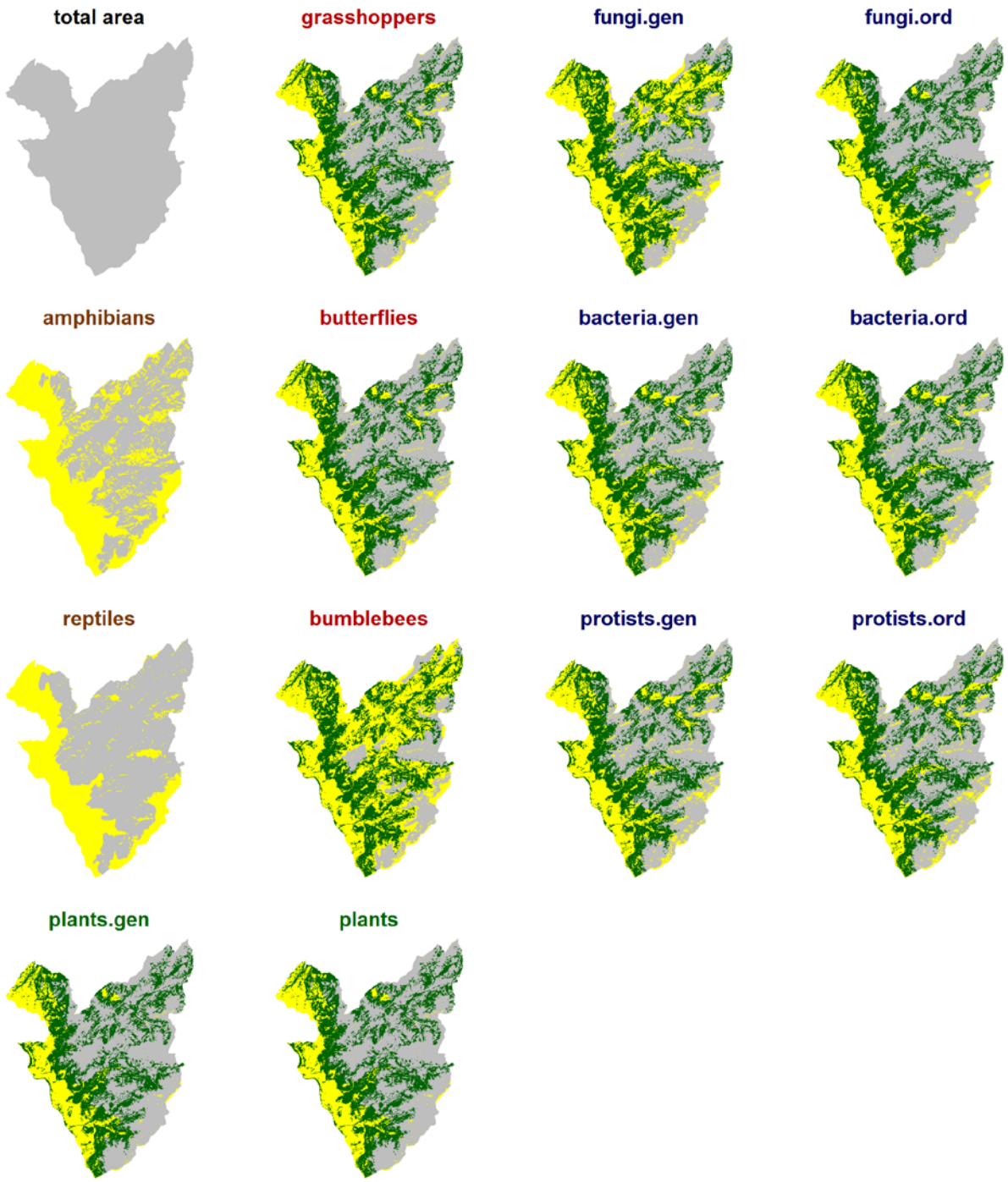

Figure S25. Maps of non-analogous space (in yellow) respective to all environmental predictors and scenarios, and coverage of sampling of taxonomic groups. Forest, masked from the projections of groups sampled in non-forested sites, is shown in green.

REFERENCES:

Chen, W., Simpson, J., & Levesque, C.A. (2016). RAM: R for Amplicon-Sequencing-Based Microbial-Ecology. R package (Version 1.2.1.3). Retrieved from http://cran.r-project.org/package=RAM

DeSantis, T.Z., Hugenholtz, P., Larsen, N., Rojas, M., Brodie, E.L., Keller, K., . . . Andersen, G.L. (2006). Greengenes, a chimera-checked 16S rRNA gene database and workbench compatible with ARB. Applied and Environmental Microbiology, 72(7), 5069-5072. doi:10.1128/AEM.03006-05

Dubuis, A., Pottier, J., Rion, V., Pellissier, L., Theurillat, J.-P., & Guisan, A. (2011). Predicting spatial patterns of plant species richness: a comparison of direct macroecological and species stacking modelling approaches. Diversity and Distributions, 17(6), 1122-1131. doi:10.1111/j.1472-4642.2011.00792.x

Guillou, L., Bachar, D., Audic, S., Bass, D., Berney, C., Bittner, L., . . . Christen, R. (2013). The Protist Ribosomal Reference database (PR(2)): a catalog of unicellular eukaryote Small Sub-Unit rRNA sequences with curated taxonomy. Nucleic Acids Research, 41(Database issue), D597-D604. doi:10.1093/nar/gks1160

Mahe, F., Rognes, T., Quince, C., de Vargas, C., & Dunthorn, M. (2015). Swarm v2: highly-scalable and high-resolution amplicon clustering. PeerJ, 3, e1420. doi:10.7717/peerj.1420

Pagni, M., Niculita-Hirzel, H., Pellissier, L., Dubuis, A., Xenarios, I., Guisan, A., . . . Guex, N. (2013). Density-based hierarchical clustering of pyro-sequences on a large scale--the case of fungal ITS1. Bioinformatics, 29(10), 1268-1274. doi:10.1093/bioinformatics/btt149

Pearson, W.R. (2000). Flexible sequence similarity searching with the FASTA3 program package. Methods in Molecular Biology, 132, 185-219.

Pellissier, L., Niculita-Hirzel, H., Dubuis, A., Pagni, M., Guex, N., Ndiribe, C., . . . Guisan, A. (2014). Soil fungal communities of grasslands are environmentally structured at a regional scale in the Alps. Molecular Ecology, 23(17), 4274-4290. doi:10.1111/mec.12854

Pellissier, L., Pinto-Figueroa, E., Niculita-Hirzel, H., Moora, M., Villard, L., Goudet, J., . . . Guisan, A. (2013a). Plant species distributions along environmental gradients: do belowground interactions with fungi matter? Frontiers in Plant Science, 4, 500. doi:10.3389/fpls.2013.00500

Pellissier, L., Pradervand, J.-N., Pottier, J., Dubuis, A., Maiorano, L., & Guisan, A. (2012). Climate-based empirical models show biased predictions of butterfly communities along environmental gradients. Ecography, 35(8), 684-692. doi:10.1111/j.1600-0587.2011.07047.x

Pellissier, L., Pradervand, J.-N., Williams, P.H., Litsios, G., Cherix, D., Guisan, A., & Baselga, A. (2013b). Phylogenetic relatedness and proboscis length contribute to structuring bumblebee communities in the extremes of abiotic and biotic gradients. Global Ecology and Biogeography, 22(5), 577-585. doi:10.1111/geb.12026

Pinto-Figueraoa, E.A. (2016). *FUNGAL BIOGEOGRAPHY IN THE WESTERN SWISS ALPS: Linking high-throughput sequencing and spatial ecology to characterize the diversity, distribution patterns and environmental niche of soil fungi along environmental gradients.* (PhD), University of Lausanne, Lausanne.

Pinto-Figueroa, E.A., Seddon, E., Yashiro, E., Buri, A., Niculita-Hirzel, H., van der Meer, J.R., & Guisan, A. (2019). Archaeorhizomycetes Spatial Distribution in Soils Along Wide Elevational and Environmental Gradients Reveal Co-abundance Patterns With Other Fungal Saprobes and Potential Weathering Capacities. Front Microbiol, 10(656), 656. doi:10.3389/fmicb.2019.00656

Pittet, M. (2017). *Impact of global warming on the distribution and dispersal of reptiles in the Western Swiss Alps.* (Master of Science), Université de Lausanne, Lausanne.

Pradervand, J.-N., Dubuis, A., Reymod, A., Sonnay, V., Gelin, A., & Guisan, A. (2013). Quel facteurs influencent la richesse en orthoptères des Préalpes vaudoises? Bulletin de la Societe Vaudoise des Sciences Naturelles, 93(4), 155-173.

Schmidt, B.R., & Zumbach, S. (2019). Amphibian conservation in Switzerland. In H. Heatwole & J.W. Wilkinson (Eds.), *Status of Conservation and Decline of Amphibians: Eastern Hemisphere* (Vol. 5, pp. 46-51). Exeter: Pelagic Publishing.

Seppey, C.V.W., Broennimann, O., Buri, A., Yashiro, E., Pinto-Figueroa, E., Singer, D., . . . Lara, E. (2019). Soil protist diversity in the Swiss western Alps is better predicted by topo-climatic than by edaphic variables. Journal of Biogeography, 571760. doi:10.1111/jbi.13755

Yashiro, E., Pinto-Figueroa, E., Buri, A., Spangenberg, J.E., Adatte, T., Niculita-Hirzel, H., . . . van der Meer, J.R. (2016). Local Environmental Factors Drive Divergent Grassland Soil Bacterial Communities in the Western Swiss Alps. Applied and Environmental Microbiology, 82(21), 6303-6316. doi:10.1128/AEM.01170-16

Yashiro, E., Pinto-Figueroa, E., Buri, A., Spangenberg, J.E., Adatte, T., Niculita-Hirzel, H., . . . van der Meer, J.R. (2018). Meta-scale mountain grassland observatories uncover commonalities as well as specific interactions among plant and non-rhizosphere soil bacterial communities. Scientific Reports, 8(1), 5758. doi:10.1038/s41598-018-24253-x

Zimmermann, N.E., & Kienast, F. (1999). Predictive mapping of alpine grasslands in Switzerland: Species versus community approach. Journal of Vegetation Science, 10(4), 469-482. doi:10.2307/3237182

Zubler, E.M., Fischer, A.M., Liniger, M.A., Croci-Maspoli, M., Scherrer, S.C., & Appenzeller, C. (2014). Localized climate change scenarios of mean temperature and precipitation over Switzerland. Climatic Change, 125(2), 237-252. doi:10.1007/s10584-014-1144-x

Supplementary material for *Greater climate control of above- versus belowground communities* by Mod et al.

Appendix 2: Additional results

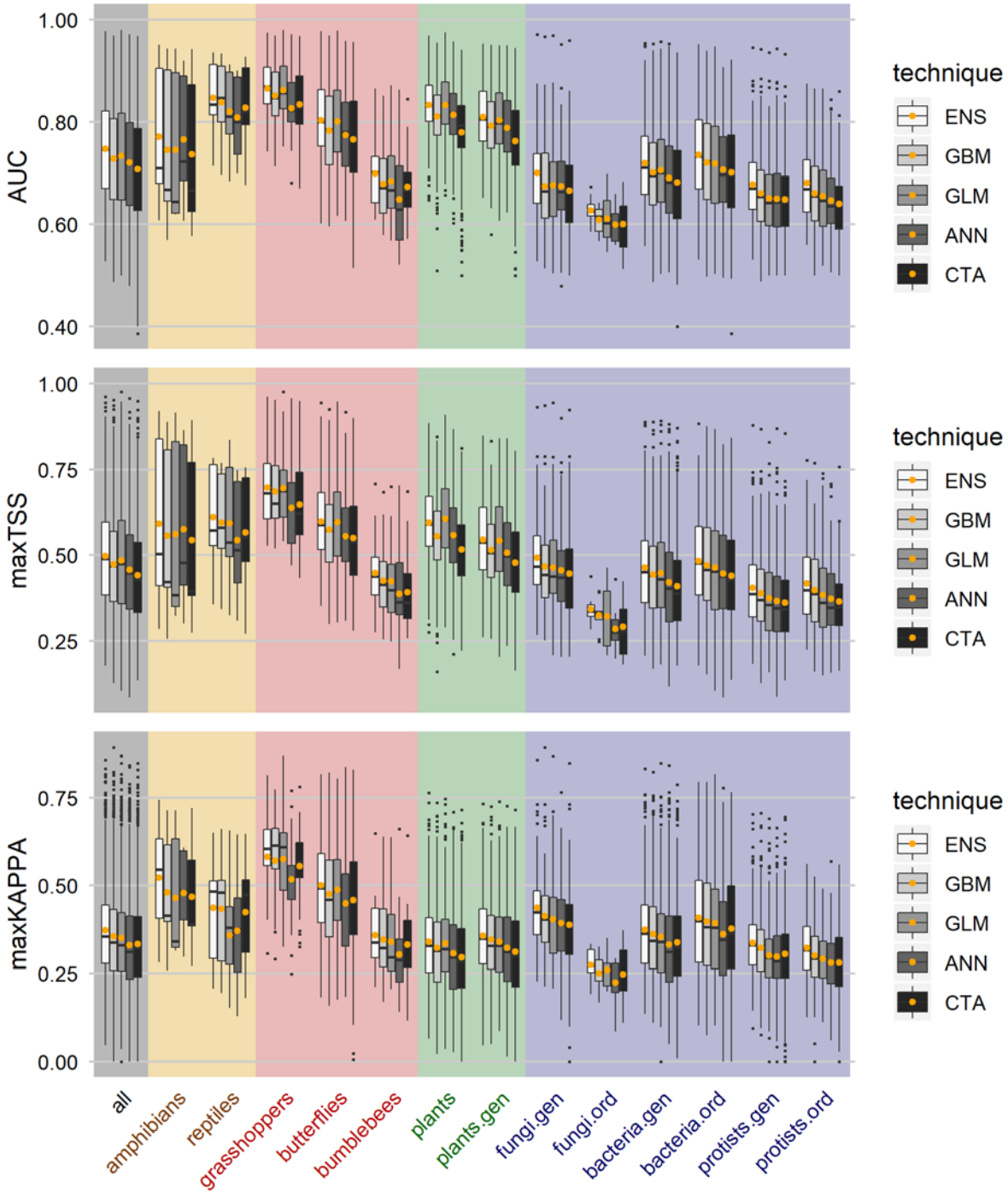

Figure S26. Model evaluation scores per taxon and technique (ENS=ensemble of the four techniques, GBM=generalized boosting method, GLM=generalized linear model, ANN=artificial neural network and CTA=classification tree analyses) as measured by AUC, maxTSS and maxKAPPA. Boxes in boxplots span the 25th to 75th quartile, with median (black bar) and mean (orange point) in the middle. Whiskers span the lowest and highest scores, yet in maximum to 1.5(75th-25th quartile); outlier scores are indicated by black points.*

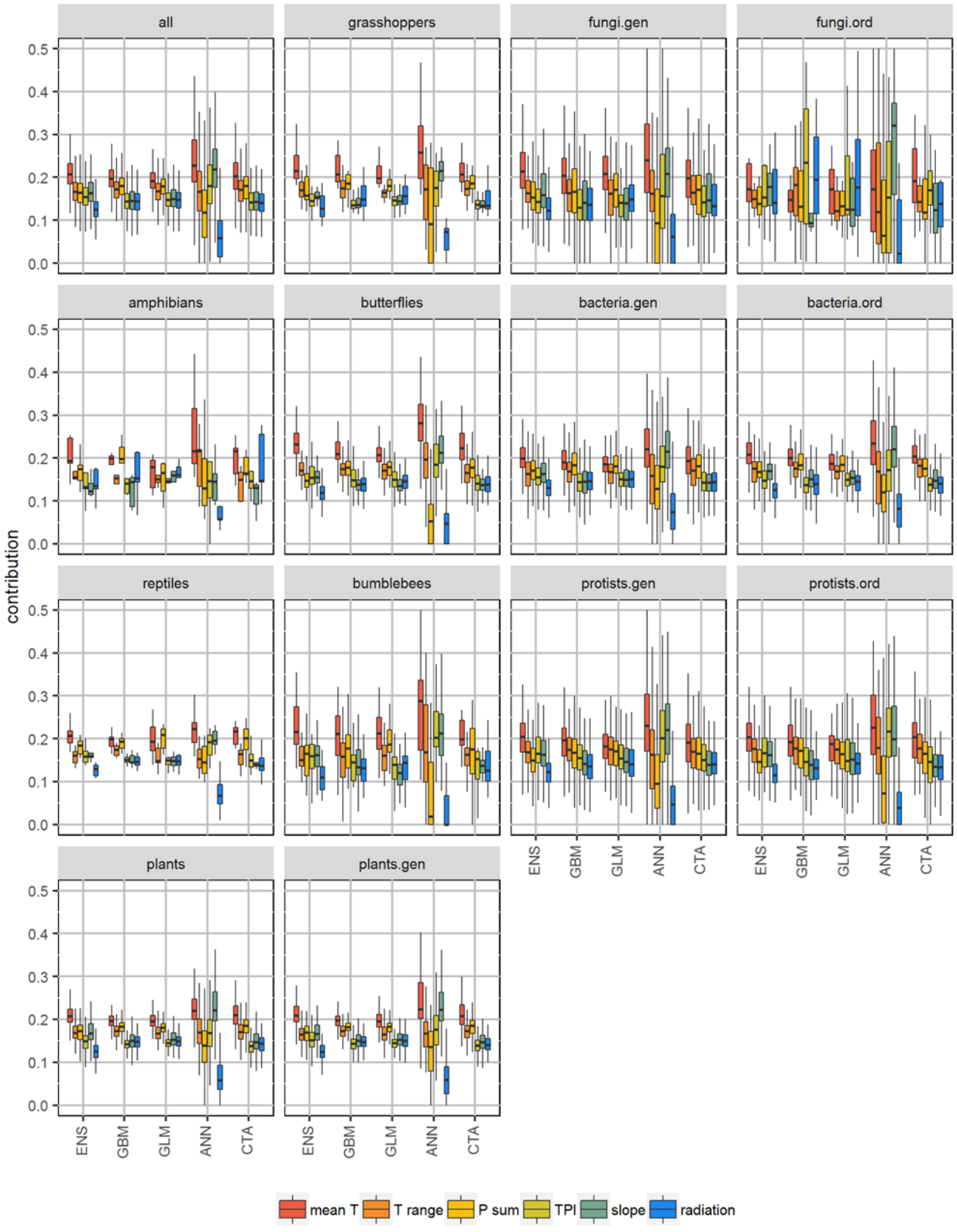

Figure S27. Boxplots of relative variable contributions per taxon and technique. Boxes span from 25th to 75th quartile, with median in the middle. Whiskers span to the lowest and highest scores, yet in maximum to 1.5(75th-25th quartile); outlier scores are indicated by points.*

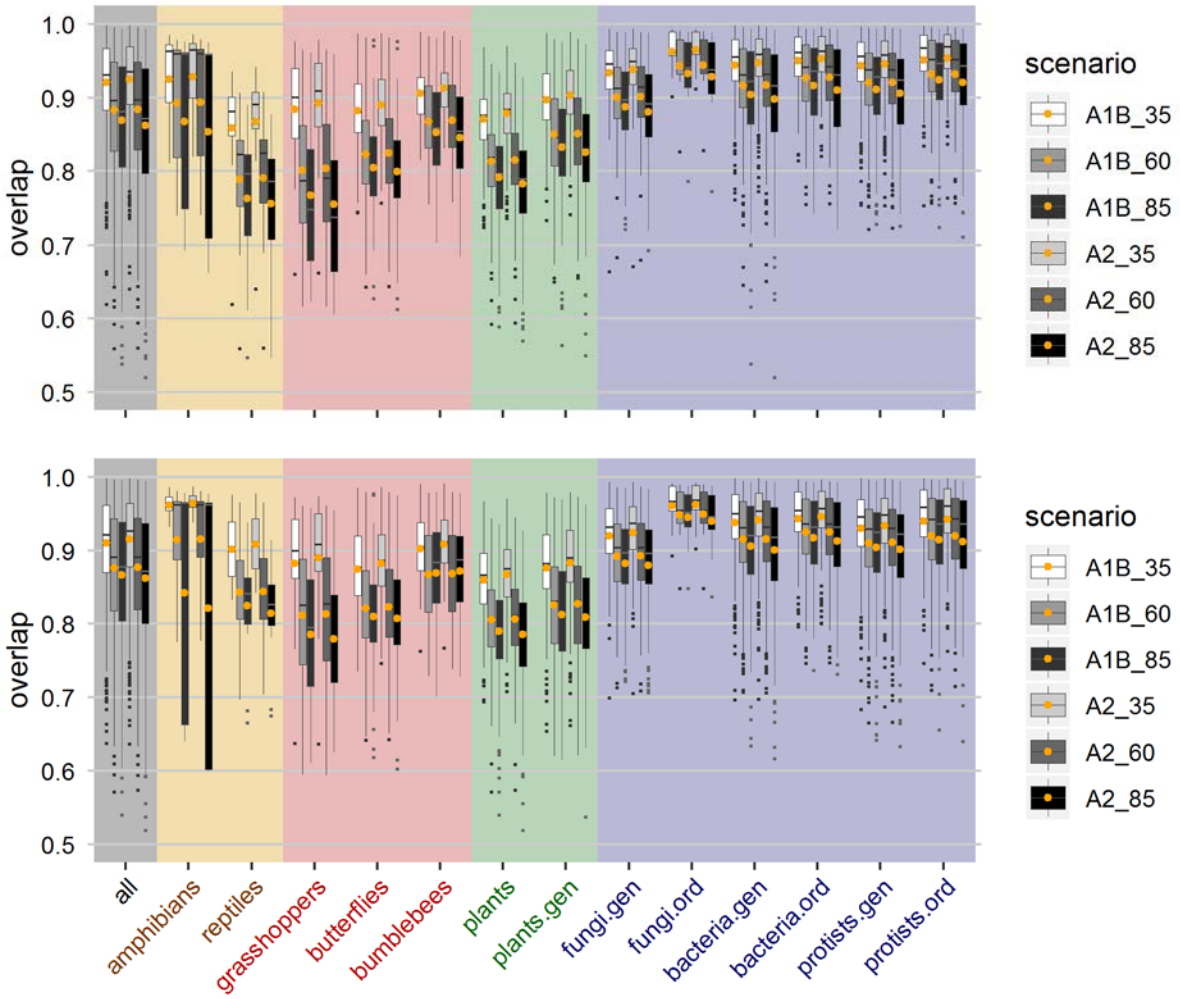

Figure S28. Overlap of habitat suitability between current and future projections within the whole study area (top) and environmentally analogous study area (bottom). Boxes in boxplots span the 25th to 75th quartile, with median (black bar) and mean (orange point) in the middle. Whiskers span the lowest and highest scores, yet in maximum to 1.5(75th-25th quartile); outlier scores are indicated by black points.*

*Table S1. Spearman correlations (with significance levels as * p < 0.05, ** p < 0.01, *** p < 0.001) between niche overlap and prevalence of taxa.*

	A1B 2035	A1B 2060	A1B 2085	A2 2035	A2 2060	A2 2085
all	0.81***	0.81***	0.81***	0.81***	0.81***	0.8***
amphibians	0.6	0.6	0.6	0.6	0.6	0.6
reptiles	0.42	0.14	0.14	0.43	0.24	0.15
grasshoppers	0.73***	0.84***	0.88***	0.72***	0.83***	0.88***
butterflies	0.39***	0.3**	0.28*	0.42***	0.3**	0.28*
bumblebees	0.75***	0.73***	0.69***	0.78***	0.72***	0.7***
plants	0.46***	0.34***	0.32***	0.49***	0.34***	0.31***
plants.gen	0.65***	0.57***	0.54***	0.67***	0.58***	0.52***
fungi.gen	0.52***	0.59***	0.6***	0.52***	0.59***	0.61***
fungi.ord	0.75*	0.89**	0.89**	0.67*	0.89**	0.89**
bacteria.gen	0.83***	0.85***	0.85***	0.83***	0.85***	0.84***
bacteria.ord	0.86***	0.86***	0.86***	0.86***	0.86***	0.86***
protists.gen	0.77***	0.78***	0.79***	0.77***	0.78***	0.79***
protists.ord	0.81***	0.85***	0.85***	0.81***	0.85***	0.86***

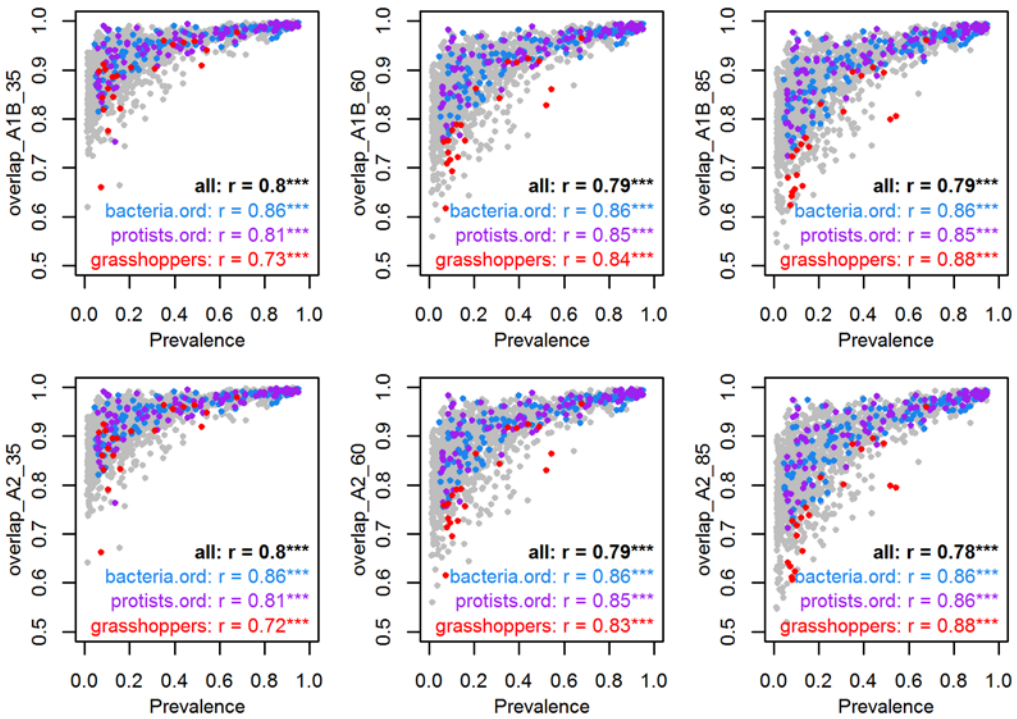

Figure S29. Relationship between overlap in habitat suitability and prevalence of taxa. The groups with the strongest and most significant Spearman correlations (p < 0.05, ** p < 0.01, *** p < 0.001) are shown in addition to all taxa.*

*Table S2. Spearman correlations (with significance levels as * p < 0.05, ** p < 0.01, *** p < 0.001) between overlap in habitat suitability and niche breadth of taxa.*

	A1B 2035	A1B 2060	A1B 2085	A2 2035	A2 2060	A2 2085
all	**0.66*** **	**0.67*** **	**0.68*** **	**0.66*** **	**0.67*** **	**0.67*** **
amphibians	0.8	0.8	0.8	0.8	0.8	0.8
reptiles	**0.59***	0.49	0.49	**0.61***	**0.63***	0.52
grasshoppers	**0.64****	**0.75*** **	**0.76*** **	**0.65****	**0.72*** **	**0.75*** **
butterflies	**0.34****	**0.32****	**0.31****	**0.34****	**0.32****	**0.31****
bumblebees	0.36	0.37	0.34	0.33	0.37	0.38
plants	**0.48*** **	**0.51*** **	**0.56*** **	**0.48*** **	**0.51*** **	**0.58*** **
plants.gen	**0.69*** **	**0.69*** **	**0.7*** **	**0.68*** **	**0.69*** **	**0.69*** **
fungi.gen	**0.27****	0.2	0.18	**0.28****	0.2	0.17
fungi.ord	-0.19	-0.39	-0.39	-0.13	-0.39	-0.39
bacteria.gen	**0.34*** **	**0.34*** **	**0.36*** **	**0.34*** **	**0.34*** **	**0.37*** **
bacteria.ord	0.1	0.13	0.15	0.1	0.13	0.16
protists.gen	**0.39*** **	**0.42*** **	**0.43*** **	**0.38*** **	**0.42*** **	**0.42*** **
protists.ord	**0.38****	**0.38*** **	**0.36*** **	**0.38*** **	**0.38*** **	**0.38*** **

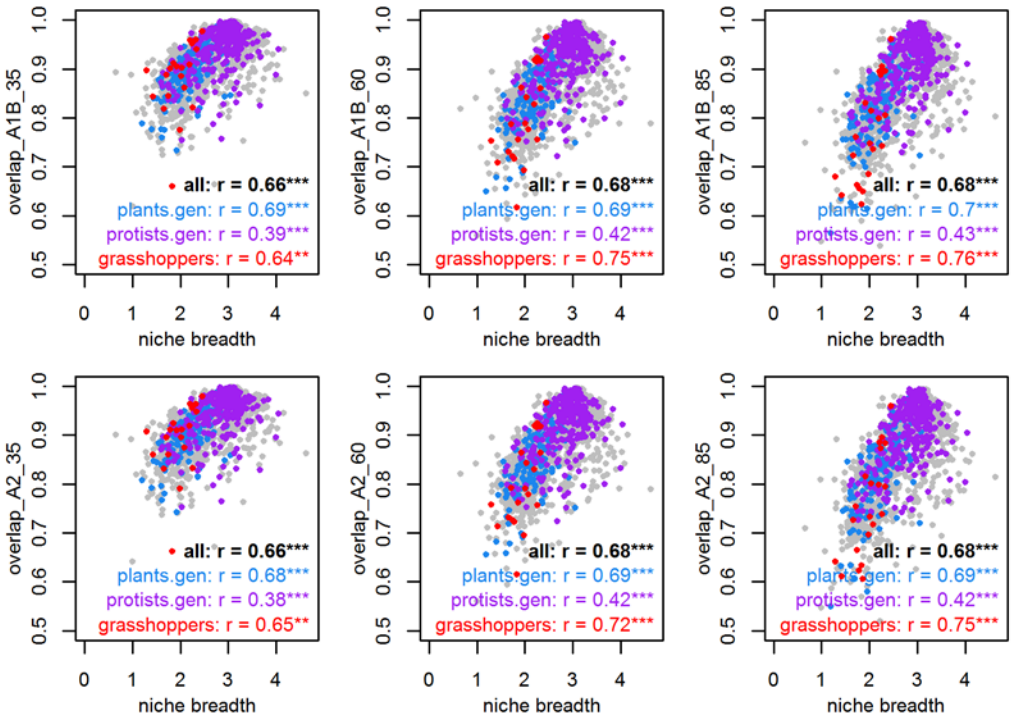

Figure S30. Relationship between overlap in habitat suitability and niche breadth of taxa. The groups with the strongest and most significant Spearman correlations (p < 0.05, ** p < 0.01, *** p < 0.001) are shown in addition to all taxa.*

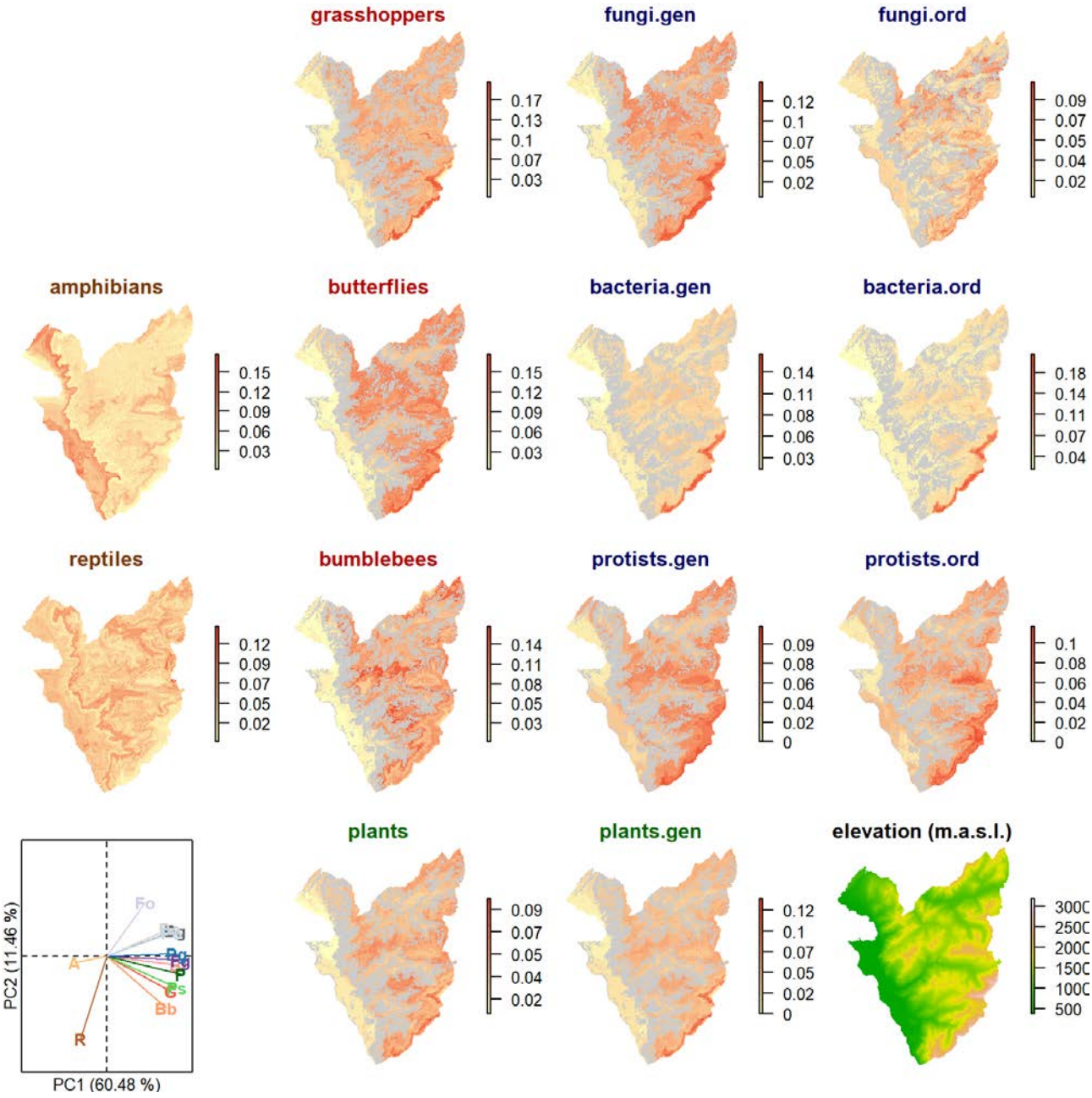

*Figure S31. Spatial variation in the magnitude of the predicted future changes in community structure between current conditions and future scenario **A1b for year 2035**. The maximum possible magnitude is 1, meaning that PPOs of all taxa are predicted to change from 1 to 0 or from 0 to 1, and the minimum possible magnitude is 0, meaning that PPOs of none of the taxa are predicted to change between current and future prediction. Grey areas mark the forest cover masked from the predictions of taxa which sampling targeted non-forested sites. The panel in bottom left, shows the (dis)similarity in the spatial variations among the taxonomic groups (based on a PCA of the maps), i.e. groups with lines pointing to the same direction have similar spatial patterns in the magnitude of community changes in non-forested areas, whereas lines of varying directions indicate varying patterns. The panel in bottom right, shows elevation of the study area. A = amphibians, R = reptiles, G = grasshoppers, Bf = butterflies, Bb = bumblebees, Ps = plant species, P = plant genera, Fg = fungus genera, Fo = fungus orders, Bg = bacteria genera, Bo = bacteria orders, Pg = protist genera, Po = protist orders. For relationship against elevation, and for comparison to analogous environmental space, see Figure S37.*

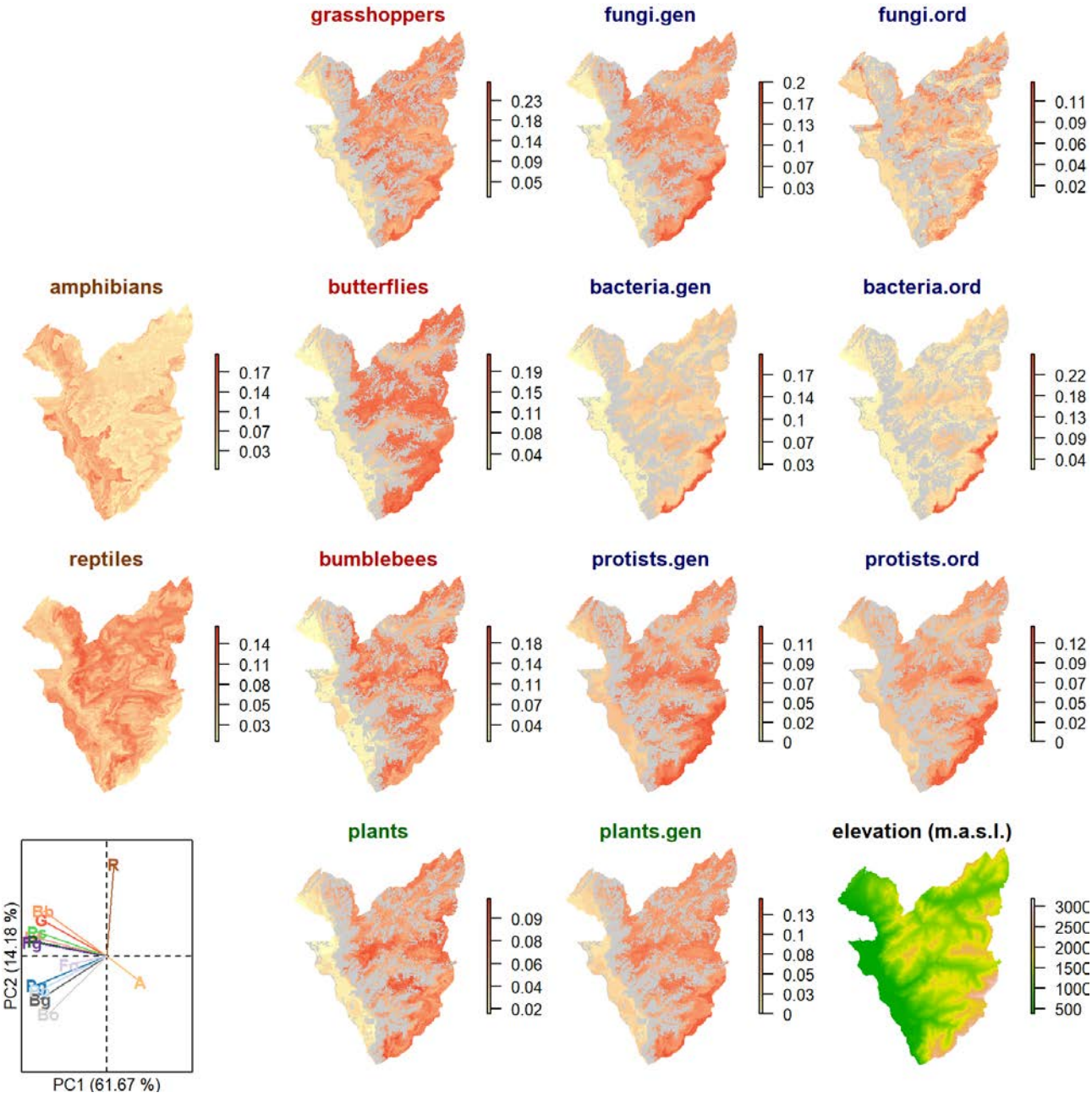

*Figure S32. Spatial variation in the magnitude of the predicted future changes in community structure between current conditions and future scenario **A1b for year 2060**. The maximum possible magnitude is 1, meaning that PPOs of all taxa are predicted to change from 1 to 0 or from 0 to 1, and the minimum possible magnitude is 0, meaning that PPOs of none of the taxa are predicted to change between current and future prediction. Grey areas mark the forest cover masked from the predictions of taxa which sampling targeted non-forested sites. The panel in bottom left, shows the (dis)similarity in the spatial variations among the taxonomic groups (based on a PCA of the maps), i.e. groups with lines pointing to the same direction have similar spatial patterns in the magnitude of community changes in non-forested areas, whereas lines of varying directions indicate varying patterns. The panel in bottom right, shows elevation of the study area.. A = amphibians, R = reptiles, G = grasshoppers, Bf = butterflies, Bb = bumblebees, Ps = plant species, P = plant genera, Fg = fungus genera, Fo = fungus orders, Bg = bacteria genera, Bo = bacteria orders, Pg = protist genera, Po = protist orders. For relationship against elevation, and for comparison to analogous environmental space, see Figure S38.*

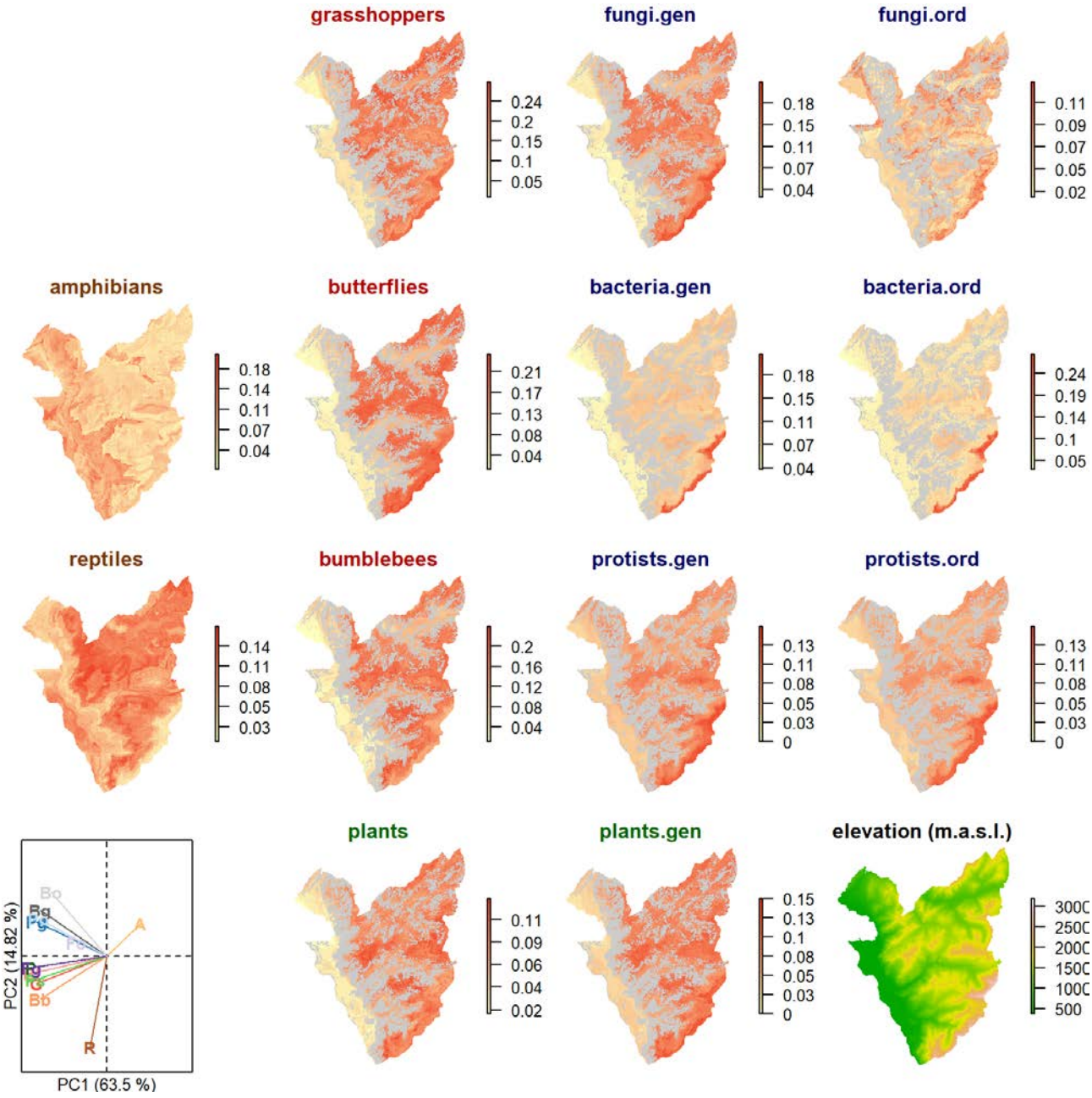

*Figure S33. Spatial variation in the magnitude of the predicted future changes in community structure between current conditions and future scenario **A1b for year 2085**. The maximum possible magnitude is 1, meaning that PPOs of all taxa are predicted to change from 1 to 0 or from 0 to 1, and the minimum possible magnitude is 0, meaning that PPOs of none of the taxa are predicted to change between current and future prediction. Grey areas mark the forest cover masked from the predictions of taxa which sampling targeted non-forested sites. The panel in bottom left, shows the (dis)similarity in the spatial variations among the taxonomic groups (based on a PCA of the maps), i.e. groups with lines pointing to the same direction have similar spatial patterns in the magnitude of community changes in non-forested areas, whereas lines of varying directions indicate varying patterns. The panel in bottom right, shows elevation of the study area. A = amphibians, R = reptiles, G = grasshoppers, Bf = butterflies, Bb = bumblebees, Ps = plant species, P = plant genera, Fg = fungus genera, Fo = fungus orders, Bg = bacteria genera, Bo = bacteria orders, Pg = protist genera, Po = protist orders. For relationship against elevation, and for comparison to analogous environmental space, see Figure S39.*

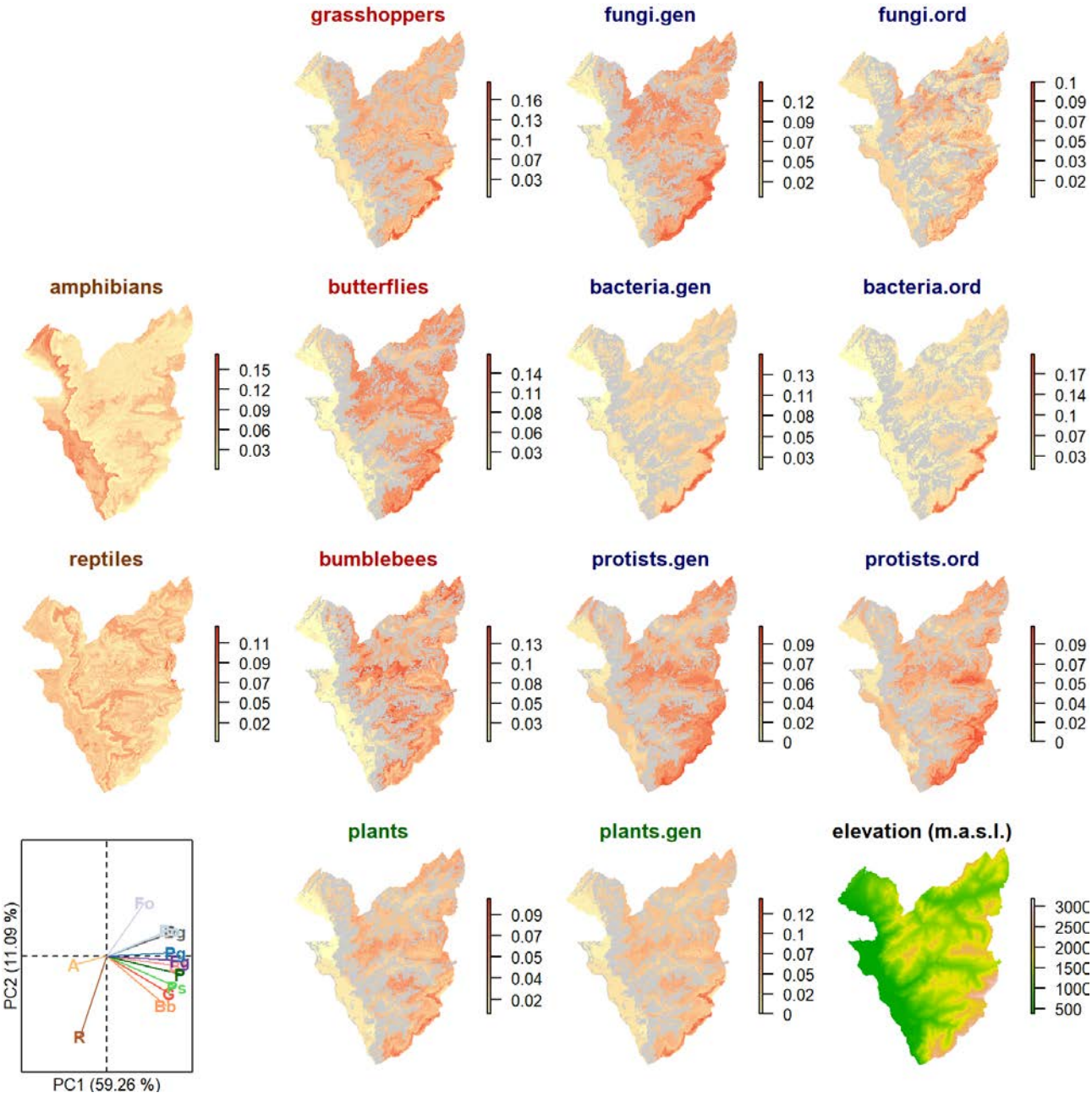

*Figure S34. Spatial variation in the magnitude of the predicted future changes in community structure between current conditions and future scenario **A2 for year 2035**. The maximum possible magnitude is 1, meaning that PPOs of all taxa are predicted to change from 1 to 0 or from 0 to 1, and the minimum possible magnitude is 0, meaning that PPOs of none of the taxa are predicted to change between current and future prediction. Grey areas mark the forest cover masked from the predictions of taxa which sampling targeted non-forested sites. The panel in bottom left, shows the (dis)similarity in the spatial variations among the taxonomic groups (based on a PCA of the maps), i.e. groups with lines pointing to the same direction have similar spatial patterns in the magnitude of community changes in non-forested areas, whereas lines of varying directions indicate varying patterns. The panel in bottom right, shows elevation of the study area. A = amphibians, R = reptiles, G = grasshoppers, Bf = butterflies, Bb = bumblebees, Ps = plant species, P = plant genera, Fg = fungus genera, Fo = fungus orders, Bg = bacteria genera, Bo = bacteria orders, Pg = protist genera, Po = protist orders. For relationship against elevation, and for comparison to analogous environmental space, see Figure S40.*

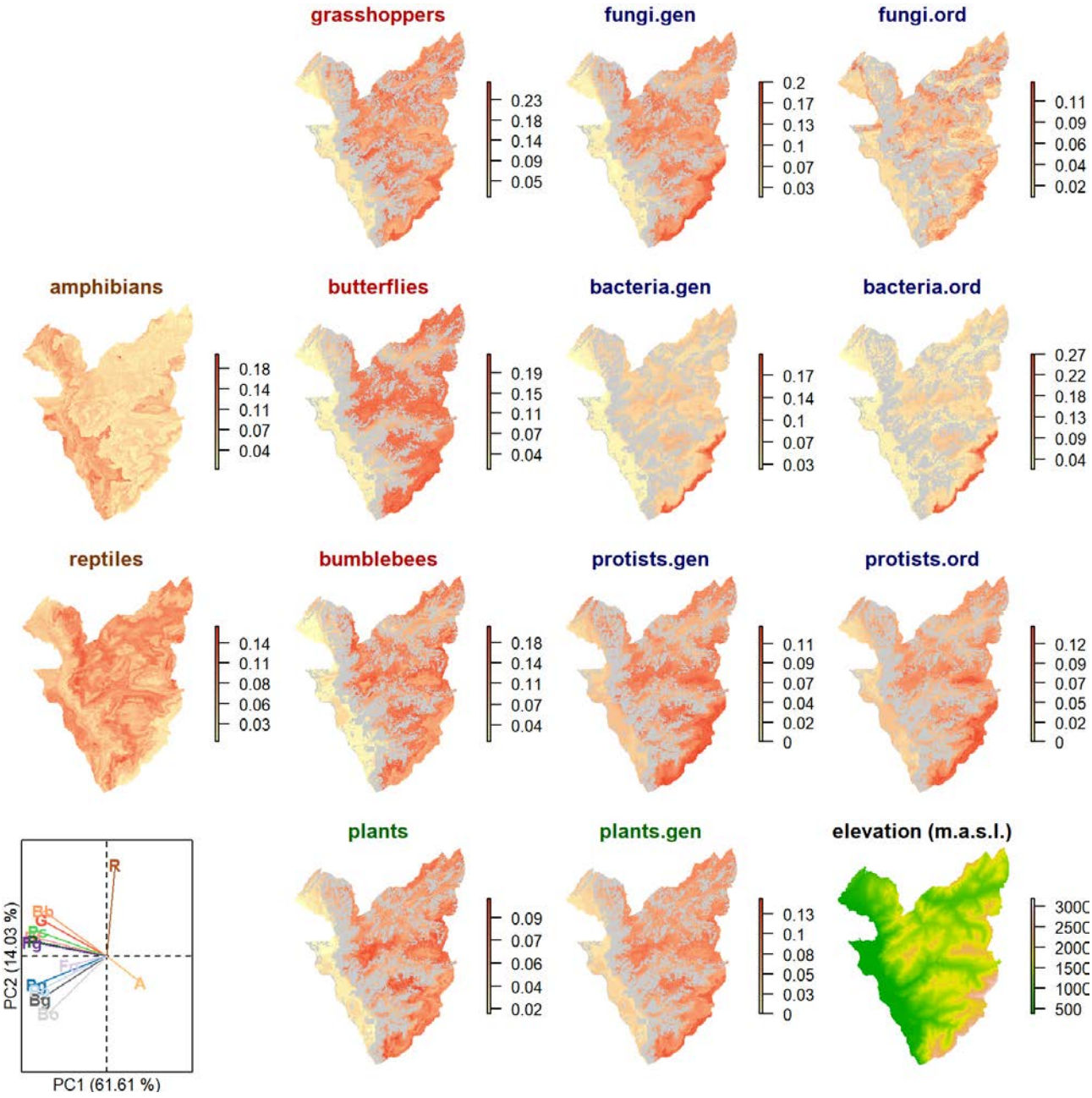

*Figure S35. Spatial variation in the magnitude of the predicted future changes in community structure between current conditions and future scenario **A2 for year 2060**. The maximum possible magnitude is 1, meaning that PPOs of all taxa are predicted to change from 1 to 0 or from 0 to 1, and the minimum possible magnitude is 0, meaning that PPOs of none of the taxa are predicted to change between current and future prediction. Grey areas mark the forest cover masked from the predictions of taxa which sampling targeted non-forested sites. The panel in bottom left, shows the (dis)similarity in the spatial variations among the taxonomic groups (based on a PCA of the maps), i.e. groups with lines pointing to the same direction have similar spatial patterns in the magnitude of community changes in non-forested areas, whereas lines of varying directions indicate varying patterns. The panel in bottom right, shows elevation of the study area. A = amphibians, R = reptiles, G = grasshoppers, Bf = butterflies, Bb = bumblebees, Ps = plant species, P = plant genera, Fg = fungus genera, Fo = fungus orders, Bg = bacteria genera, Bo = bacteria orders, Pg = protist genera, Po = protist orders. For relationship against elevation, and for comparison to analogous environmental space, see Figure S41.*

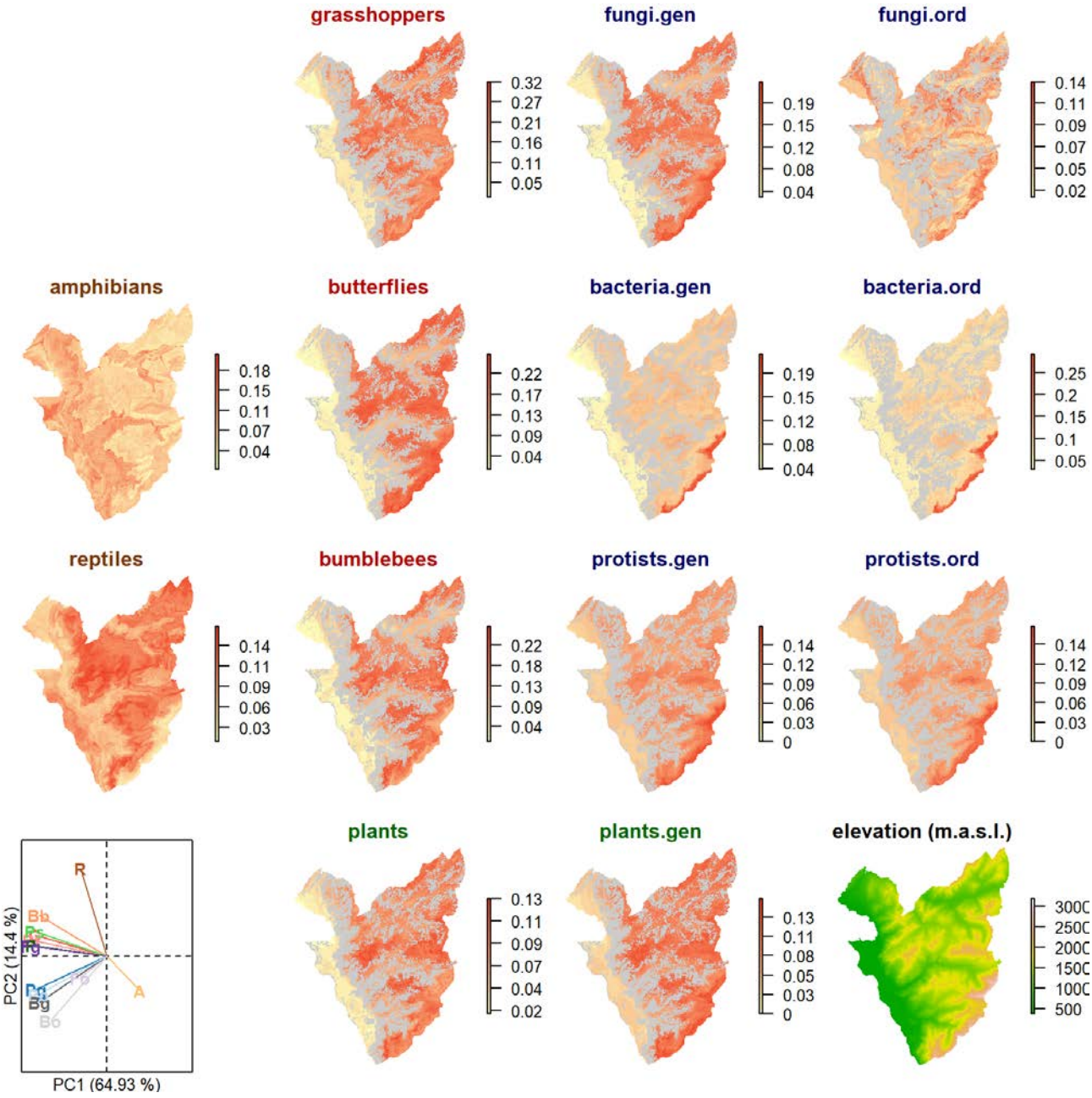

*Figure S36. Spatial variation in the magnitude of the predicted future changes in community structure between current conditions and future scenario **A2 for year 2085**. The maximum possible magnitude is 1, meaning that PPOs of all taxa are predicted to change from 1 to 0 or from 0 to 1, and the minimum possible magnitude is 0, meaning that PPOs of none of the taxa are predicted to change between current and future prediction. Grey areas mark the forest cover masked from the predictions of taxa which sampling targeted non-forested sites. The panel in bottom left, shows the (dis)similarity in the spatial variations among the taxonomic groups (based on a PCA of the maps), i.e. groups with lines pointing to the same direction have similar spatial patterns in the magnitude of community changes in non-forested areas, whereas lines of varying directions indicate varying patterns. The panel in bottom right, shows elevation of the study area. A = amphibians, R = reptiles, G = grasshoppers, Bf = butterflies, Bb = bumblebees, Ps = plant species, P = plant genera, Fg = fungus genera, Fo = fungus orders, Bg = bacteria genera, Bo = bacteria orders, Pg = protist genera, Po = protist orders. For relationship against elevation, and for comparison to analogous environmental space, see Figure S42.*

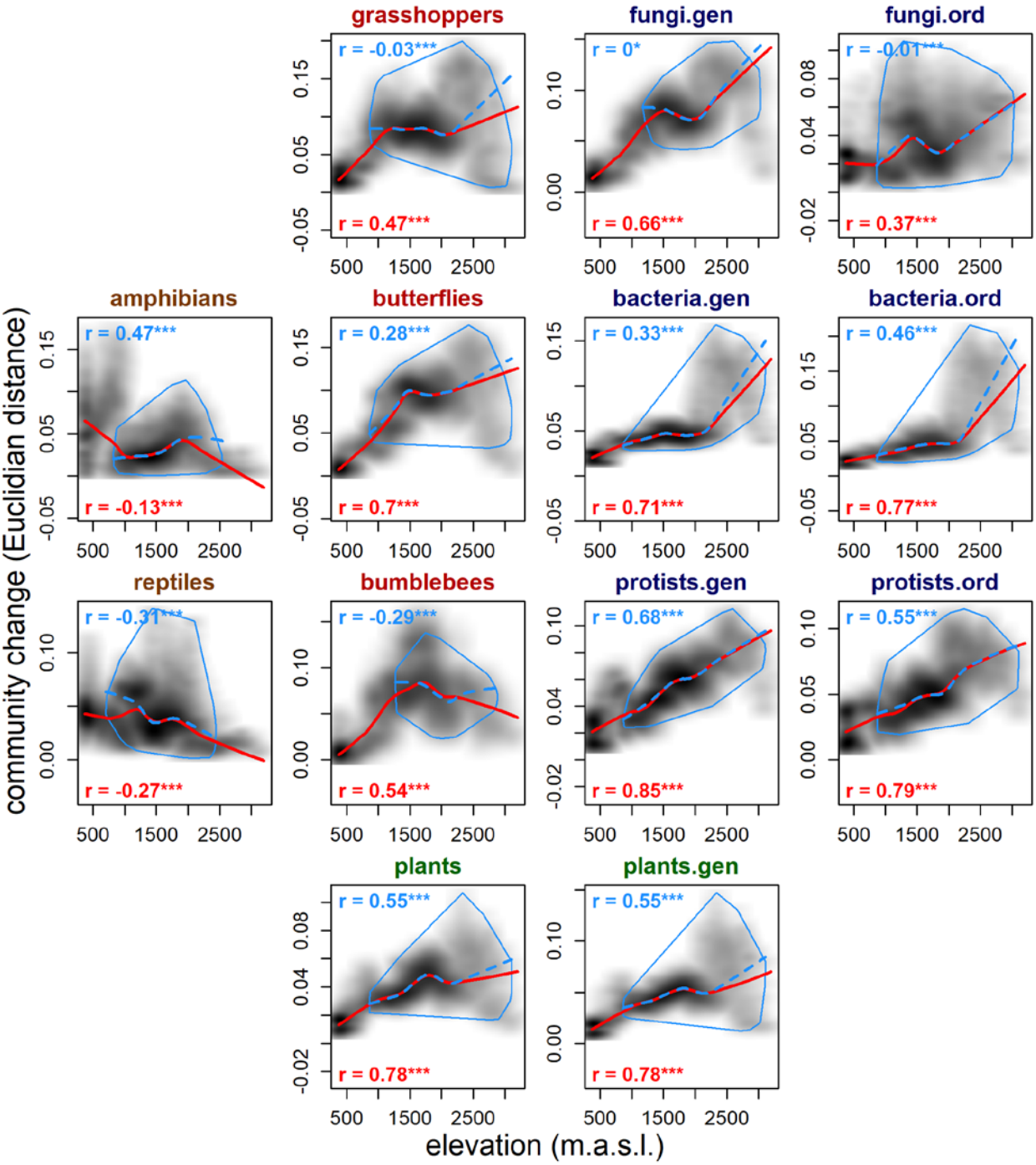

*Figure S37. Relationships between elevation and magnitude of community change between current conditions and future scenario **A1B for year 2035**. From the scatter plot in grey (for the total study area), the pixels within the environmentally analogous area are bordered by the blue polygon. The relationships (as LOWESS) and Spearman correlation are indicated in red for the total study area and in blue for environmentally analogous area.*

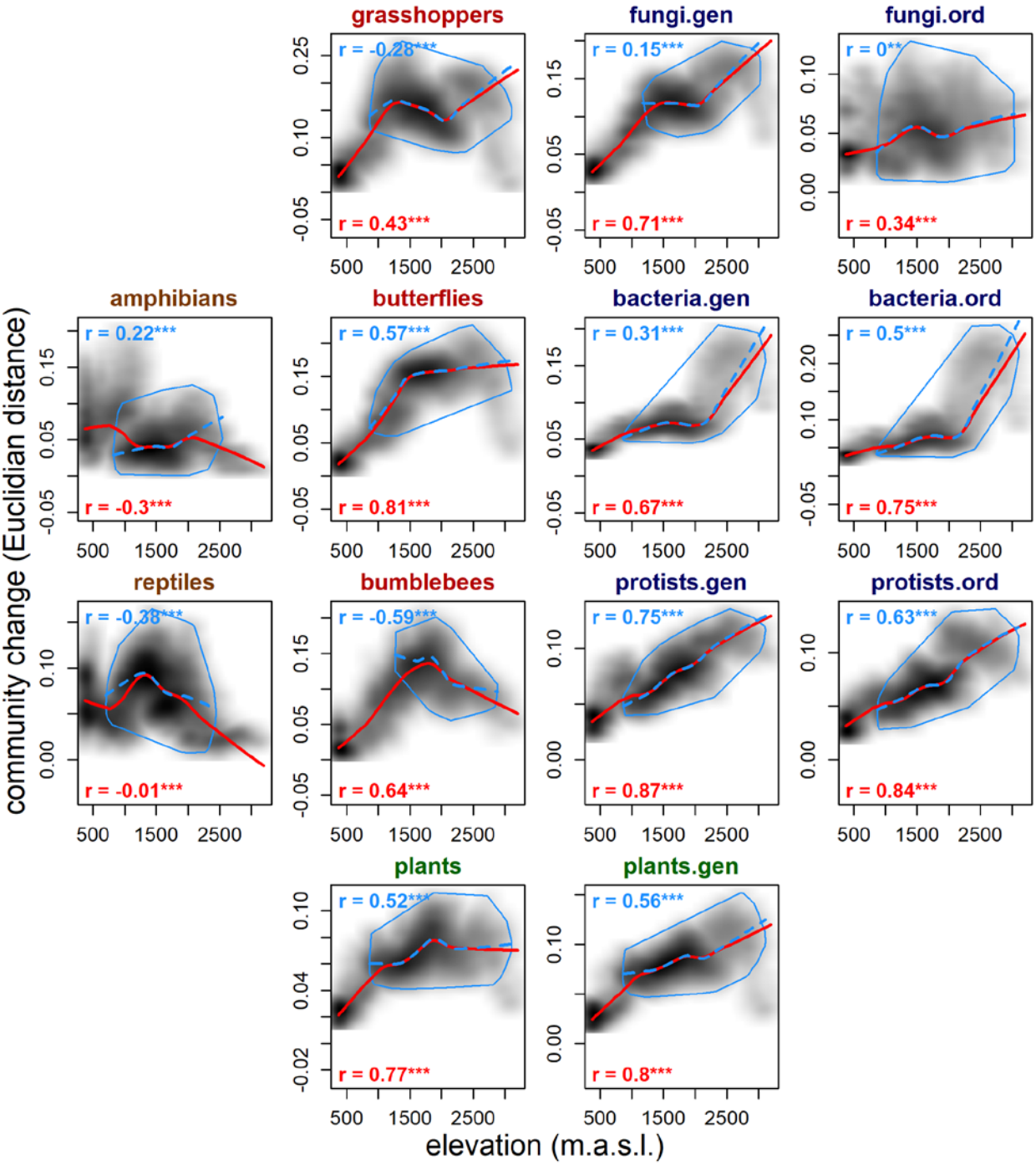

*Figure S38. Relationships between elevation and magnitude of community change between current conditions and future scenario **A1B for year 2060**. From the scatter plot in grey (for the total study area), the pixels within the environmentally analogous area are bordered by the blue polygon. The relationships (as LOWESS) and Spearman correlation are indicated in red for the total study area and in blue for environmentally analogous area.*

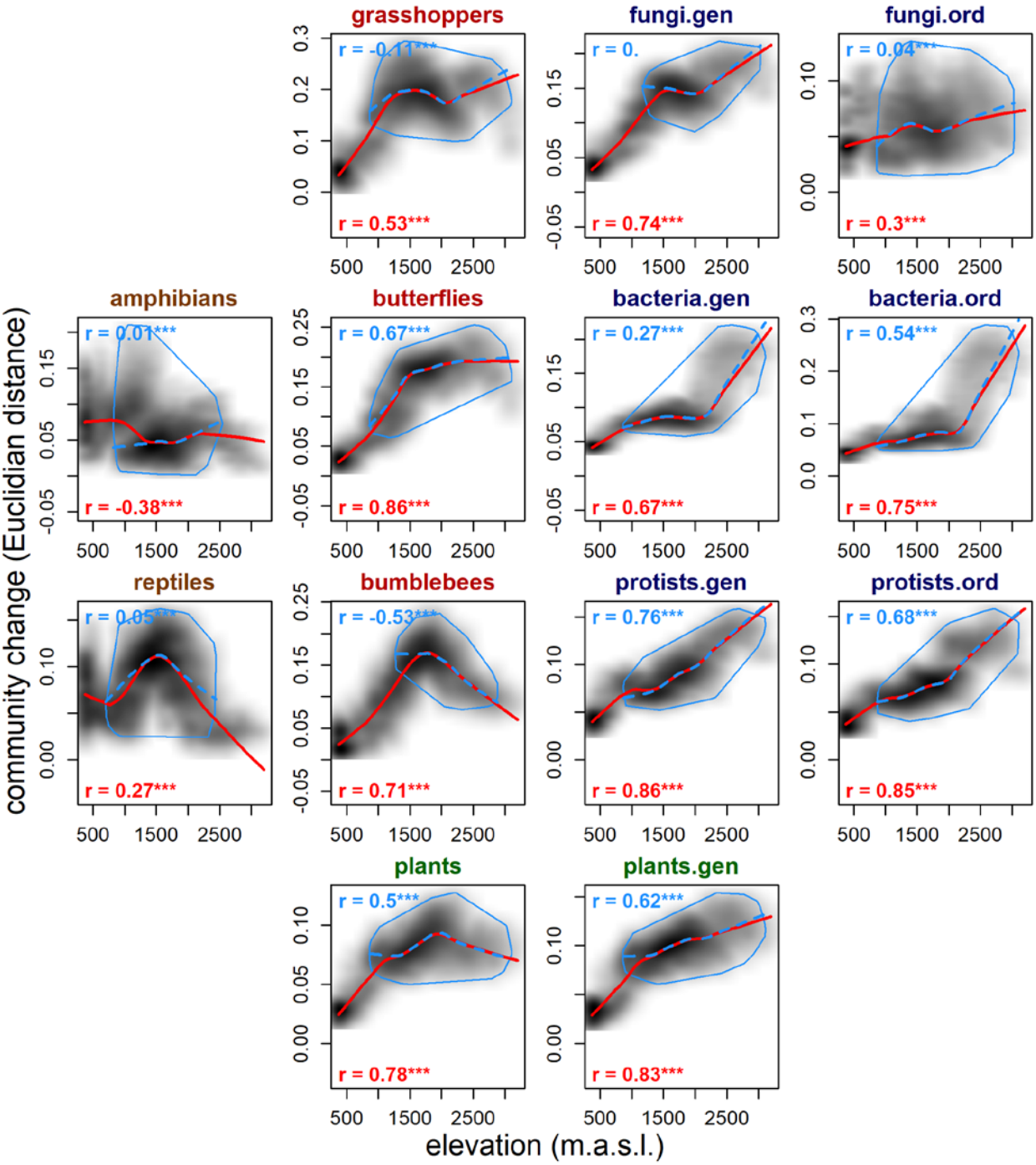

*Figure S39. Relationships between elevation and magnitude of community change between current conditions and future scenario **A1B for year 2085**. From the scatter plot in grey (for the total study area), the pixels within the environmentally analogous area are bordered by the blue polygon. The relationships (as LOWESS) and Spearman correlation are indicated in red for the total study area and in blue for environmentally analogous area.*

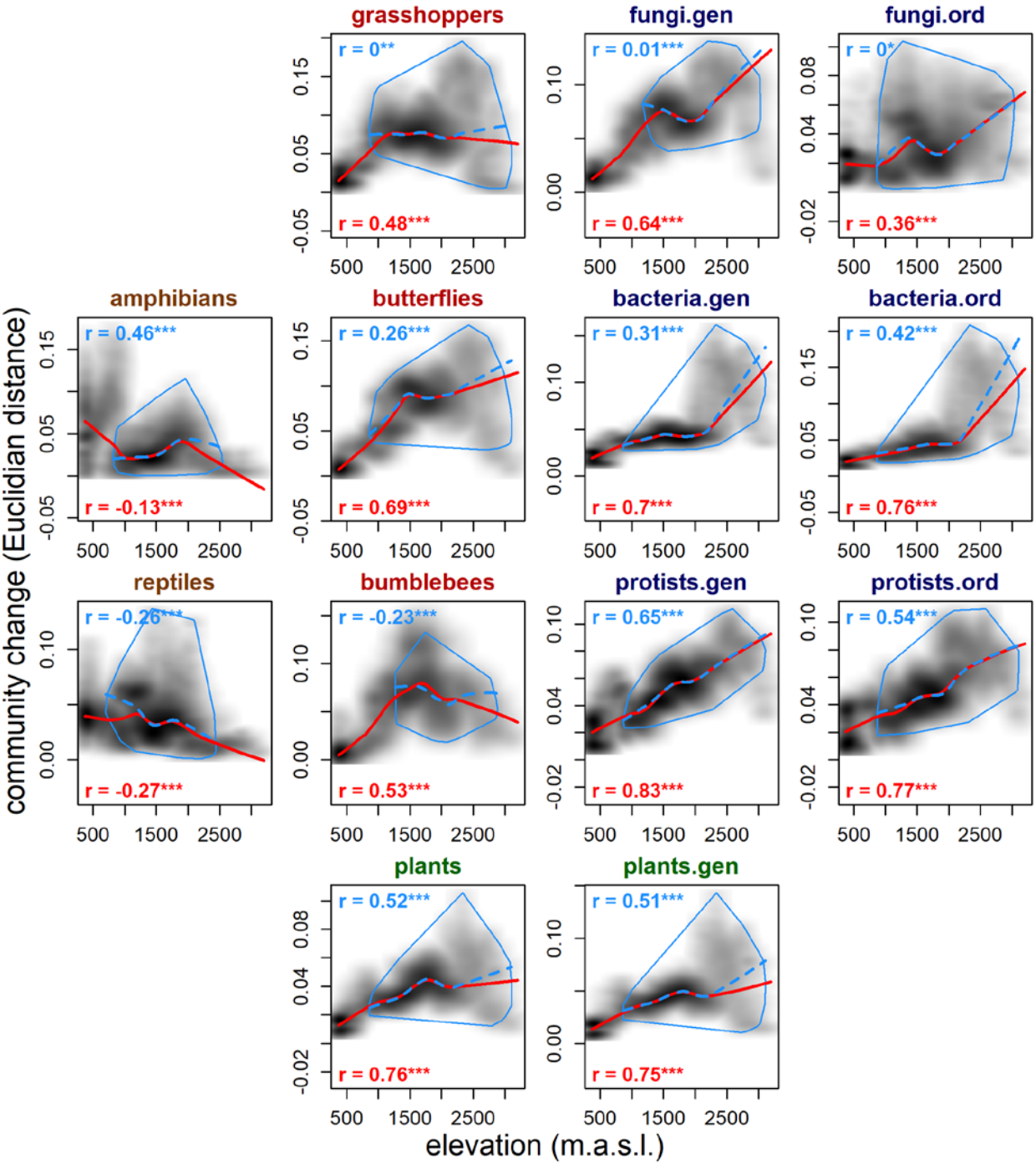

*Figure S40. Relationships between elevation and magnitude of community change between current conditions and future scenario **A2 for year 2035**. From the scatter plot in grey (for the total study area), the pixels within the environmentally analogous area are bordered by the blue polygon. The relationships (as LOWESS) and Spearman correlation are indicated in red for the total study area and in blue for environmentally analogous area.*

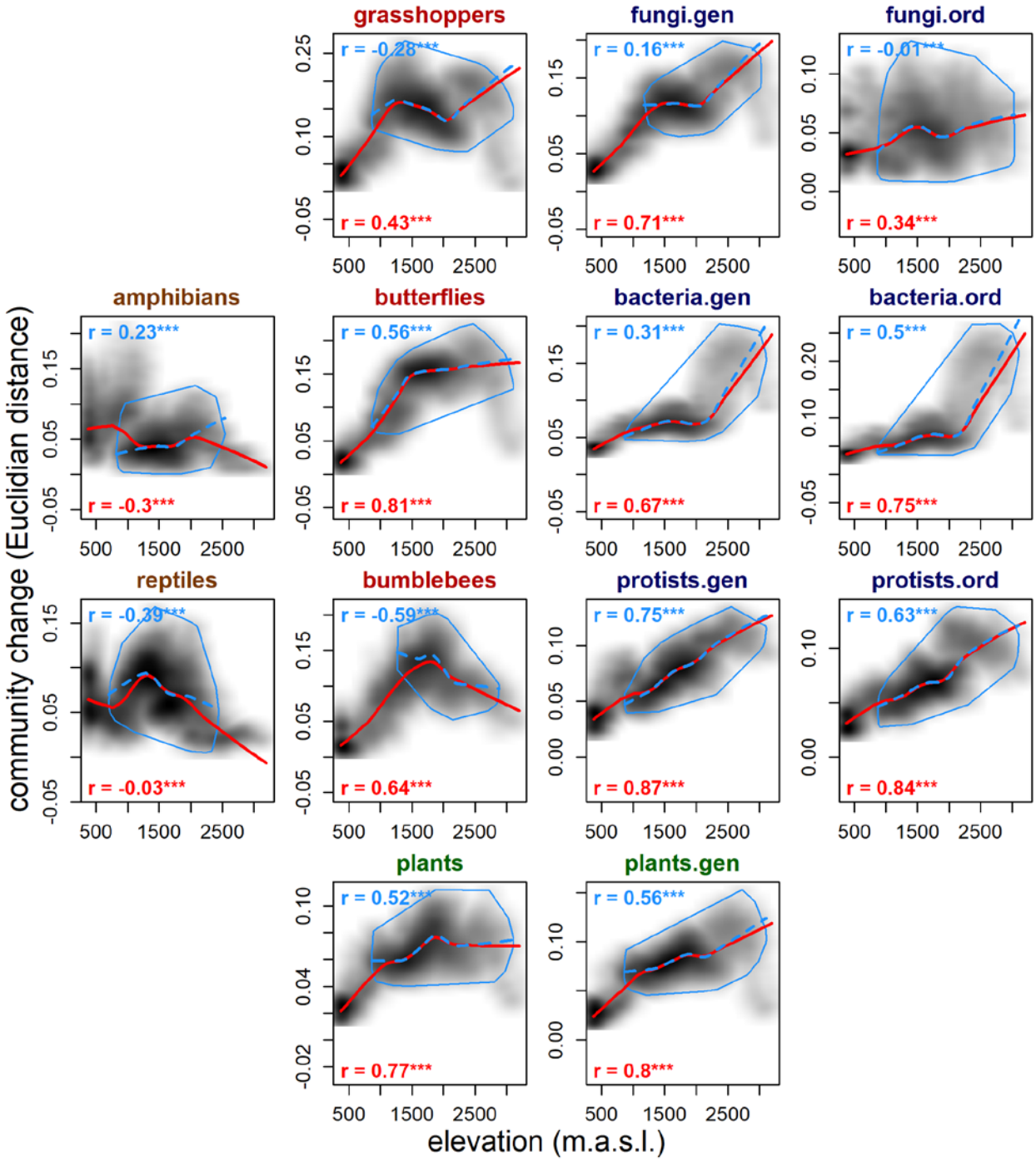

*Figure S41. Relationships between elevation and magnitude of community change between current conditions and future scenario **A2 for year 2060**. From the scatter plot in grey (for the total study area), the pixels within the environmentally analogous area are bordered by the blue polygon. The relationships (as LOWESS) and Spearman correlation are indicated in red for the total study area and in blue for*

environmentally analogous area.

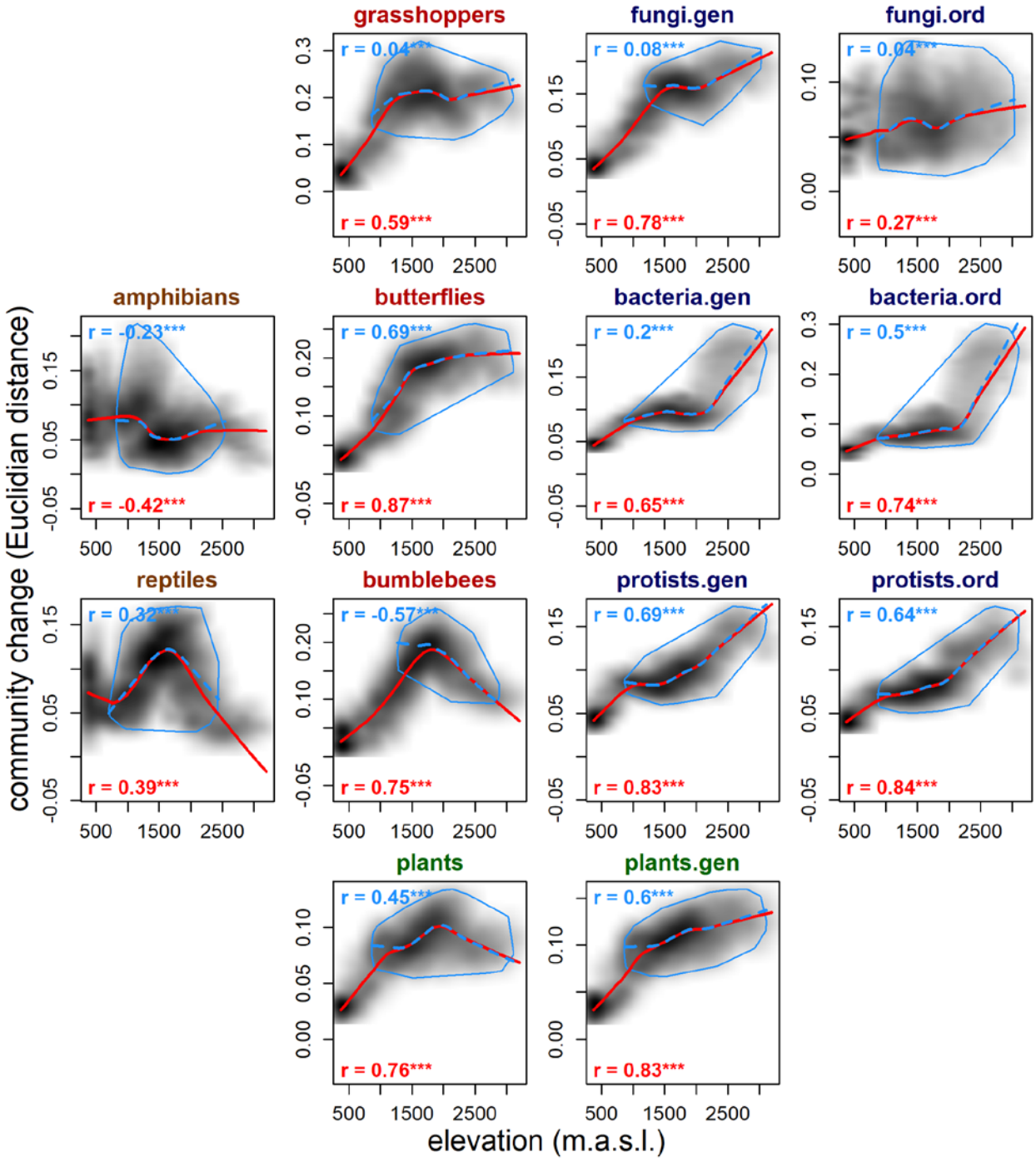

*Figure S42. Relationships between elevation and magnitude of community change between current conditions and future scenario **A2 for year 2085**. From the scatter plot in grey (for the total study area), the pixels within the environmentally analogous area are bordered by the blue polygon. The relationships (as LOWESS) and Spearman correlation are indicated in red for the total study area and in blue for environmentally analogous area.*

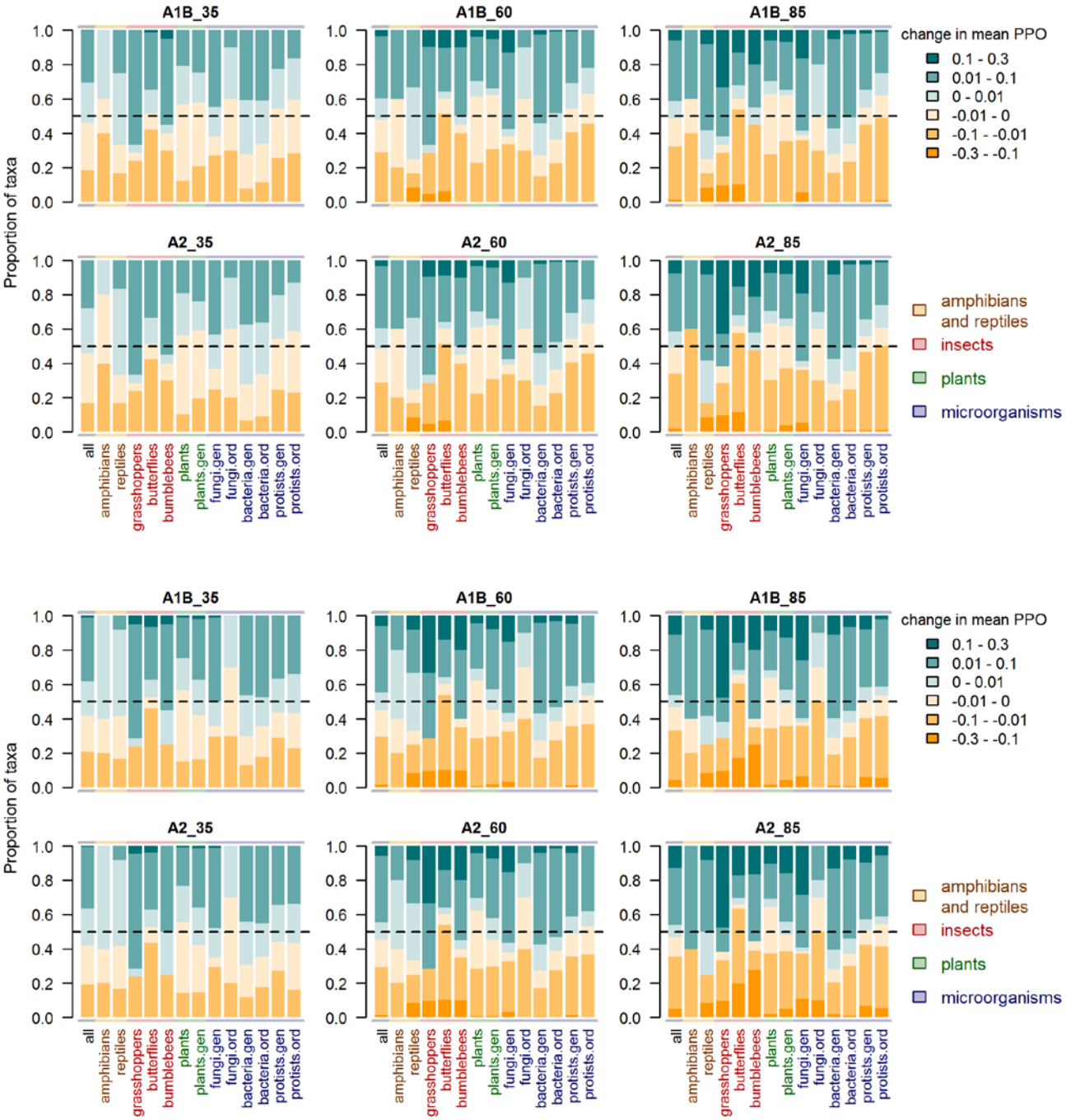

*Figure S43. Proportions of taxa with different mean changes in predicted probability of occurrence (PPO) between current and future conditions across the whole study area (**top**) and across the analogous environmental space (**bottom**). Positive values (in green) indicate increase in mean PPO, classified to three classes, whereas negative values (in orange) indicate decrease in mean PPO, classified to three classes.*

*Table S3. Spearman correlations (with significance levels as * p < 0.05, ** p < 0.01, *** p < 0.001) between mean change in predicted probability of occurrence (PPO) and prevalence of taxa.*

	A1B 2035	A1B 2060	A1B 2085	A2 2035	A2 2060	A2 2085
all	**0.06***	0.01	-0.02	**0.06****	0.01	-0.04
amphibians	-0.9	-0.9	-0.8	-0.9	-0.9	-0.8
reptiles	-0.2	-0.19	-0.14	-0.2	-0.19	-0.07
grasshoppers	0.02	-0.28	-0.34	0.02	-0.28	-0.4
butterflies	-0.12	**-0.22***	**-0.26***	-0.11	-0.22	**-0.28***
bumblebees	-0.08	-0.05	-0.09	-0.06	-0.05	-0.14
plants	0.02	-0.1	**-0.14***	0.04	-0.1	**-0.19****
plants.gen	-0.03	-0.1	-0.14	-0.02	-0.1	**-0.16***
fungi.gen	-0.06	-0.06	-0.09	-0.06	-0.06	-0.1
fungi.ord	-0.53	-0.59	-0.58	-0.53	-0.59	-0.58
bacteria.gen	**0.11***	0.05	-0.01	**0.12***	0.05	-0.04
bacteria.ord	0.12	0.06	0.01	0.13	0.06	0
protists.gen	**-0.16****	**-0.19****	**-0.22*****	**-0.16****	**-0.19****	**-0.23*****
protists.ord	-0.17	-0.2	**-0.22***	-0.16	-0.19	**-0.23***

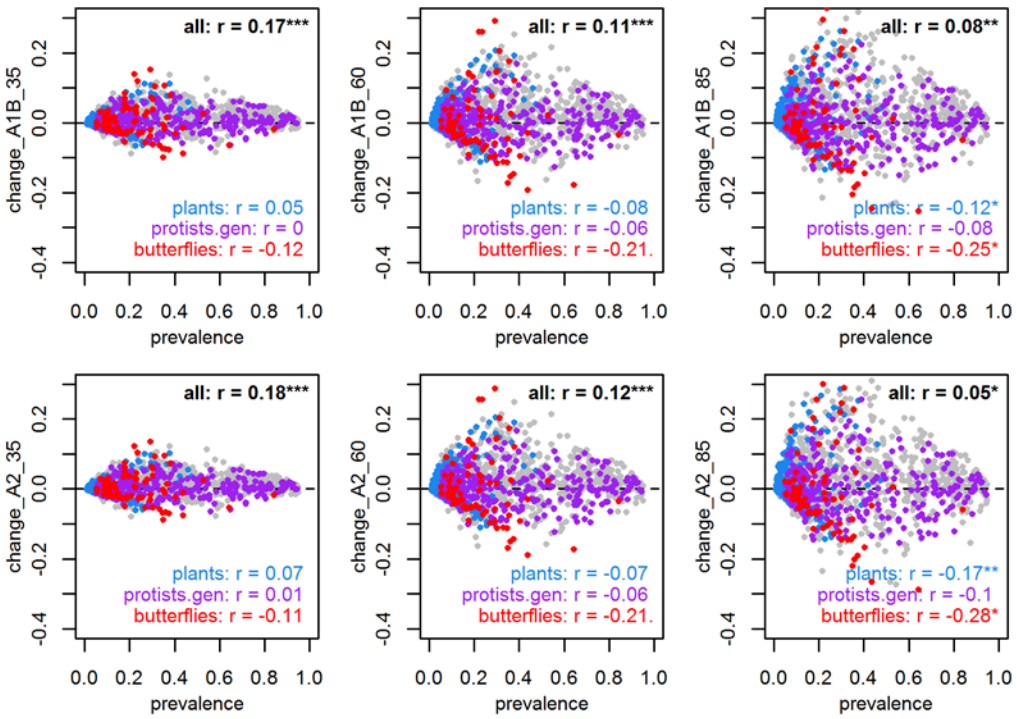

Figure S44. Relationship between mean change in predicted probability of occurrence (PPO) and prevalence of taxa. The taxonomic groups with the strongest and most significant Spearman correlations (p < 0.05, ** p < 0.01, *** p < 0.001) are shown in addition to all taxa.*

*Table S4. Spearman correlations (with significance levels as * p < 0.05, ** p < 0.01, *** p < 0.001) between mean change in predicted probability of occurrence (PPO) and niche breadth within study area of taxa.*

	A1B 2035	A1B 2060	A1B 2085	A2 2035	A2 2060	A2 2085
all	-0.03	0.01	0.01	-0.03	0	0.02
amphibians	-0.8	-0.8	-0.9	-0.8	-0.8	-0.9
reptiles	0.02	-0.06	-0.08	0.02	-0.06	-0.14
grasshoppers	-0.07	-0.24	-0.25	-0.08	-0.24	-0.29
butterflies	-0.14	-0.09	-0.08	-0.15	-0.09	-0.08
bumblebees	-0.26	-0.2	-0.18	-0.25	-0.2	-0.18
plants	-0.02	-0.08	**-0.12***	-0.01	-0.08	**-0.15***
plants.gen	0.13	0.11	0.07	0.14	0.11	0.06
fungi.gen	0.16	0.2	0.23*	0.14	0.2	**0.24***
fungi.ord	**0.82****	**0.9*****	**0.88****	**0.82****	**0.9*****	**0.88****
bacteria.gen	**-0.16****	-0.08	-0.07	**-0.17****	-0.09	-0.04
bacteria.ord	**-0.2***	-0.07	-0.04	**-0.21***	-0.08	0.01
protists.gen	**-0.49*****	**-0.44*****	**-0.41*****	**-0.5*****	**-0.44 *****	**-0.39 *****
protists.ord	**-0.4*****	**-0.39*****	**-0.37*****	**-0.41*****	**-0.39*****	**-0.35*****

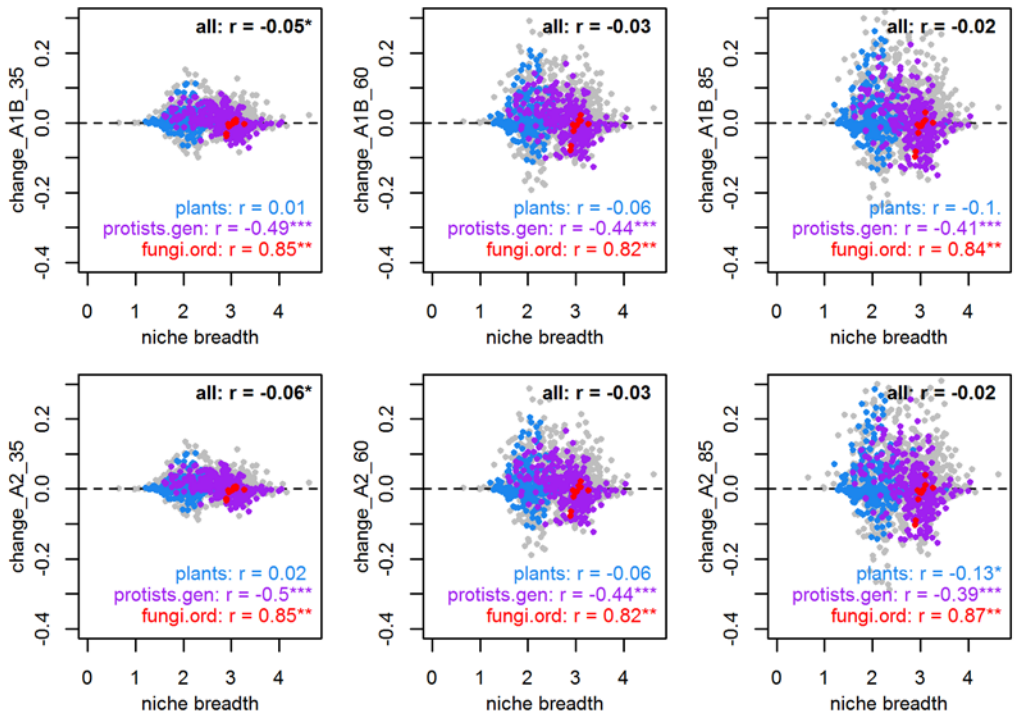

Figure S45. Relationship between mean change in predicted probability of occurrence (PPO) and niche breadth of taxa. The groups with the strongest and most significant Spearman correlations (p < 0.05, ** p < 0.01, *** p < 0.001) are shown in addition to all taxa.*

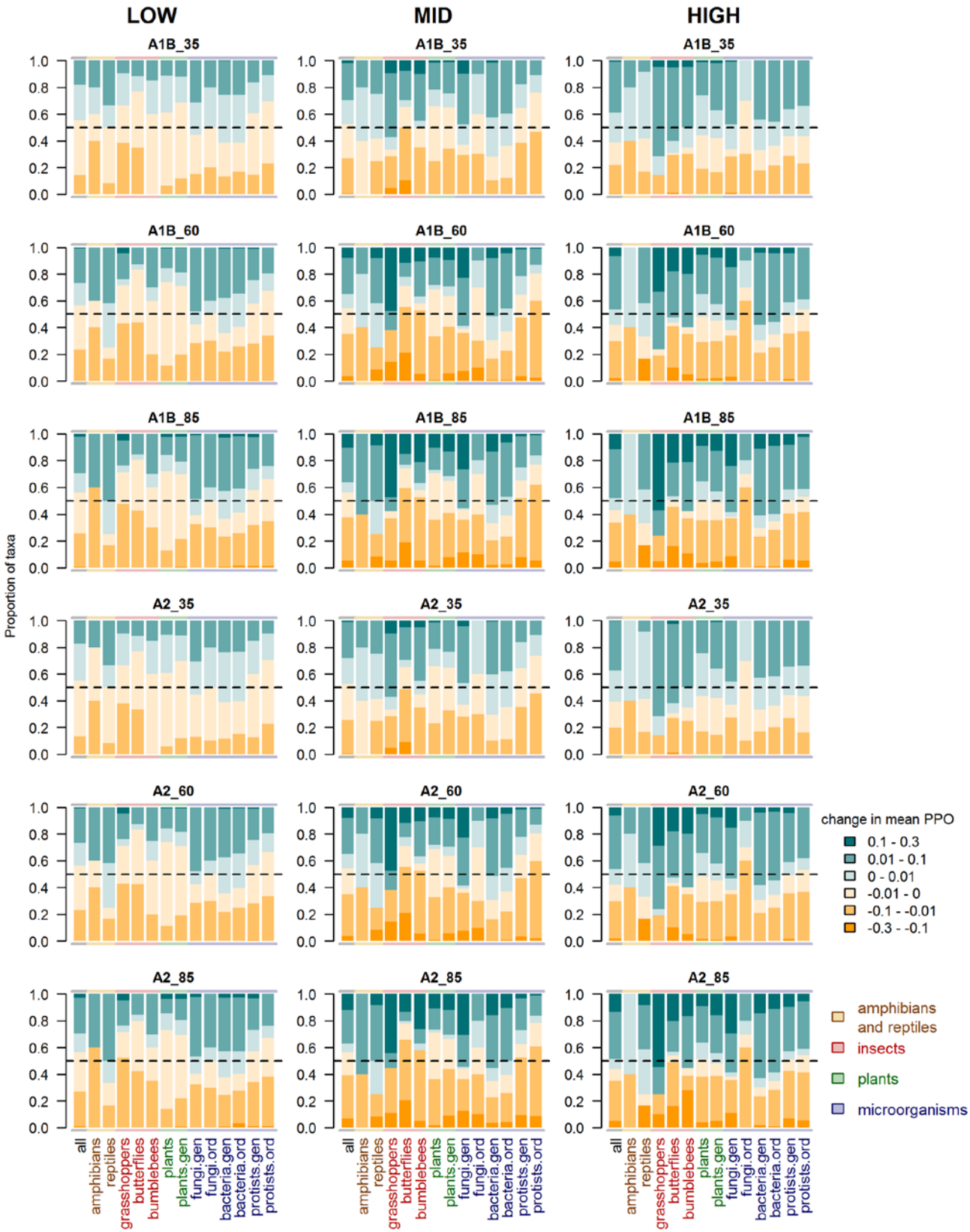

Figure S46. Proportion of taxa with different mean changes in predicted probability of occurrence (PPO) across elevational bands (low = <1180 m.a.s.l., mid = 1180-1650 m.a.s.l., high > 1650 m.a.s.l.) and under different future scenarios. Positive values (in green) indicate increase in mean PPO, classified to three classes, whereas negative values (in orange) indicate decrease in mean PPO, classified to three classes.

Supplementary material for *Greater climate control of above- versus belowground communities* by Mod et al.

Appendix 3: Comparisons between mean and median changes in PPOs of taxa, between ESM and standard SDM, and between different taxonomic resolutions

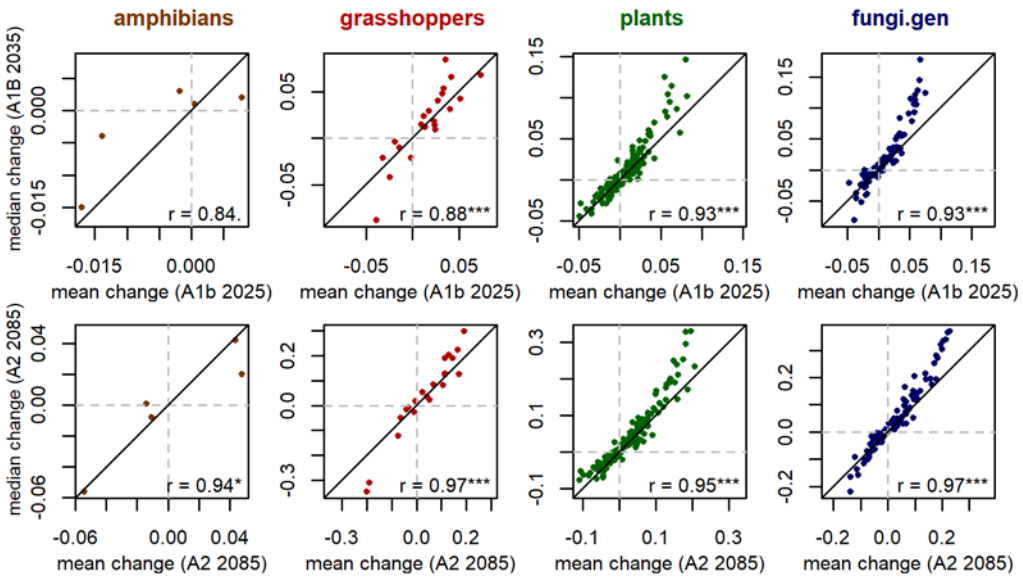

*Figure S47. Relationships between mean and median changes in taxa's PPOs **across the whole study area** under future scenarios A1b for year 2035 and A2 for 2085. Correlations (as Pearson) with significance levels (* p < 0.05, ** p < 0.01, *** p < 0.001) are indicated at bottom-right corner of each panel. As an example, only subset of taxonomic groups and future scenarios are presented.*

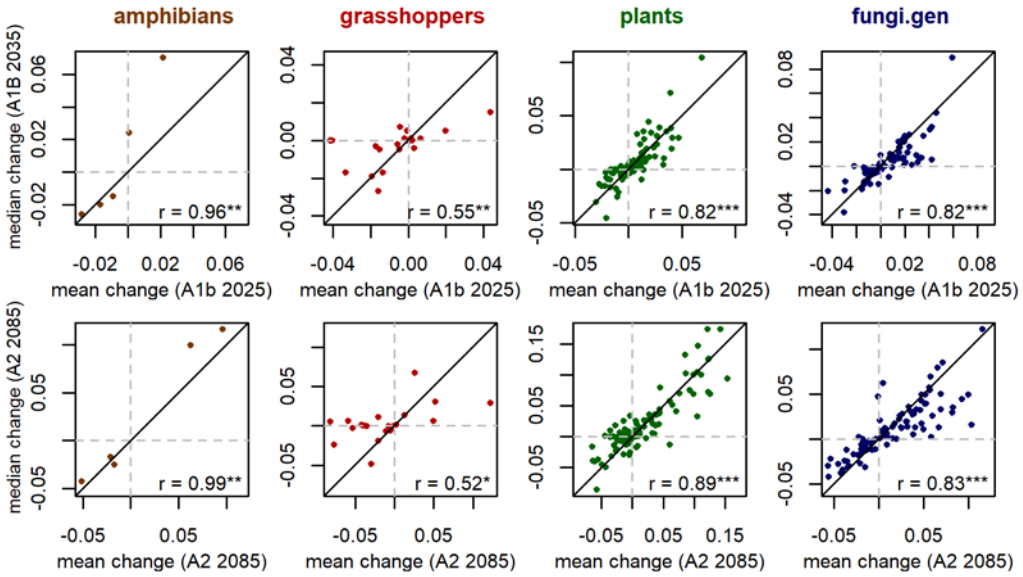

*Figure S48. Relationships between mean and median changes in taxa's PPOs **in low elevations** under future scenarios A1b for year 2035 and A2 for 2085. Correlations (as Pearson) with significance levels (* p < 0.05, ** p < 0.01, *** p < 0.001) are indicated at bottom-right corner of each panel. As an example, only subset of taxonomic groups and future scenarios are presented.*

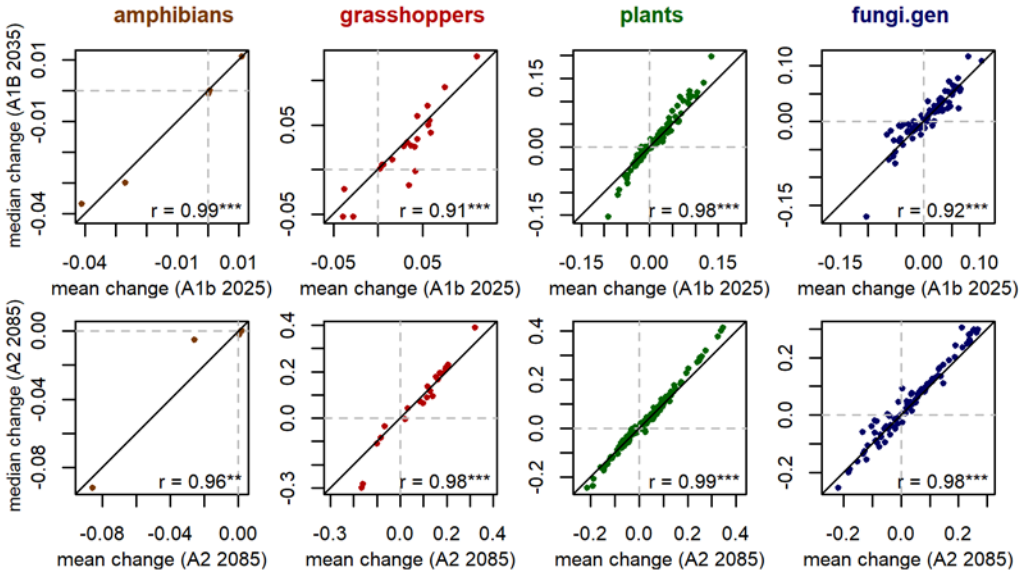

*Figure S49. Relationships between mean and median changes in taxa's PPOs **in high elevations** area under future scenarios A1b for year 2035 and A2 for 2085. Correlations (as Pearson) with significance levels (* p < 0.05, ** p < 0.01, *** p < 0.001) are indicated at bottom-right corner of each panel. As an example, only subset of taxonomic groups and future scenarios are presented.*

While ensembles of small models (ESMs) have been found to over-perform standard species distribution models (SDMs; i.e. models fitted with all predictors at one time) for rare species and current predictions

(Breiner, Guisan, Bergamini, & Nobis, 2015), the use of ESMs to derive future climate change predictions had not been tested so far. Thus, for comparison to ESMs (results shown in the main manuscript), standard ensemble SDMs were fitted for the subset of 468 taxa of groups with sufficient prevalence, i.e. taxa that had at least 50 presences and absences in each CCV-fold of training data and at least one presence and absence in each CCV-fold of evaluation data (Table S5). Standard SDMs followed the approach used for ESM (e.g. final ensemble model weighted based on AUC of single techniques) except that they were fitted within Biomod2-platform implementing ensemble modelling of Generalized Boosting Models (GBM), Generalized Linear Models (GLM), Generalized Additive Models (GAM) and Random Forest (RF) with default modelling options (Thuiller, Lafourcade, Engler, & Araújo, 2009; Thuiller, Georges, Engler, & Breiner, 2016; Hao, Elith, Guillera-Arroita, & Lahoz-Monfort, 2019). A selection of model evaluations and analyses of predicted changes were performed to compare ESMs and standard SDMs of the same subset of taxa and groups (see below).

Table S5. Number of taxa per group modelled with standard SMDs. Amphibians and fungi genera did not have any taxa meeting the rule when randomly dividing the sites to training and evaluation cross-validation folds.

8	*reptile species*
6	*grasshopper species*
15	*butterfly species*
3	*bumblebee species*
104	*plant species*
3	*fungi orders*
114	*bacteria genus*
49	*bacteria orders*
71	*protist genus*
24	*protist orders*

Model performances of final ensemble ESMs and final ensemble standard SDMs are highly correlated (0.964-0.983; Figure S50) but in general, ESMs perform better for most taxonomic groups (except for reptile, grasshopper and plant species for which SDM performs better; Table S6). Mean relative variable contributions across taxa are similar for ESMs and standard SDMs (Figure S51). The mean change in predicted probability of occurrence (PPO) of ESMs and standard SDMs are highly correlated but predictions of SDMs shows a larger variation (Figures S52-55 and Table S7).

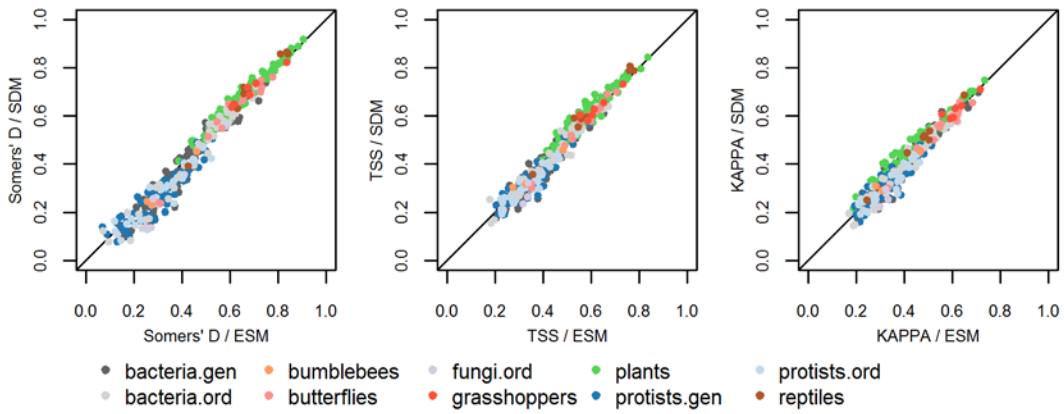

Figure S50. Relationship of Somers' D (AUC scaled between -1 and 1), maxTSS and maxKAPPA of taxa based on ESM and standard SDM. Correlations of evaluation metrics between ESM and standard SDM are 0.983, 0.977 and 0.964 for Somers' D, maxTSS and maxKAPPA, respectively. All correlations are statistically significant (p-value < $2.2*10^{-16}$).

Table S6. Mean AUC, maxTSS and maxKAPPA across taxa based on ESM and standard SDM, and p-values of significance of difference between means of metrics (based on paired t.test). In bold, the higher mean between ESM and standard SDM, and in bold italics, significant p-values (<0.05).

	AUC			maxTSS			maxKAPPA		
	ESM	**SDM**	**p-value**	**ESM**	**SDM**	**p-value**	**ESM**	**SDM**	**p-value**
all	**0.7225**	0.7155	***0.000***	**0.433**	0.427	***0.000***	**0.388**	0.383	***0.001***
reptiles	0.8465	**0.8565**	0.096	0.610	**0.633**	***0.015***	0.447	**0.467**	***0.008***
grasshoppers	0.844	**0.8535**	0.074	0.624	**0.633**	0.365	0.620	**0.628**	0.465
butterflies	**0.804**	0.801	0.535	**0.566**	0.557	0.119	**0.543**	0.535	0.122
bumblebees	**0.6655**	0.654	0.196	**0.362**	0.358	0.838	**0.354**	0.349	0.744
plants	0.8265	**0.8395**	***0.000***	0.565	**0.587**	***0.000***	0.417	**0.442**	***0.000***
fungi.ord	**0.6335**	0.5885	0.114	**0.331**	0.271	0.108	**0.319**	0.256	0.065
bacteria.gen	**0.7155**	0.7065	***0.000***	**0.420**	0.413	***0.018***	**0.406**	0.399	***0.021***
bacteria.ord	**0.7115**	0.7015	***0.001***	**0.419**	0.412	0.062	**0.408**	0.396	***0.003***
protists.gen	**0.6515**	0.633	***0.000***	**0.340**	0.319	***0.000***	**0.330**	0.310	***0.000***
protists.ord	**0.6575**	0.6375	***0.000***	**0.344**	0.321	***0.000***	**0.333**	0.311	***0.003***

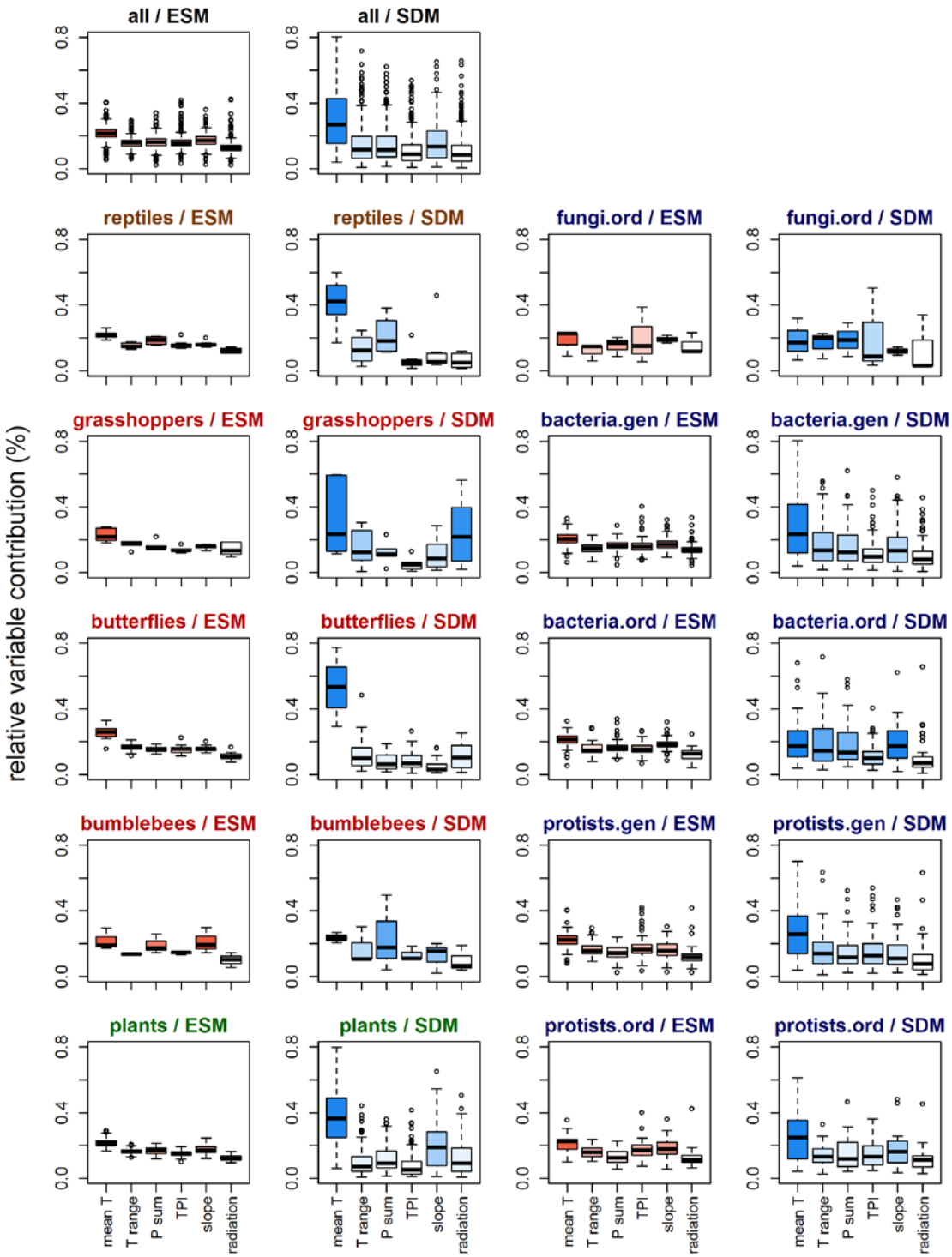

Figure S51. Relative variable contributions per taxonomic group based on ESM (in red) and standard SDM (in blue). Note that the calculation of relative variable contribution vary between ESM and standard SDM. For SDM, relative variable contributions were calculated following the methodology of biomod2 with three permutations. For ESM, see methods in the main text.

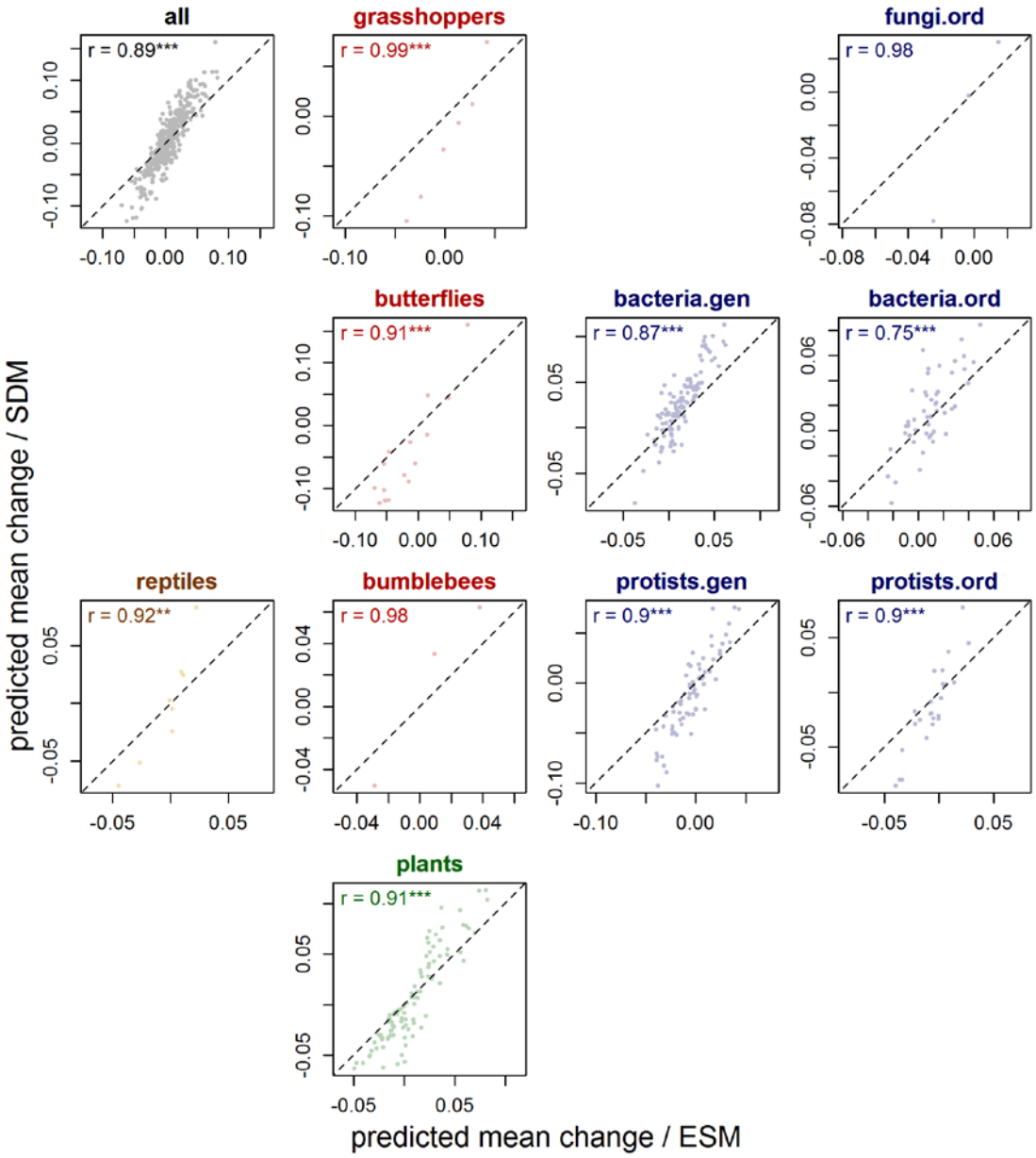

Figure S52. Relationship of predicted mean change from current to future conditions under A1b 2035-scenario across the study area as based on ESM and standard SDM. Correlations with significance levels (p < 0.05, ** p < 0.01, *** p < 0.001) are indicated at top-left corner of each panel.*

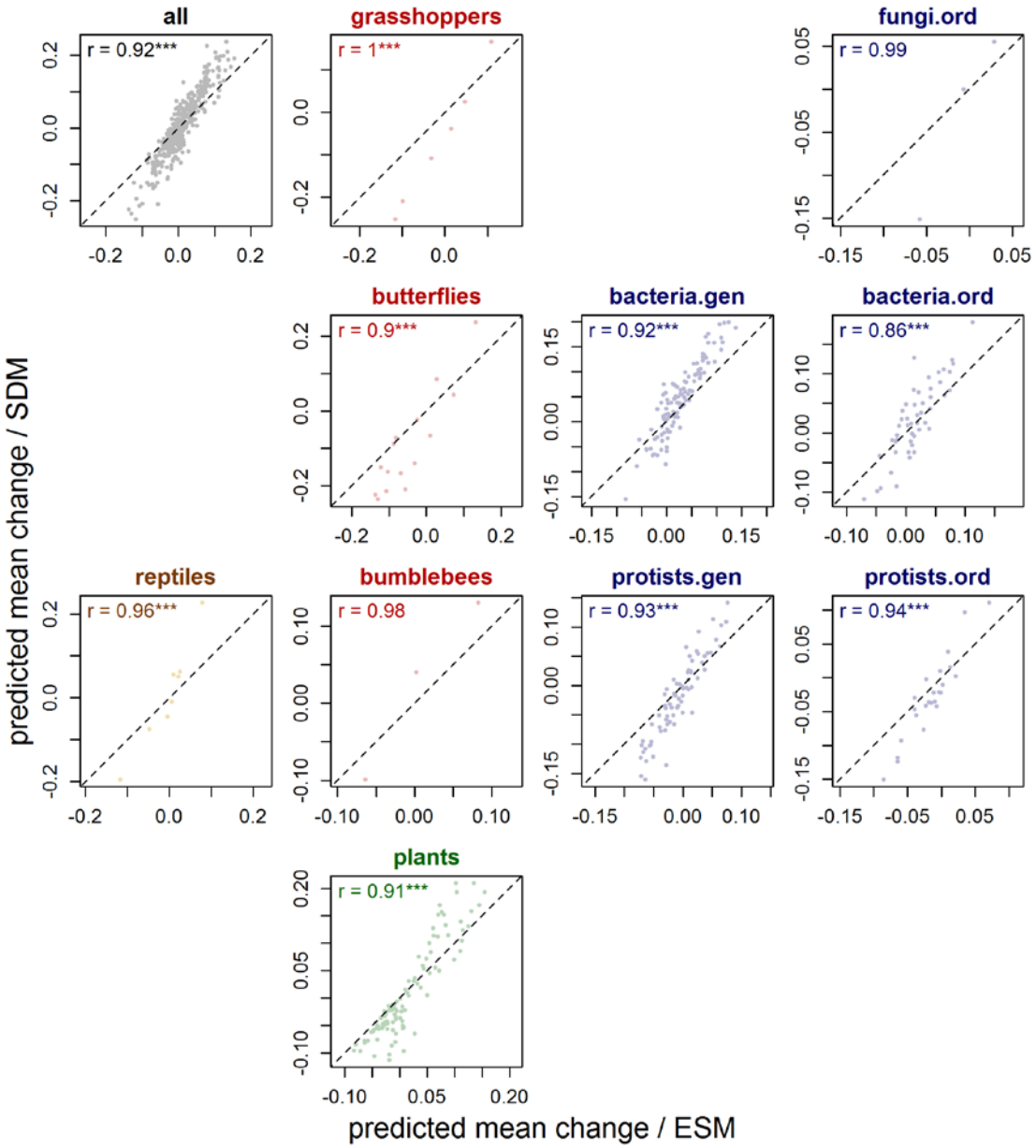

Figure S53. Relationship of predicted mean change from current to future conditions under A1b60-scenario across the study area as based on ESM and standard SDM. Correlations with significance levels (p < 0.05, ** p < 0.01, *** p < 0.001) are indicated at top- left corner of each panel.*

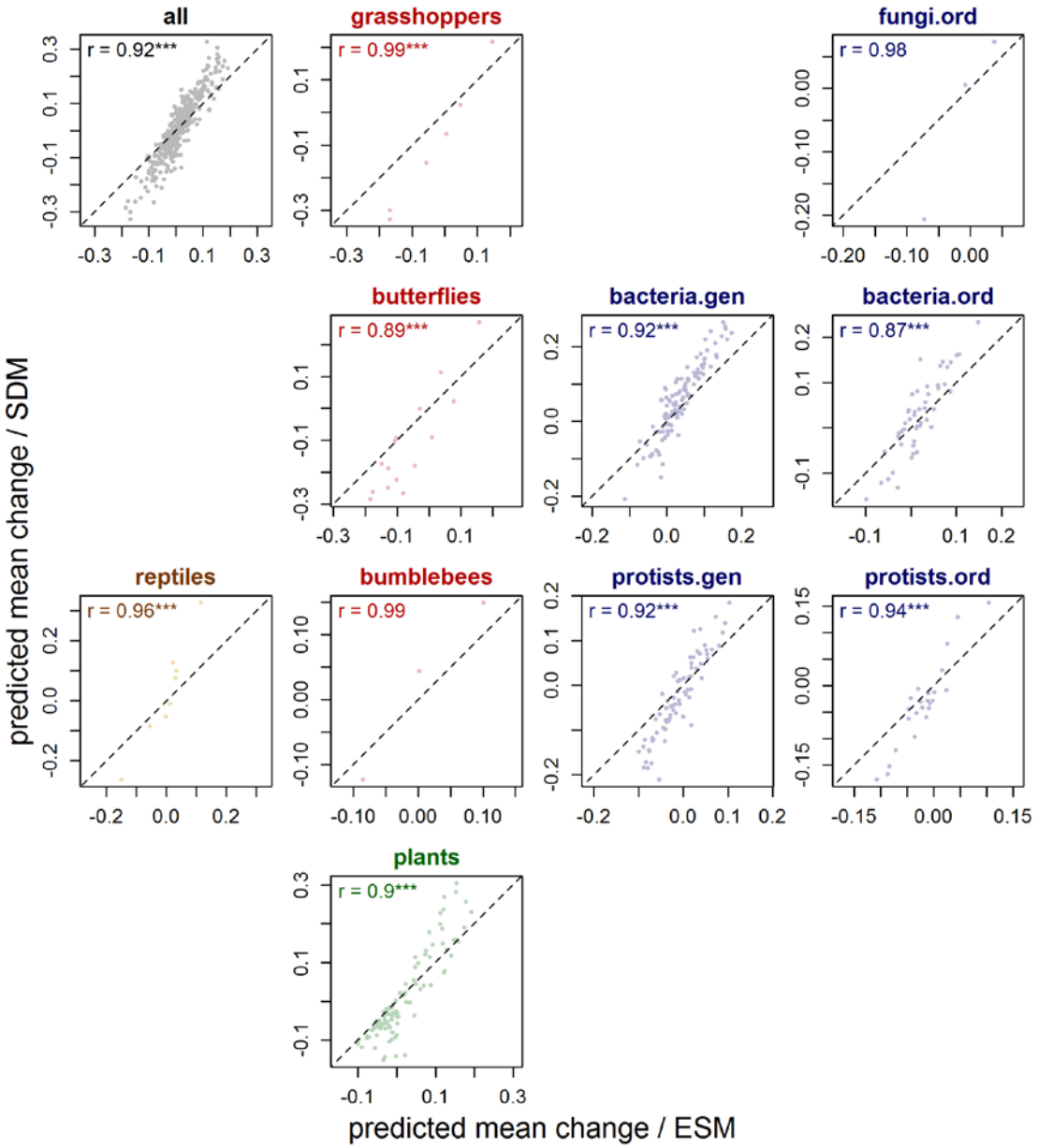

Figure S54. Relationship of predicted mean change from current to future conditions under A1b85-scenario across the study area as based on ESM and standard SDM. Correlations with significance levels (p < 0.05, ** p < 0.01, *** p < 0.001) are indicated at top- left corner of each panel.*

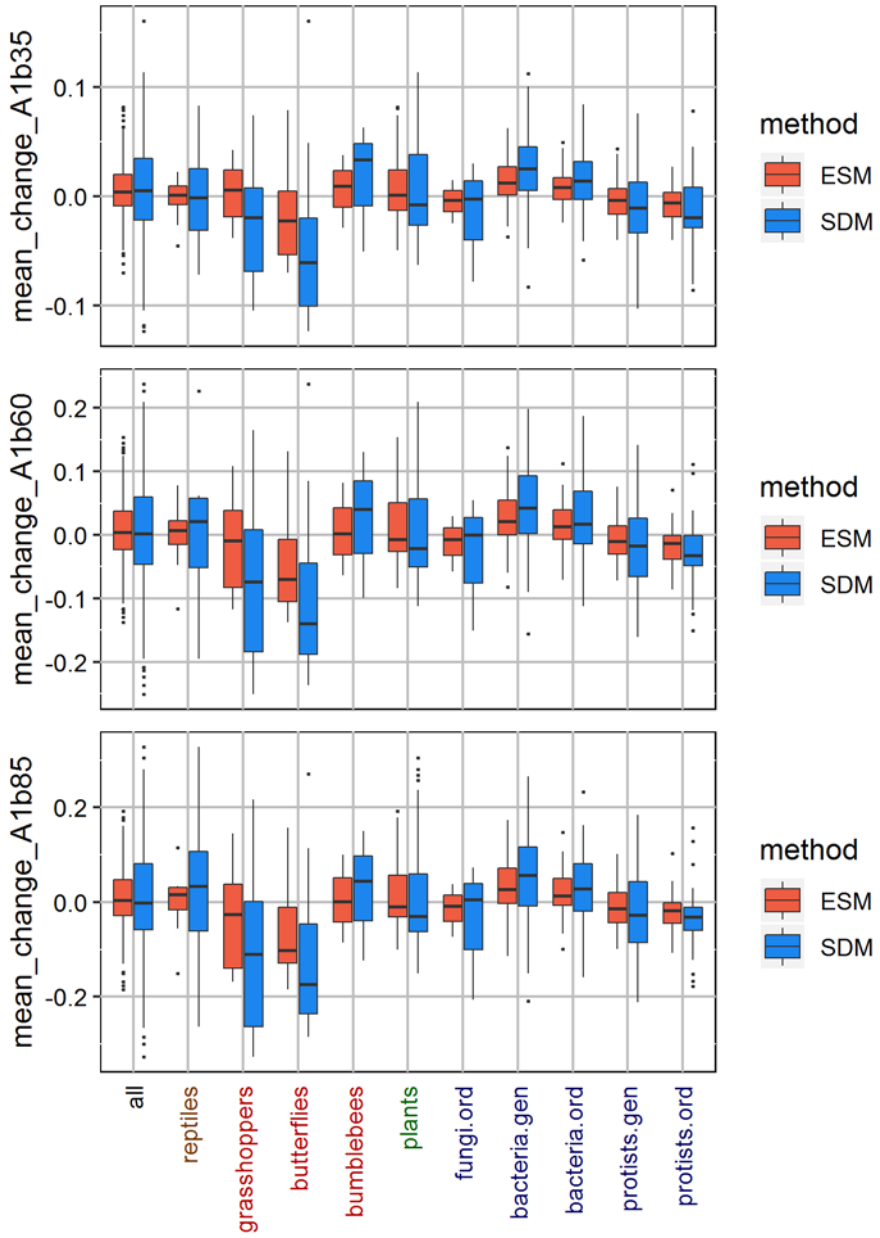

Figure S55. Mean change in predicted probability of occurrence across study area of taxa from current to future conditions under A1b-scenario as based on ESM and standard SDM.

Table S7. Mean change in predicted probability across study area based on ESM and standard SDM, and p-values of significance of difference between means of mean changes (based on paired t.test). In bold italics, significant p-values (<0.05).

	A1b 2035			A1b 2060			A1b 2085		
	ESM	**SDM**	**p-value**	**ESM**	**SDM**	**p-value**	**ESM**	**SDM**	**p-value**
all	0.005	0.006	0.166	0.008	0.008	0.890	0.010	0.009	0.951
reptiles	-0.003	-0.002	0.876	-0.004	0.009	0.621	0.000	0.028	0.477
grasshoppers	0.003	-0.023	0.126	-0.013	-0.070	0.098	-0.033	-0.101	0.098
butterflies	-0.019	-0.045	***0.035***	-0.047	-0.092	**0.027**	-0.064	-0.114	**0.037**
bumblebees	0.006	0.015	0.607	0.007	0.024	0.585	0.005	0.023	0.586
plants	0.007	0.005	0.371	0.013	0.008	0.185	0.015	0.008	0.170
fungi.ord	-0.005	-0.017	0.622	-0.012	-0.032	0.641	-0.015	-0.042	0.652
bacteria.gen	0.014	0.027	***0.000***	0.027	0.045	**0.000**	0.035	0.057	**0.000**
bacteria.ord	0.009	0.016	***0.031***	0.016	0.024	0.156	0.020	0.029	0.186
protists.gen	-0.004	-0.010	***0.028***	-0.008	-0.020	**0.010**	-0.010	-0.025	**0.015**
protists.ord	-0.007	-0.014	0.176	-0.016	-0.029	0.058	-0.020	-0.034	0.105

Table S8. Average (mean across taxa) model performance of final ensemble ESMs for plants and microorganisms at the different taxonomic resolutions (species vs. genus for plants and genus vs. order for microorganisms). p-values indicate the statistical significance that the difference in model performance deviates from zero (based on two-sample Mann-Whitney test). Note, that fungi genera and orders result from different type of data production (see Appendix 1)

taxonomic	**Somers' D**			**maxTSS**			**maxKAPPA**		
group	**species**	**genus**	**p-value**	**species**	**genus**	**p-value**	**species**	**genus**	**p-value**
plants	**0.666**	0.619	***0.000***	**0.595**	0.545	***0.000***	0.340	**0.357**	0.130
	genus	**order**	**p-value**	**genus**	**order**	**p-value**	**genus**	**order**	**p-value**
fungi	**0.399**	0.255	***0.001***	**0.492**	0.343	***0.000***	**0.437**	0.274	***0.000***
bacteria	0.438	**0.470**	0.058	0.463	**0.483**	0.168	0.375	**0.408**	***0.028***
protists	0.356	**0.361**	0.804	0.405	**0.418**	0.422	**0.337**	0.322	0.246

REFERENCES

Breiner, F.T., Guisan, A., Bergamini, A., & Nobis, M.P. (2015). Overcoming limitations of modelling rare species by using ensembles of small models. Methods in Ecology and Evolution, 6(10), 1210-1218. doi:10.1111/2041-210x.12403

Hao, T.X., Elith, J., Guillera-Arroita, G., & Lahoz-Monfort, J.J. (2019). A review of evidence about use and performance of species distribution modelling ensembles like BIOMOD. Diversity and Distributions, 25(5), 839-852. doi:10.1111/ddi.12892

Thuiller, W., Georges, D., Engler, R., & Breiner, F. (2016). biomod2: Ensemble Platform for Species Distribution Modeling R-package (Version 3.3-7.). Retrieved from https://CRAN.R-project.org/package=biomod2

Thuiller, W., Lafourcade, B., Engler, R., & Araújo, M.B. (2009). BIOMOD - a platform for ensemble forecasting of species distributions. Ecography, 32(3), 369-373. doi:10.1111/j.1600-0587.2008.05742.x